Buckling Behaviour Improvement of Steel Plate Shear Walls with and without Openings

Mohammad Sabouri Ghomi

A Thesis

In The Department of

Building, Civil and Environmental Engineering

Presented in partial fulfillment of the requirements

For the degree of

Doctor of Philosophy (Civil Engineering) at

Concordia University

Montreal, Québec, Canada

April 2023

© Mohammad Sabouri Ghomi, 2023

CONCORDIA UNIVERSITY

School of Graduate Studies

This is to certify that the thesis prepared

By: Mohammad Sabouri Ghomi

Entitled: Buckling Behaviour Improvement of Steel Plate Shear Walls with and without Openings

and submitted in partial fulfillment of the requirements for the degree of

Doctor of Philosophy Civil Engineering

complies with the regulations of the University and meets the accepted standards with respect to originality and quality.

Signed by the final examining committee:

_____ Chair

Dr. Ahmed Soliman

_____ Thesis supervisor

Dr. Anjan Bhowmick

_____ Examiner

Dr. Lucia Tirca

_____ Examiner

Dr. Emre Erkmen

_____ Examiner

Dr. M. Zahangir Kabir

_____ External Examiner

Dr. Sreekanta Das

Approved by _____

Dr. Mazdak Nik-Bakht   , Graduate Program Director

_____

Dr. Mourad Debbabi   , Dean

Date of Defense: 2023-06-19

Abstract

Buckling Behaviour Improvement of Steel Plate Shear Walls with and without Openings

Mohammad Sabouri Ghomi, Ph.D.

Concordia University, 2023

Steel plate shear wall (SPSW) is an effective lateral load-resisting system rapidly gaining the attention of many researchers and structural engineers. The system is designed and constructed primarily in seismically active regions. Conventional SPSW uses thin unstiffened steel infill plates, which act as the main ductile fuse of the lateral load-resisting system. It is often required to have openings in the infill plate. One of the main reasons for having an opening in the infill plate is to provide a place for nonstructural elements such as windows or doors. However, when subjected to lateral loads, deformations around the openings are a concern that must be considered. The main objective of this study is to prevent the out-of-plane deformation of the openings and find a practical and efficient solution for this issue. A recognized method commonly used to prevent the buckling of thin steel plate shear walls is attaching stiffeners on the infill plate. Thus, using stiffeners around the opening is the main consideration as a solution for the addressed issue. Commonly used stiffened plates are extensively stiffened and have a relatively large number of stiffeners. This can make the stiffened SPSW system quite expensive and unpopular. This study aims to prevent the deformation of the openings by using as few stiffeners as possible.

In the first part of this research work, the behaviour of stiffened steel plate shear walls is studied analytically and numerically. The analytical study is done by the plate-frame interaction (PFI) model, and the numerical analysis is done using ABAQUS. The analytical study shows that stiffeners in the stiffened infill plate can increase elastic stiffness by 53% and the shear strength by about 15%. A series of SPSW models with horizontal and vertical stiffeners are analyzed, and their buckling behaviour is studied. A close agreement between the PFI method and the finite element analysis is observed. Based on the analysis, an improved stiffness criterion for designing stiffeners in stiffened SPSWs is proposed. FE analysis shows that the proposed stiffness criterion is effective in preventing the global buckling of the stiffened infill plates in SPSWs

In the second part, SPSWs with a rectangular opening are studied using finite element analysis. The results for unstiffened plates show very large deformations around the opening. Different stiffener layouts to prevent deformations are considered and analyzed. The results show that all considered layouts are effective in preventing the deformation around the opening. Based on the analysis, an effective stiffener layout is selected. FE analysis shows that the proposed stiffener layout can improve the behaviour of SPSWs with rectangular openings. FE models with different opening locations and sizes are also analyzed. Analysis shows that the shear strength of the stiffened infill plate depends only on the length of the rectangular opening. It is also observed that the location of the rectangular opening does not have any significant effect on the strength of the infill plate. Finally, a shear strength equation is proposed for the infill plate stiffened with the proposed stiffener layout around the rectangular opening.

In the last part, two one-third-scale single-storey SPSWs are tested. The specimens have a rectangular opening at the center of the plate, and the openings are reinforced using the proposed stiffener layout. The two specimens are identical in size, and the only difference between the specimens is the size of the opening. Cyclic quasi-static loading is applied at the top of the specimens. Various instruments are used to monitor the behaviour of the specimens during the experiment. Both tests show that deformations around the opening are successfully restrained. Test results also show stable hysteresis curves and good energy dissipation capacity for both specimens. In the end, a 4-storey finite element model with a large rectangular opening is selected, and seismic analysis is performed on the model with and without stiffeners. Eleven historical records are selected and scaled for the seismic analysis. Seismic analysis shows that the proposed stiffener layout around the opening can prevent out-of-plane deformation around the opening in the SPSW system.

Acknowledgements

Words cannot express my gratitude to my supervisor, Dr. Anjan Bhowmick, for his invaluable support and guidance throughout this research. This research would have never been possible without his continuous help, encouragement, and patience. His immense knowledge and valuable feedback have guided me during the course of my Ph.D. degree. It was a great honour to be one of his graduate students and work under his guidance. I would also like to thank the examination committee, Dr. Lucia Tirca, Dr. Emre Erkmen, Dr. Zahangir Kabir, and Dr. Sreekanta Das, for their thorough review of the thesis. I could not have undertaken this journey without their valuable suggestions and remarks.

Lastly, I would like to express my deep gratitude to my family, especially my parents and my sister, for their endless support and encouragement. Their belief in me has kept my spirits and motivation high during this period of my life.

Dedications

To my beloved parents,

& To my sister

Co-Authorship

This thesis has been prepared in accordance with the regulations for a sandwich thesis format. This research presents numerical and experimental work carried out solely by Mohammad Sabouri Ghomi. Advice and guidance were provided for the whole thesis by the academic supervisor Dr. Anjan Bhowmick. This thesis consists of the following chapters:

Chapter 3

Sabouri-Ghomi, Mohammad, and Bhowmick, Anjan K. 2023. "Analytical and numerical investigation of stiffened steel plate shear walls." *Asian Journal of Civil Engineering* 24: 1841–1857.

Chapter 4

Sabouri-Ghomi, Mohammad, and Bhowmick, Anjan K. 2022. "Numerical analysis of steel plate shear walls with rectangular openings." *Journal of Steel & Composite Structures*, submitted and is under review.

Chapter 5

Sabouri-Ghomi, Mohammad, Bhowmick, Anjan K. and Sabouri-Ghomi, Saied. 2023. "Experimental and numerical study of stiffened steel plate shear walls with rectangular openings " ASCE Journal of Structural Engineering, revision submitted and is under review.

TABLE OF CONTENTS

List of Figures

List of tables

List of Symbols

t_p = infill plate thickness

L = infill plate length

h = infill plate height

A_b = boundary beam gross section area

A_c = boundary column gross section area

b   = infill plate length

t   = infill plate thickness

τ_{cr} = infill plate critical shear stress

σ_{ty} = infill plate tension field stress at yielding

θ = tension field angle of inclination

d   = infill plate height

E = elastic modulus

G = shear modulus

M_{fp} = boundary column plastic moment

I_f = boundary column moment of inertia

τ_{crg} = critical shear buckling stress for global buckling mode

τ_{crl} = critical shear buckling stress for local buckling mode

I_x = vertical stiffeners moment of inertia

I_y = horizontal stiffeners moment of inertia

S_x = vertical stiffeners spacing

S_y = horizontal stiffeners spacing

υ = Poisson ratio

k_g = global shear buckling coefficient

k_l = local shear buckling coefficient

V_{op} = perforated plate shear strength

V_p = solid plate shear strength

D = circular opening diameter

w = infill plate thickness

I_c = boundary column moment of inertia

T_1 = fundamental period

$T_{90\%}$ = period of the highest vibration mode for a minimum of 90% mass participation

CHAPTER 1

INTRODUCTION

1.1. Introduction and problem definition

Building structures require appropriate load-resisting systems to resist lateral loads such as wind and earthquakes. Generally, three different types of load-resisting systems are used to resist lateral loads in steel buildings: Moment resisting frames, Braced frames, and shear walls. Each load-resisting system has its advantages and disadvantages. Steel Plate Shear Wall (SPSW) is an innovative lateral load-resisting system that is used in buildings in moderate to high seismic regions. An SPSW consists of a steel plate attached (welded or bolted) to the surrounding beams and columns. While the SPSW system can be stiffened or unstiffened, in North America unstiffened SPSW system is popular. The Canadian steel design standard, CAN/CSA S16-19, and the American steel design standard, AISC 341-16, have adopted unstiffened SPSW system and provided design guidelines for the lateral load-resisting system. Several studies (numerical and experimental) have been conducted on the SPSW system (Roberts and Sabouri-Ghomi 1992; Driver et al. 1998b; Bhowmick et al. 2009; Bhowmick et al. 2011; Chatterjee et al. 2015). These studies have shown that a properly designed SPSW system has significantly higher initial stiffness, ultimate strength, and higher energy dissipation capacity than conventional steel lateral load-resisting systems. In some cases, using SPSWs instead of moment-resisting frames can reduce the use of steel by up to 50% (Caccese et al. 1993).

Another important advantage of SPSWs is the option to have openings in the infill plates. In general, there are two main reasons, structural and architectural, for providing openings in SPSWs. Current Canadian and American steel design standards require that SPSWs be designed according to the capacity design approach. Capacity design approach requires preselecting a ductile fuse where the seismic energy is dissipated. In the SPSW system, yielding in the infill plate and plastic hinging at the end of the boundary beams are considered ductile fuses. Often, in the structural design of buildings, the lowest commercially available thickness for the infill plate is higher than that required by seismic demand. In this situation, the overstrength of the infill plate increases the demand on the boundary framing members, making the SPSW system expensive. A known

1

solution to reduce the overstrength of the infill plate is using perforated infill plates. In this case, the perforation is usually circular and various forms and configurations of perforations have been suggested in recent years (Purba and Bruneau 2009; Bhowmick et al. 2014). Openings can also provide a place for nonstructural elements such as windows and doors. This is a desirable advantage of the SPSW system, especially from an architectural point of view. While some research has been conducted on SPSWs with circular openings, research on SPSWs with rectangular openings is limited. Also, because of the early buckling of the infill plates under lateral loads, relatively large deformations occur around the openings in SPSWs. The main focus of this study is finding an efficient solution to this problem, and since the considered approach includes using stiffeners, stiffened plates and their design and behaviour are also investigated.

1.2. Motivation

The most common steel plate shear wall type currently designed and used is an unstiffened thin plate wall. With growing interest in SPSW as a reliable system against later loads, it is necessary to direct more attention to the broader range of options the system can provide. The possibility of having openings on the plate is one of the options that is much required but usually overlooked. This is due to the uncertainty of the SPSW system's behaviour when there is an opening and a lack of sufficient studies on the subject. As mentioned before, a major drawback of having a rectangular opening in the infill plate is the deformation around the opening. At the time of this writing, the issue has not been adequately addressed. There is no mention of having rectangular openings in the infill plate in the Canadian steel standard (CSA S16-19). Although AISC seismic provisions for structural steel buildings recognize the possibility of having a rectangular opening in the infill plate, the issue of deformation is not cited in the provision, and the only consideration for openings is to add local boundary elements around the opening (ANSI/AISC 2016). This consideration is very costly and difficult to design and construct. Therefore, developing an efficient method to prevent the deformation of the opening can lead to a more reliable and efficient design of the system. Furthermore, evaluating the effectiveness of such a method in an experimental test will also contribute to the development of the system. Since experimental testing is a very reliable method to study the real-life performance of engineering structures, the results of such an experiment can be used in other studies and also design standards.

1.3. Objectives of the study

The main objective of this research work is to develop an efficient solution to prevent the out-of-plane deformation of openings in SPSWs. Due to the nature of the considered approach, stiffened steel plate shear walls are also investigated in this study. Thus, the key objectives of the present study can be summarized below:

- To evaluate the performance of stiffened steel plate shear walls and study the effects of the number of stiffeners on different parameters such as shear strength and stiffness.
- To develop a rational and efficient method to prevent the out-of-plane deformation of the openings in steel plate shear walls based on the findings of the previous step.
- To evaluate the real-life performance of the developed method by designing and conducting experimental tests and comparing the results of the experimental test to the numerical study.

1.4. The Thesis Layout

The thesis is structured into six chapters as follows:

- Chapter 1 consists of an introduction, motivation, and objectives of the study.
- Chapter 2 presents a comprehensive literature review on various topics, such as analytical models for SPSWs, stiffened steel plate shear walls, perforated steel plate shear walls, and the use of SPSWs with rectangular openings.
- Chapter 3 focuses on "Theoretical and numerical investigation on the design and behaviour of stiffened steel plate shear walls." This chapter explores the effect of the number of stiffeners on the behaviour of stiffened SPSWs using a theoretical method. The accuracy of the theoretical predictions is then validated using numerical models, and design recommendations for stiffened steel plate shear walls are provided.
- Chapter 4 consists of "Numerical analysis of steel plate shear walls with rectangular openings.". This chapter investigates unstiffened SPSWs with rectangular openings through numerical models and identifies some of the associated issues. Different stiffener layouts around the openings are proposed, and their effectiveness in improving the

behaviour of SPSWs with rectangular openings is examined. Based on the results, the best stiffener layout is selected.

- Chapter 5 focuses on the "Experimental and numerical study of stiffened steel plate shear walls with rectangular openings." This chapter evaluates the performance of the proposed stiffener layout around rectangular openings in real life by conducting experimental tests. Seismic performance of stiffened SPSWs using the proposed stiffener layout is also investigated by conducting nonlinear dynamic finite element analysis in this chapter.

- Chapter 6 concludes the thesis with a summary of the research work, highlighting the main contributions and conclusions. Recommendations for future work are also provided in this chapter.

CHAPTER 2
Literature Review

2.1. Introduction

Considering the present research work's objectives, this chapter focuses on two main areas of SPSW. The first subject matter is the topic of stiffened steel plate shear walls which is related to the first and second parts of this study. It has been observed by several numerical and experimental studies that a thin steel infill plate can have significant load-carrying capacity after buckling due to the development of tension fields in the plate (Timler and Kulak 1983; Thorburn et al. 1983; Driver et al. 1998b; Bhowmick 2009; Bhowmick et al. 2010; Bhowmick et al. 2011). Therefore, most of the currently designed SPSWs use a thin infill plate. However, the behaviour of the SPSW system can be improved by preventing the buckling of the infill plate by using stiffeners.

The concept of welding plate stiffeners on one or both sides of the infill plate was first adopted in an experimental study in Japan in 1973. This study has become the foundation for using stiffeners in steel plate shear walls (Takahashi et al. 1973). Different stiffener configurations were considered in this study, and the effectiveness of these configurations in preventing the buckling of the infill plate was examined. In recent years, stiffened SPSWs have been investigated by several different studies. Farahbakhshtooli and Bhowmick (2019) evaluated the seismic performance of stiffened shear walls, and the results showed that the force modification factors that are currently used in seismic design for unstiffened SPSWs could be used for stiffened SPSWs as well. The elastic buckling strength of stiffened plates was also studied in Japan, and a method to estimate the strength was proposed (Ikarashi et al. 2020). Amongst the studies on SPSWs, a few more closely related to this study are selected for review.

The second subject that is required to be studied for this research is openings in SPSWs. A number of studies have shown that having an opening in the infill plate will reduce the shear strength of the infill plate (Vian et al. 2003; Roberts and Sabouri-Ghomi 1992; Bhowmick 2014). Thus, perforations in SPSWs are usually employed as a solution to decrease the overstrength of the infill plate when it is not possible to reduce plate thickness. Circular openings are commonly used for

this purpose. Openings can also be rectangular and be used as a place for windows or doors, but the performance of SPSWs with rectangular openings is not well investigated.

Several important experimental studies have been carried out on SPSW systems (Timler and Kulak 1983; Timler et al. 1998; Driver et al. 1998b; Choi and Park 2009; Lubell et al. 2000). These studies lead to a better understanding of the real-life behaviour and performance of the SPSW system. Since one of the key objectives of the present study is to conduct experimental tests, an emphasis was put on related experimental studies when selecting publications for the literature review.

2.2. Analytical Models for SPSWs

Analytical models are used to design the system and calculate important parameters such shear strength. Analytical models for steel plate shear usually adopt the similarity between SPSWs and plate girders. In this analogy, the columns are similar to flanges of a plate girder, the infill plate is similar to web of a plate girder and the beams are similar to the stiffeners. The first analytical model for steel plate shear walls was proposed by Thorburn et al. (1983) in Canada at university of Alberta. This model was based on earlier researches on plate girder webs by Basler (Basler 1961) and diagonal tension filed action theory by Wagner (Wagner 1931). In this model the plate is allowed to buckle under lateral loads and the post buckling strength of the steel plate due to diagonal tension field action is considered. Therefore, the researchers proposed replacing the plate with a series of inclined tension strips to represent the plate and the model was named *the strip model*. In this model, the proposed strips have equal width and they are pin ended. Fig 2.1 shows a general example of the strip model. The inclination angle, α, here can be calculated using Eq. (2.1).

$$\tan^4\alpha = \left[\frac{1 + \dfrac{Lt_p}{2A_c}}{1 + \dfrac{ht_p}{A_b}} \right] \qquad (2.1)$$

where t_p is the panel thickness, L is the panel width, h is the panel height and A_b and A_c are gross section area of the boundary beams and columns.
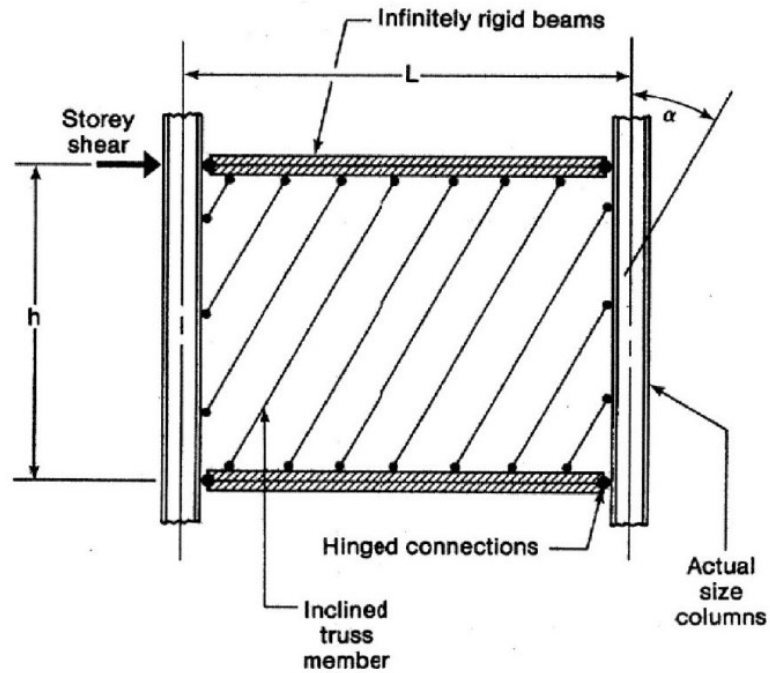
Fig 2.1. A general presentation of the strip model (Thorburn et al. 1983)

By conducting analytical investigations, the researchers also suggested that considering 10 strips for a panel could represent the behaviour of a panel sufficiently.

To validate the proposed model, Kulak conducted an experiment on single storey large scale SPSW specimen with a thin plate (Kulak 1991). The test specimen had a width of 3750 mm and height of 2500 mm. A built-up section similar to W310x29 and another built-up section similar to W460x144 were used for column and beam sections respectively. The plate thickness was 5 mm and it was connected to the frame by using a 6 mm fishplate. The test specimen details can be seen in Fig 2.2. Cyclic loading was applied to the specimen until allowable serviceability drift was reached and then loading was continued until the failure of the structure.

Later, a multi angle strip model was proposed by the researchers at the University of British Columbia (Rezai 1999) which is shown in Fig 2.3. The researchers used a nonlinear analysis software for the proposed strip model and also conducted finite element analysis and compared the results with conducted experimental tests. Their results showed reasonable predictions for the yield and ultimate shear strength by the proposed model and finite element model. However, the elastic stiffness was reported to be overestimated by the models.
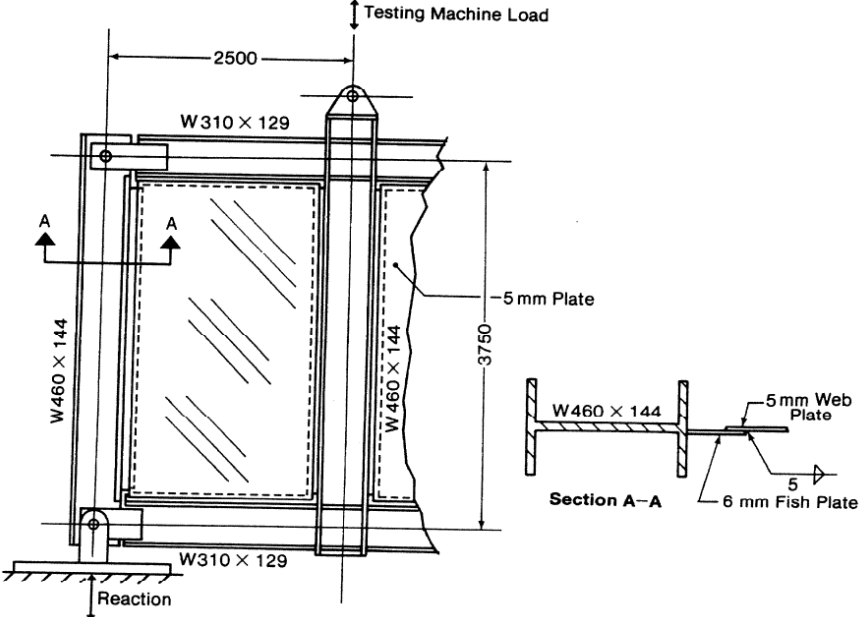
Fig 2.2. Test specimen details (Kulak 1991)
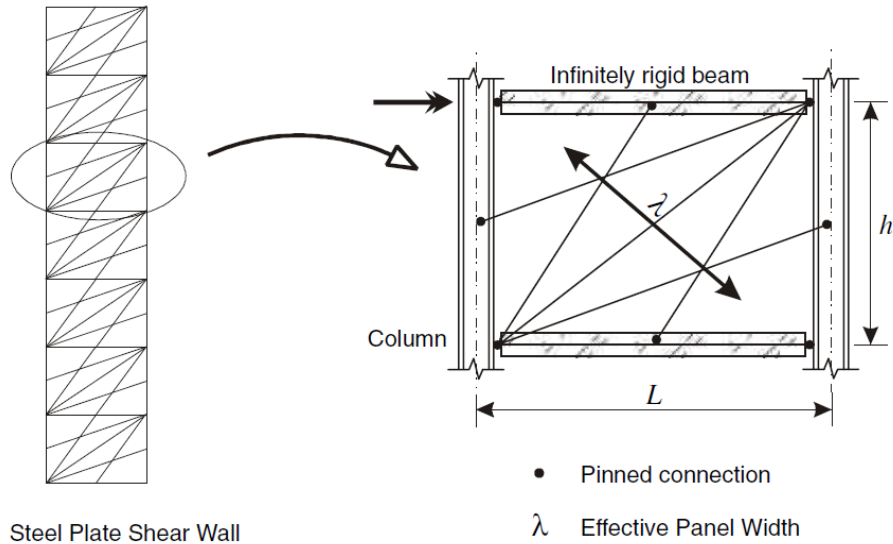
Fig 2.3. multi angle strip model (Rezai, Ventura, and Prion 2004)

The strip model is applicable for analysis of PSPSWs with thin plates; however, there are some limitations when using the model. This model is not appropriate for analysis of SPSWs with thick plates or stiffened plates and there are no methods for SPSWs with openings. Therefore a general analytical model was developed (Sabouri-Ghomi and Roberts 1991; Sabouri-Ghomi, Ventura, and Kharrazi 2005) to overcome these limitations. The proposed model was name *the plate-frame interaction model (PFI)* and the shear buckling stress and tension field stress of the plate as well as the interaction between plate and boundary frame are taken into account in this model.

The state of stress in the web plate are shown in Fig 2.4. The PFI model calculates the shear strength of the web plate is calculated using Eq. (2.2). Where b is web plate width, t is web plate thickness, τ_{cr} is critical shear stress of the plate, σ_{ty} is value of the tension field stress at yielding of the plate and θ is angle of inclination of the tension field.
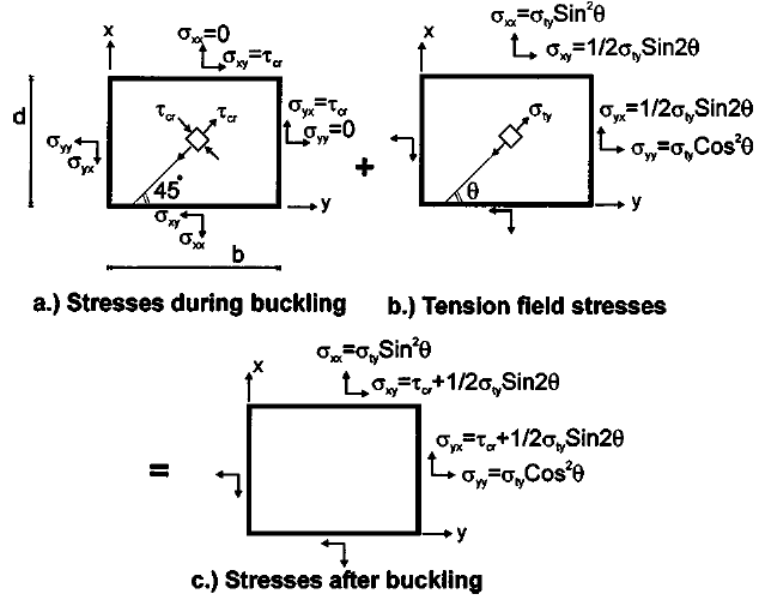
Fig 2.4. The state of stress in the web plate (Sabouri-Ghomi et al. 2005)

$$F_{wu} = bt(\tau_{cr} + 0.5\sigma_{ty}\sin2\theta) \tag{2.2}$$

The elastic shear displacement of the web plate is calculated from Eq. (2.3), where d is the height of the plate and E and G are the elastic and shear modulus of the plate respectively.

$$U_{we} = d\left(\frac{\tau_{cr}}{G} + \frac{2\sigma_{ty}}{E.\sin2\theta}\right) \tag{2.3}$$

By assuming rigid connection for beam to column, the shear strength and the elastic shear displacement of boundary frame can also be calculated using Eq. (2.4) and Eq. (2.5) respectively. In which M_{fp} and I_f are the plastic moment and the moment of inertia of the column.

$$F_{fu} = \frac{4M_{fp}}{d} \qquad\qquad (2.4)$$

$$U_{fe} = \frac{M_{fp}d^2}{6EI_f} \qquad\qquad (2.5)$$

By calculating all of the mentioned parameters the shear load-displacement of the panel can be obtained as displayed in Fig 2.5.

The researchers also compared the results calculated from the PFI model to results from previous experimental tests and concluded the model can predict the backbone curve of the tests reasonably well. Other studies also evaluated the accuracy of the PFI model by comparing the results to experimental and finite elements results. An investigation on low yield point steel plate shear walls by Zirakian (Zirakian and Zhang 2015) studied the effectiveness of this method. The researchers conducted finite element analysis on unstiffened SPSWs with low yield point steel to evaluate their structural performance. The selected plated in this study had moderate and thick plates. They compared the finite element analysis results with values predicted by the PFI method and validated the model predictions for moderate and thick plates.
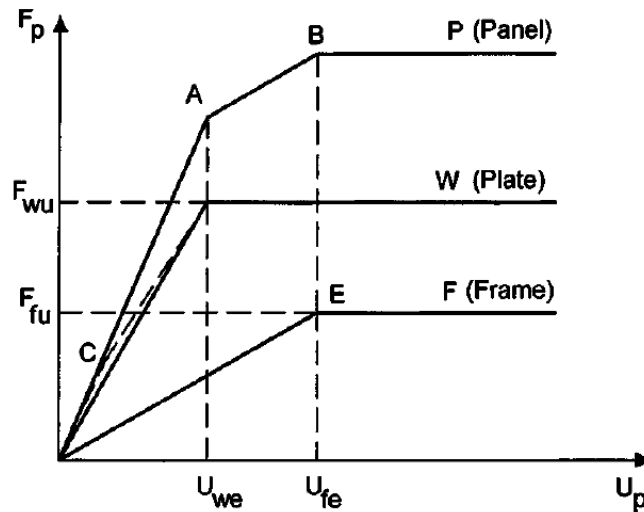
Fig 2.5. Load-displacements of the frame, plate, and panel (Sabouri-Ghomi et al. 2005)

2.3. Stiffened steel plate shear walls

The behaviour of stiffened and unstiffened SPSWs was compared in an experimental study in 2012 by Sabouri-Ghomi and Sajjadi (Sabouri-Ghomi and Sajjadi 2012). In this study, the main objective was to observe the effect of stiffeners on the system. For this purpose, three one-third scale specimen were designed, two of them being stiffened and unstiffened steel plate shear walls and the last one being only the surrounding frame without the infill plate. The stiffened specimen was named "DS-SPSW-0%" and the unstiffened specimen was named "DS-PSW". The dimensions and specifications of DS-SPSW-0% and DS-PSW specimens and their boundary frame are shown in Fig 2.6 and Fig 2.7, respectively. Low strength steel was selected for the infill plate material and high strength steel for the surrounding frame. In order to make sure that the stiffeners were strong enough to prevent the buckling of the plate, they were designed and selected by conducting finite element analysis.

Following ATC-24 (ATC-24 1992) provision, lateral load was applied on both sides of the top beam and the story shear displacement and shear load were recorded for each of the specimens. For both stiffened and unstiffened specimens the first significant yielding was reported at the sixth cycle of loading with drift of 0.16% and 0.18% in DS-SPSW-0% and DS-PSW specimens

12

receptively. Maximum drift of 6.44% and 5.34% was also observed for DS-SPSW-0% and DS-PSW specimens receptively.
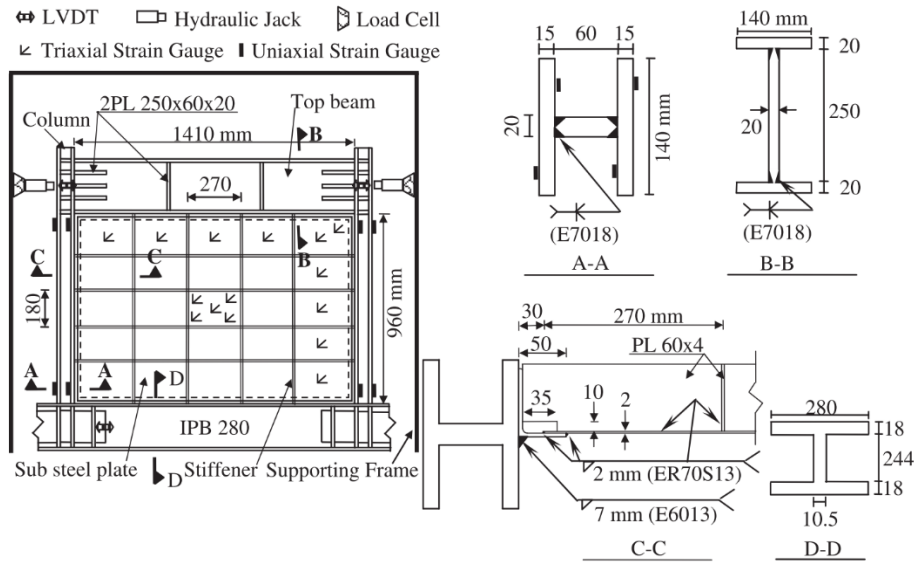
Fig 2.6. DS-SPSW-0% specimen specifications (Sabouri-Ghomi and Sajjadi 2012)
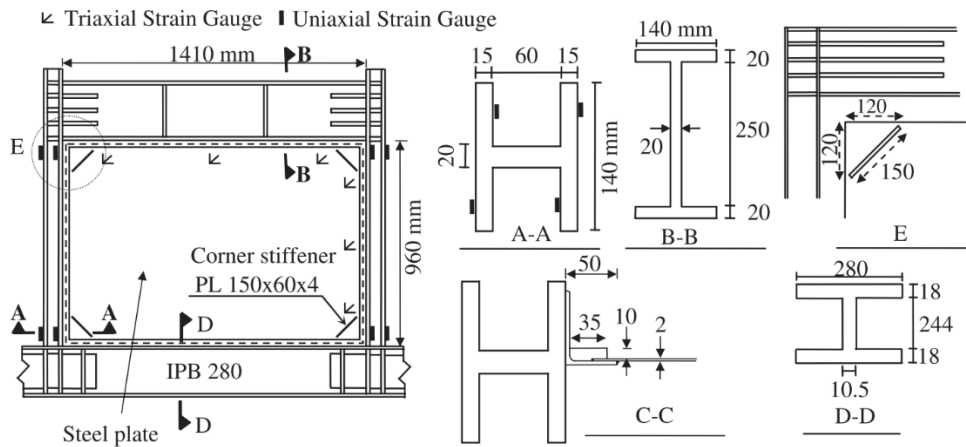
Fig 2.7. DS-SPSW specimen specifications (Sabouri-Ghomi and Sajjadi 2012)

Fig 2.8 shows both stiffened and unstiffened specimens at their maximum drifts at the end of cyclic loading. The reported hysteresis curves for the two specimen are also shown in Fig 2.9.

13

The results of this study showed the stiffened specimen had a significantly more stiffness and energy dissipation capacity in comparison to the unstiffened plate. The increase of shear strength was reported to be minor. As it is observed in Fig 2.9, installing stiffeners on the thin plate also reformed the shape of the hysteresis curves, leading to larger area under the curves hysteresis for stiffened plate. The increase of stiffness when using stiffened plate was reported around 51.1% and the increase of energy dissipation capacity around 25.4%.
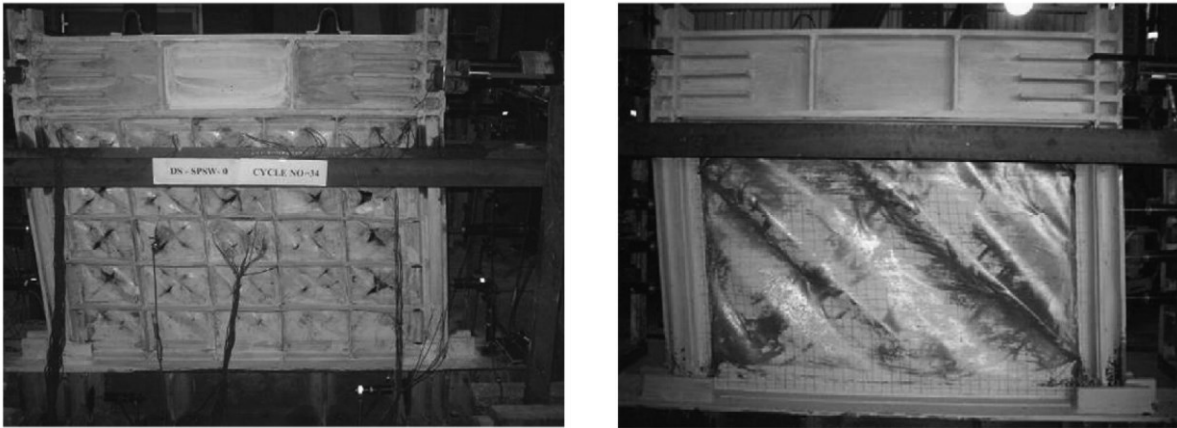
Fig 2.8. Stiffened specimen "DS-SPSW-0%" (Right) and unstiffened specimen "DS-SPSW" (Left) at maximum drift at the end of the cyclic loading (Sabouri-Ghomi and Sajjadi 2012)
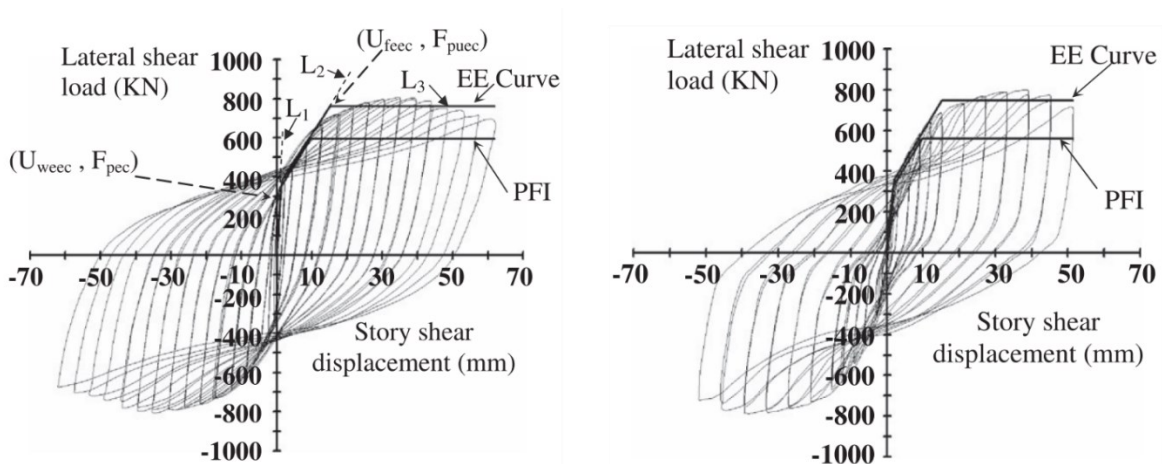
Fig 2.9. Hysteresis curves for stiffened specimen "DS-SPSW-0%" (Right) and unstiffened specimen "DS-SPSW" (Left) (Sabouri-Ghomi and Sajjadi 2012)

14

The experimental study that was reviewed is a key study that demonstrates the advantageous of installing stiffeners on the infill plate. However the authors used finite element modeling to make sure that the selected size of stiffeners was sufficient to prevent the buckling of the thin plate. Although it is possible to use finite element analysis for research purposes, it is not a rational approach when it comes to the practical design of the system. In order for structural engineers to be able to design stiffened steel plate shear walls an established design method for the system is required.

A stiffened steel plate shear wall is usually constructed by installing vertical and horizontal plate stiffeners on the infill plate. The stiffeners divide the shear panel into rectangular sub-panels. Generally, there are two possible buckling modes that can occur in a stiffened plate. If the stiffeners are not strong enough, the plate will buckle under lateral load, similar to an unstiffened steel plate. This is called global buckling mode and the purpose of properly designed stiffeners is to prevent this buckling mode in SPSW. The second buckling mode is local bucking mode which occurs when buckling takes place in the sub-panels of the stiffened plate and therefore global buckling of the plate is prevented. The two buckling modes are shown in Fig 2.10.
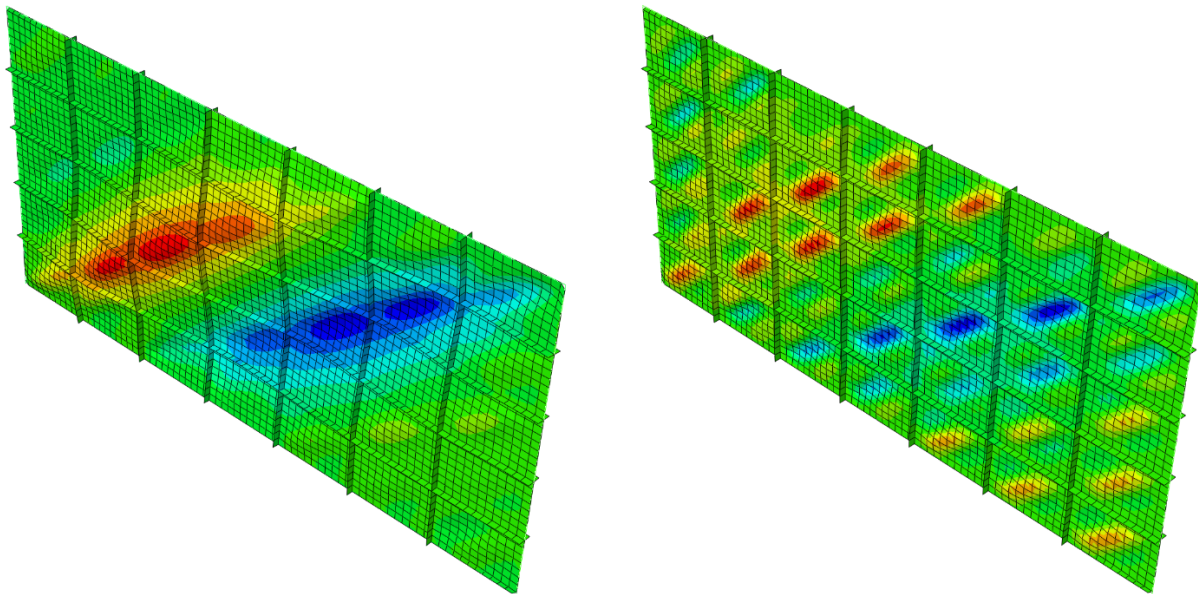
Fig 2.10. Two buckling modes of a stiffened plate: Global Buckling (left) and Local Buckling (Right)

A theoretical study that was carried out by Sabouri-Ghomi proposed a design criterion for stiffeners to improve the buckling behaviour of the stiffened SPSWs (Sabouri-Ghomi et al. 2008). The main concept that was considered in this study was that in order to force the plate into local buckling, the following equation is required to be satisfied:

$$\tau_{crg} > \tau_{crl} \tag{2.6}$$

Where τ_{crg} is the critical shear buckling stress for global buckling mode and τ_{crl} is the critical shear buckling stress for local buckling mode. In this study both equations for τ_{crg} and τ_{crl} were obtained from previous studies (Sayed-Ahmed 2001; Timoshenko and Gere 1961) and placed in Eq. (2.6). The result was the following criteria:

$$\left(\frac{I_y}{S_y} + \frac{t^3}{12(1 - \upsilon^2)}\right)^{0.25} \left(\frac{I_x}{S_x} + \frac{t^3}{12(1 - \upsilon^2)}\right)^{0.75} > 0.0916 \frac{t^3}{S_x^2}\left(\frac{k_l}{k_g}\right)d^2 \tag{2.7}$$

In this equation, I_x and I_y are moment of inertia of vertical and horizontal stiffeners, respectively; S_x and S_y are spacing between vertical and horizontal stiffeners, respectively, as it is shown in Fig 2.11. t is the infill plate thickness; υ is Poisson ratio and d is the infill plate height; k_g is the global shear buckling coefficient.

The value for k_g is 3.64 or 6.9 depending on the boundary connection of the plate. k_l is the local shear buckling coefficient and can be calculated from the two following equations:

$$k_l = 4 + 5.35\left(\frac{S_x}{S_y}\right)^2 \text{ for } \frac{S_y}{S_x} \leq 1 \tag{2.8}$$

$$k_l = 5.35 + 4\left(\frac{S_x}{S_y}\right)^2 \text{ for } \frac{S_y}{S_x} \geq 1 \tag{2.9}$$

For spacing between the vertical stiffeners equal to the spacing between the horizontal stiffeners, the following simplified equation was suggested:

$$I > 0.0916\left(\frac{d^2}{S}\left(\frac{k_l}{k_g}\right) - S\right)t^3 \tag{2.10}$$
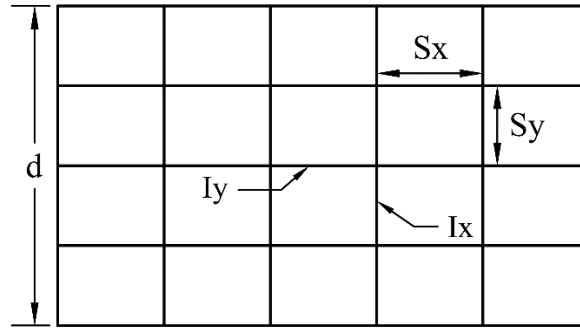
Fig 2.11. Stiffened infill plate

Finite element analyses was also conducted for this research and the proposed design criteria was evaluated by comparing FE analyses result to results of a previous experimental study (Takahashi et al. 1973). The outcomes showed that double sided stiffeners behaved better that one-sided stiffeners and also it was stated that the proposed design criteria performed better in cases that the stiffeners were more closely spaced.

2.4. Perforated steel plate shear walls

A series of quasi-static tests under cyclic loading on unstiffened SPSWs having a centrally placed circular opening was the first research on the topic of perforated SPSWs (Roberts and Sabouri-Ghomi 1992). A total number of sixteen specimens with different panel and opening sizes were tested and hysteresis loops were acquired for each specimen. Two different aspect ratios for the panels were selected and the plate thicknesses were 0.83 mm and 1.23 mm. The range of the

circular opening size for specimens was from 0 to 150 mm. The results showed that having an opening on the infill plate will result in strength and stiffness reduction in the system. According to the results, an approximate equation to calculate the shear strength and stiffness of an unstiffened panel with a centrally placed circular opening was suggested.

$$V_{op} = V_p \left(1 - \frac{D}{b}\right) \qquad (2.11)$$

In this equation, V_{op} is the strength of a perforated panel and V_p is the strength of the same panel without opening, D is the circular opening diameter and b is the panel width. Shear strength and stiffness degradation of test specimens as the opening size increases can be seen in Fig 2.12.
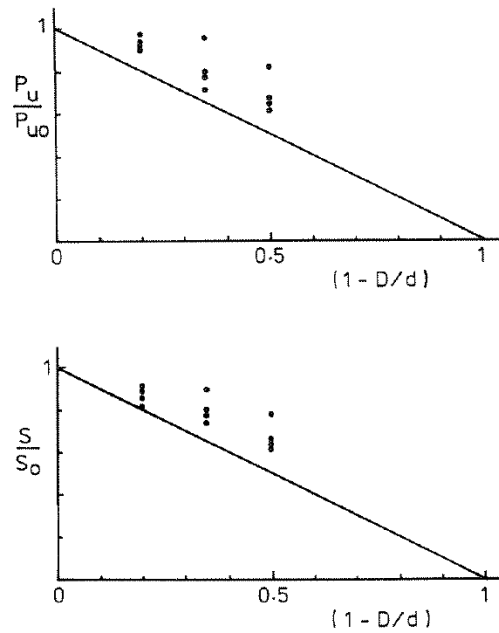
Fig 2.12. Shear strength and stiffness degradation of test specimens (Roberts and Sabouri-Ghomi 1992)

Adequate ductility and stable hysteresis loops with incensing energy dissipation capacity per cycle was also reported for all of the tested panels.

18

The effects of openings on SPSWs and validity of Eq. (2.11) was investigated later by a number of other studies. A series of finite element analyses on unstiffened SPSWs with centrally placed circular openings by Bhowmick in 2014 confirmed the validity of Eq. (2.11) (Bhowmick 2014). Three different aspect ratios for the plate were considered and for all of them, nine different perforation sizes were modeled. Fig 2.13 shows an example of one the finite element models. The results of this study showed that using perforated SPSWs will results in reduction of the strength demand on the boundary columns of system. A slight increase was also observed in the fundamental period of perforated panels; however, the amount of this increase was reported to be negligible when the opening size is small.
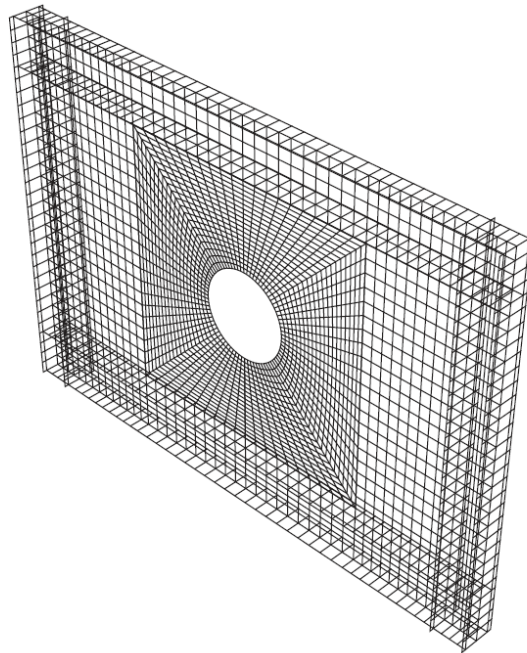
Fig 2.13. FE model and mesh with aspect ratio of 1.5 (Bhowmick 2014)

An experimental test was carried out on specially perforated SPSWs by Vian (Vian et al. 2009). In this experiment, two different approaches for plate perforations were studied. The first one placed two reinforced quarter cycle perforations at the two top corners of the plate. The second one introduced a series of regularly spaced circular perforations to the plate. The goal of these perforations was to allow utilities to pass through the plate. In addition, the second method also had the purpose of reducing the overstrength of the plate. The specimens had width of 4000 mm

and height of 2000 mm and low yield point steel with 2.6 mm thickness was used for the plate. W18X65 and W18X71 were selected as the beam and column sections respectively.

Quasi-static cyclic loading with displacement control was applied to the specimens. The two test specimens before and after the experiment can be seen in Fig 2.14. The two specimens experienced a minimum drift of three percent and ductile behaviour was reported for both. The shear strength and elastic stiffness for the perforated specimens was observed to be 15% lower than a similar solid plate.
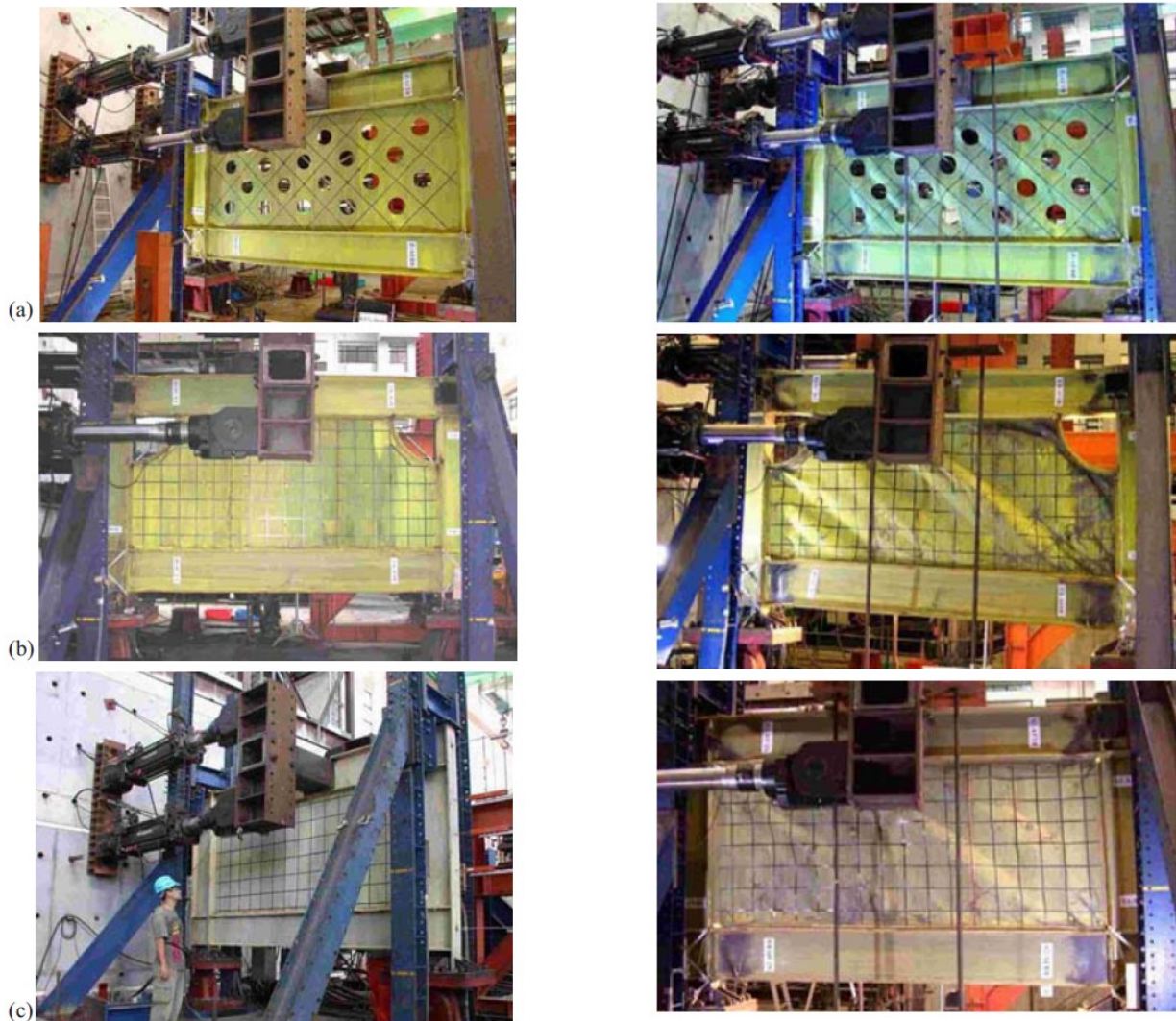
Fig 2.14. The two test specimens before (left) and after (right) the experiment (Vian et al. 2009)

The researchers also investigated finite element approach for the two proposed models (Vian et. al 2009). Full scale models and also simpler strip models were studied. The simple model only considered a quarter of strip of perforations on the plate. The two models are shown in Fig 2.15. Cyclic and monotonic quasi-static loading was conducted for the models. The results showed good agreement between the FE results and experiment results. The simple strip model was also reported to be cable of reasonably predicting the strength and displacement of initial yielding.
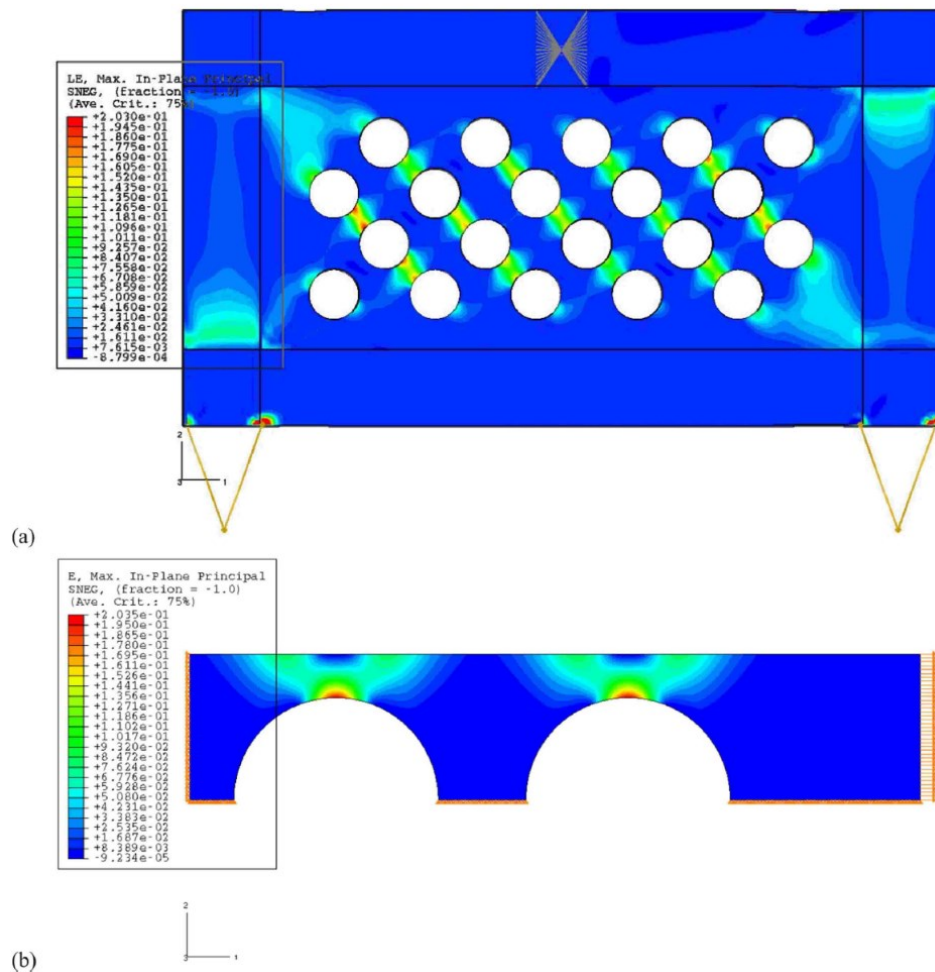
Fig 2.15. The FE results for the full panel and strip model (Vian et al. 2009)

Another study by Afshari and Gholhaki inasigated the effect of the loaction of the openings on unstiffened SPWSs behaviour (Afshari and Gholhaki 2018). Finite element analysis was carried out on models with openings on different locations on the infill plate. Fig 2.16 shows the details of the models and selected opening locations. The outcome showed that when the opening is not placed at the center of the plate, using Eq. (2.11) to calculate the shear strength of the panel will lead to conservative results. A more accurate equation that considered the place of the opening on the plate was suggested by the authors of the study.
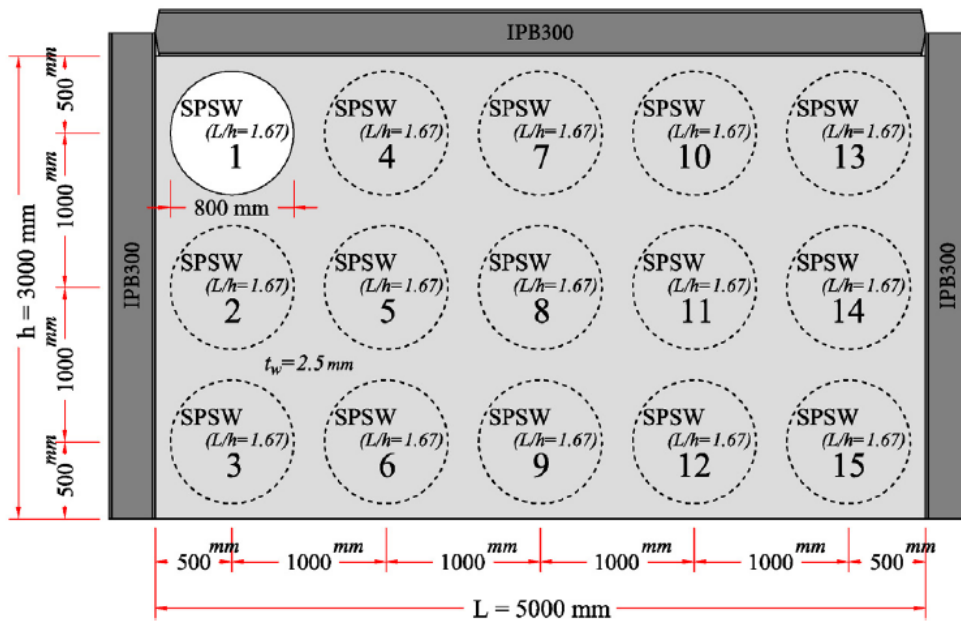
Fig 2.16. Details of the models and selected opening locations (Afshari and Gholhaki 2018)

2.5. Stiffened SPSWs with rectangular openings

One of the few studies on rectangular openings is an experimental investigation that was conducted on stiffened panels with two rectangular openings (Sabouri-Ghomi and Mamazizi 2015). Three one-third scale single-story specimens with two rectangular openings were studied. Two same size symmetrical openings were considered for all of the models and the specification of all three specimens were the same expect for the distance between the two openings that varied between the models. The specimens were named "SSW2O1", "SSW2O2" and "SSW2O3" and the

22

details for the models as well as the boundary fame and connections is shown in Fig 2.17. A fourth similar specimen without openings was also constructed for comparison purposes.

Stiffeners were installed on all of the specimens and to ensure the occurrence of local buckling mode on the plate, the stiffeners were designed according to Eq. (2.7). A box frame was applied around the openings in order to prevent large deformation and increase the stiffness against tention field action of the plate.
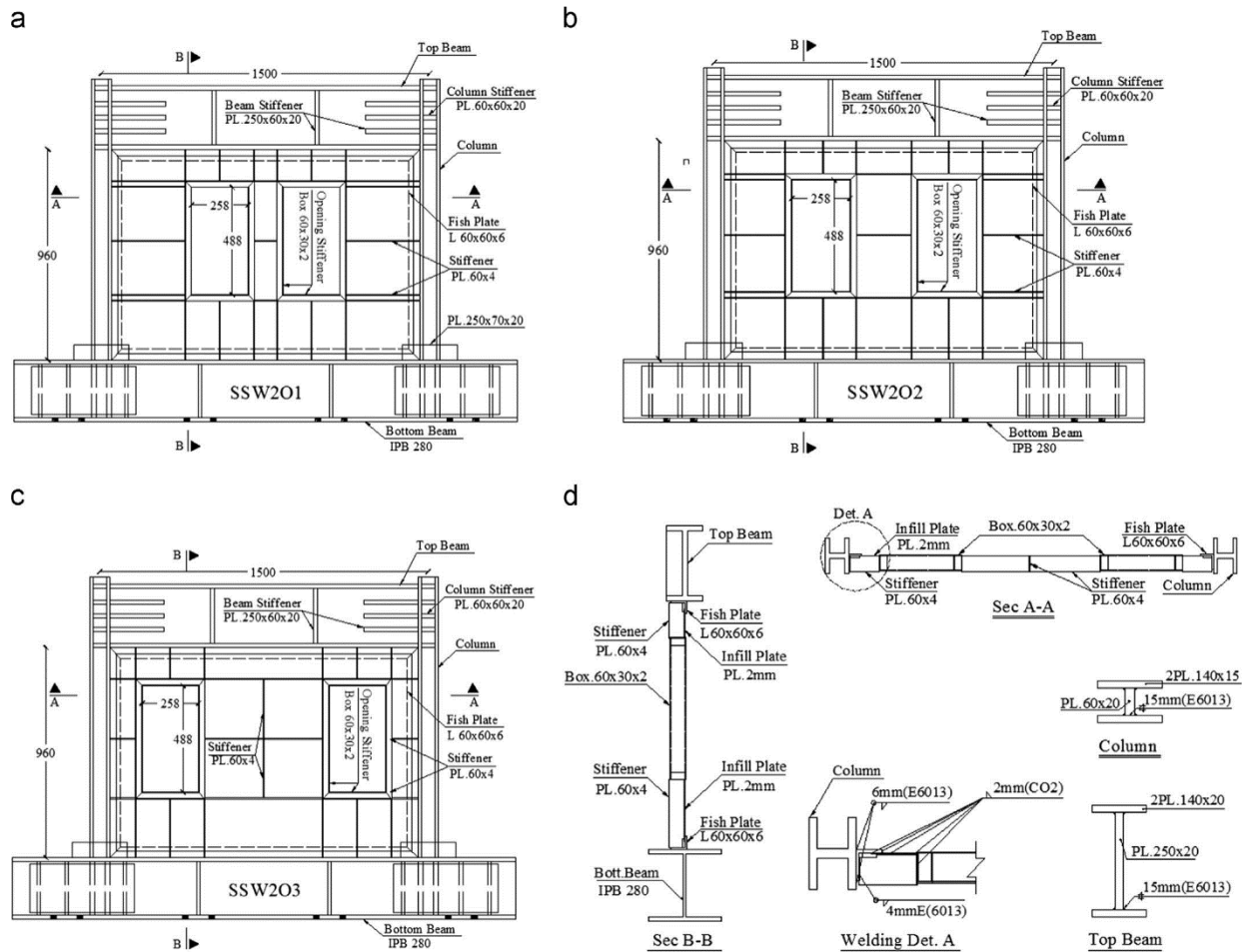
Fig 2.17. Details and specification for the three specimens. (a) SSW2O1, (b) SSW2O2, (c) SSW2O3 and (d) boundary frame and welding (Sabouri-Ghomi and Mamazizi 2015)

For all the test specimens, cyclic loading was applied horizontally at the top beam using ATC-24 protocol. The maximum drift of 5.2% and strength of 521 kN was reported for SSW2O1 at the end of the experiment. For SSW2O2, maximum drift of 6.3% and strength of 545 kN was

reported and for SSW2O3 maximum drift and strength were reported 4.8% and 573 kN respectively. Fig 2.18 shows the deformed shape of the three specimens during the experiment. Hysteresis curves were also acquired from the results of tests to calculate different parameters such as energy dissipation capacity and compare these values between the models. The hysteresis loops are shown in Fig 2.19.

Fig 2.18. Deformed shapes of SSW2O1 (left), SSW2O2 (middle) and SSW2O3 (right) during the tests (Sabouri-Ghomi and Mamazizi 2015)
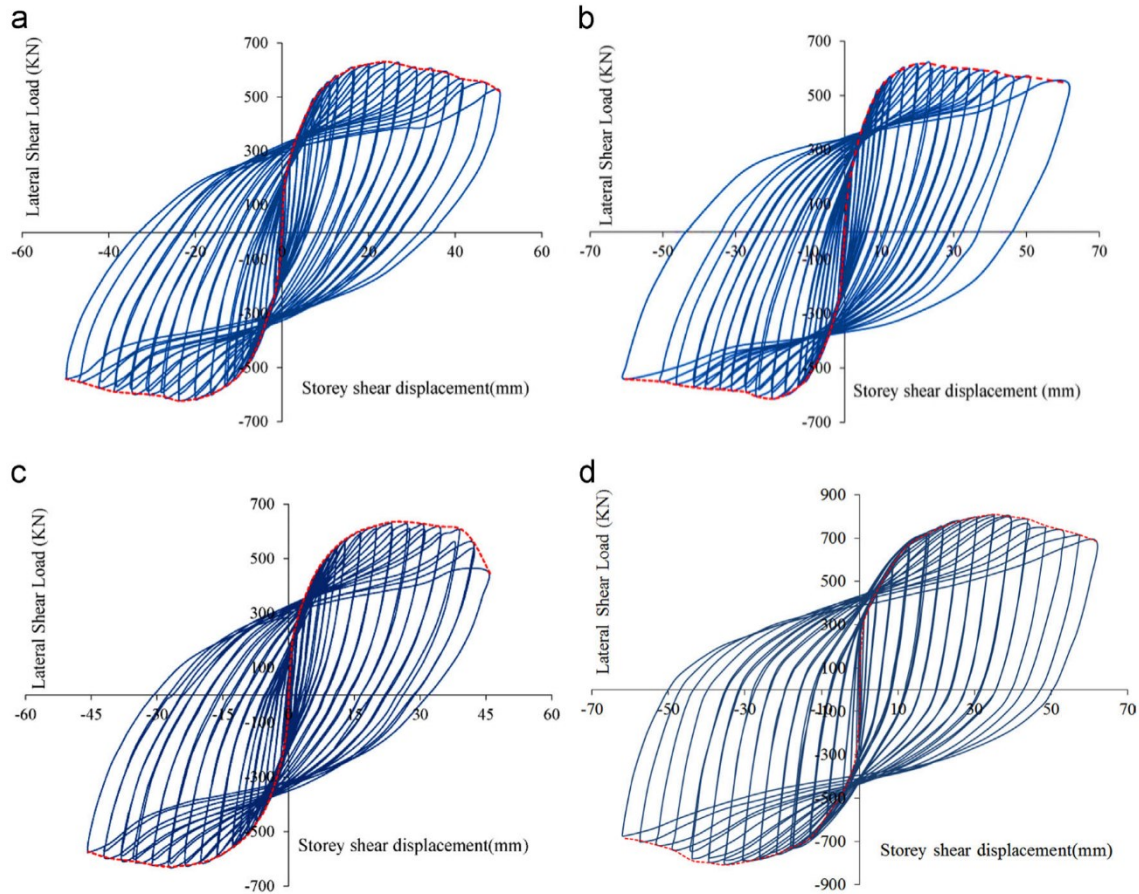
Fig 2.19. Hysteresis curves of specimens (a) SSW2O1, (b) SSW2O2, (c) SSW2O3, and (d) the panel without openings (Sabouri-Ghomi and Mamazizi 2015)

The outcomes of this experimental investigation showed that the ultimate shear strength and stiffness were very close for all panels. Energy dissipation capacity was also similar for the three specimens and most of the energy dissipation happened at the subpanels that were located between the two openings and at the lateral subpanels. It was reported that the presence of openings reduced the ultimate shear strength by 22% and initial stiffness was reduced by 36%.

At the end of the experiments, the connection of the surrounding boxes around the openings was observed to be cracked and ruptured. The deformation of the stiffeners around the corners of the openings was reported to be more than the deformation of those attached to the middle parts of the openings. The stiffeners were also found to be more effective to prevent the deformation than the boxes attached around the openings.

In 2012, a numerical study conducted on stiffened and unstiffened SPSWs investigated the effects the of a arbitrarily-located rectangular opening on the strength and stiffness of the system (Sabouri-Ghomi et al. 2012). A large number of finite element models were considered for both stiffened and unstiffened models in this study. All models had a single rectangular opening and the location and the size of the opening varied between the models. Opening ratios of 21%, 28%, 36%, 45% and 60% were selected for the models. For each of the ratios, the opening was positioned in nine different locations that are shown in Fig 2.20.
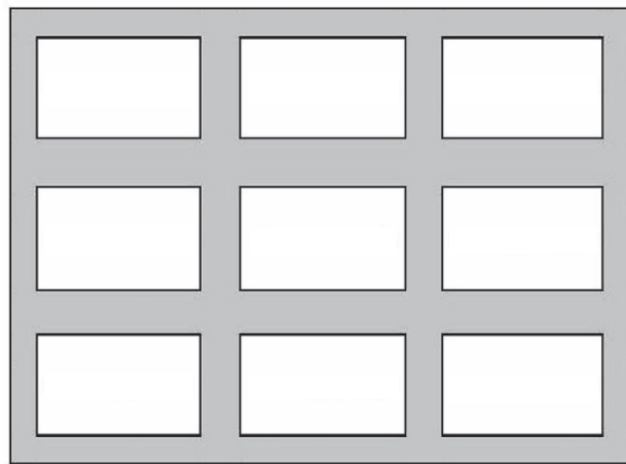
Fig 2.20. The investigated locations for the single opening (Sabouri-Ghomi et al. 2012)

Finite element analysis was carried out for the models and shear force versus lateral displacement curve was drawn for each model. As an example, Fig 2.21 shows the deformed shapes of three stiffened and three unstiffened models with opening ratio of 36% after analysis.
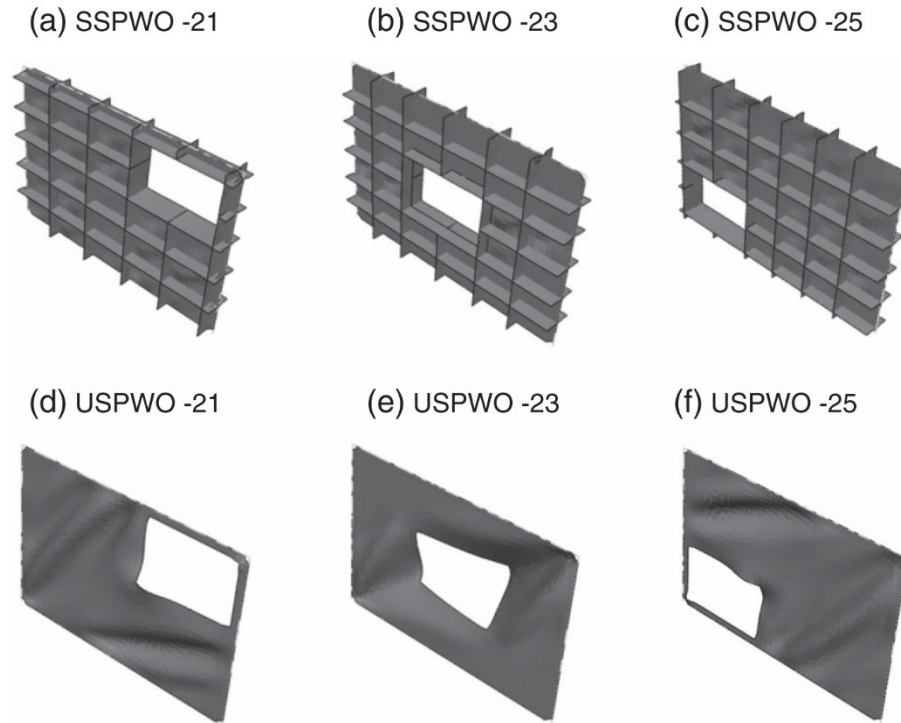
Fig 2.21. The deformed shapes of models with opening ratio of 36% after analysis (Sabouri-Ghomi et al. 2012)

The results showed that the location of the opening in unstiffened plate affected the amount of the reduction of shear strength and stiffness of the panel. The reason for this was stated to be the interference of the opening with the plate buckling and formation of tension fielded in thin unstiffened plates. The application of Eq. (2.11) in calculating the strength of unstiffened perforated SPSWs was confirmed by this study. However, unlike unstiffened plates, the location of the opening was found to have no effect on the amount of the reduction of shear strength and stiffness for stiffened panels. Therefore, it was suggested that for the design of stiffened SPSWs the location of the opening can be ignored. It was also proposed that for more accurate design of stiffened plates with a rectangular opening, the parameter D in Eq. (2.11), which is the diameter of the equivalent circular opening, can be replaced by the width of the rectangular opening.

2.6. Design requirements for openings in SPSWs

Circular perforations are allowed in seismic provisions for structural steel buildings as a mean to reduce the overstrength of the infill plate (ANSI/AISC 2016). The only consideration in regards to rectangular openings is that they should be bounded by intermediate boundary elements on all sides and these elements should extended the full height and width of the panel as it is shown in Fig 2.22. These elements are named local boundary elements (LBEs) and AISC Design Guide 20 has provided some insight and a design example for the elements (Bruneau and Sabelli 2006). It is recognized by Design Guide 20 that in many cases openings must be provided in SPSWs; however, the only reason stated for the requirement of LBEs is "to anchor the web plate tension". Use of unreinforced openings are also allowed in AISC 2016 if it has been justified by performing tests. The only research that is mentioned for the requirement of LBEs is an experimental study on unstiffened panels with a series of circular perforations (Vian et al. 2003). The tested specimen is shown in Fig 2.23 and as it is observed, there are no similarities between the tested specimen and the panel shown in Fig 2.22 beyond the fact that both panels are perforated. Although the tested specimen can provide some general understating of the behaviour of perforated SPSWs, it is not possible to fully understand the behaviour of plates with rectangular openings and justify the use LBEs solely base on this experiment. It is also recognized by Design Guide 20 that the design process for LBEs can be complicated.
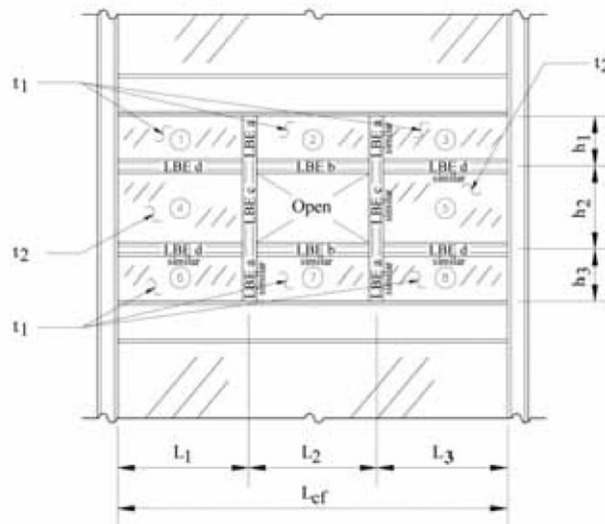
Fig 2.22. SPSW with a rectangular opening and LBEs (Bruneau and Sabelli 2006)
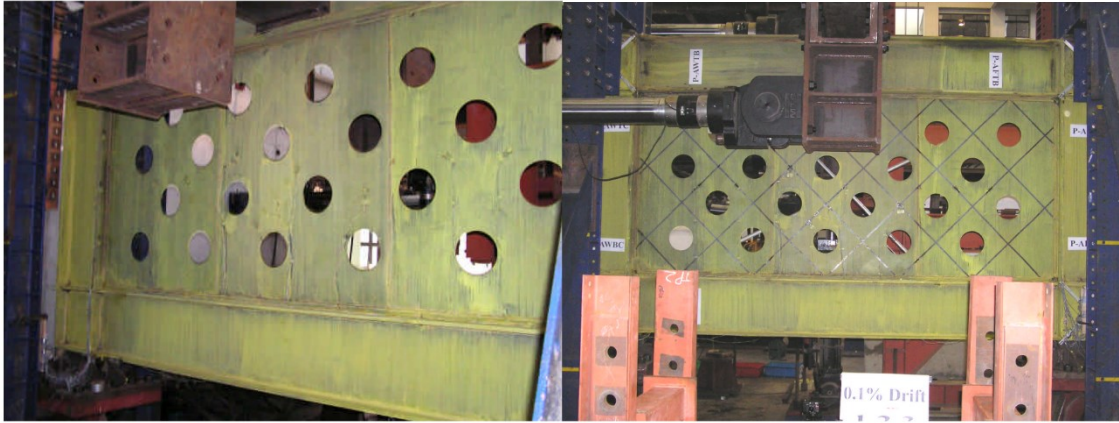
Fig 2.23. The tested specimen by Vian and Bruneau (Vian et al. 2003)

A research study on 2012 by Hosseinzadeh and Tehranizadeh investigated large rectangular openings in SPSWs and the AISC design requirements for them (Hosseinzadeh and Tehranizadeh 2012). A series of single and multi-storey SPSW finite element models were considered for the study. Rectangular openings with different aspect ratios and locations were selected and local boundary elements were designed for the openings according to Design Guide 20. Models without openings were also created for comparison purposes. The deformed shapes and mises stress distribution of three sample models after analysis are shown in Fig 2.24.
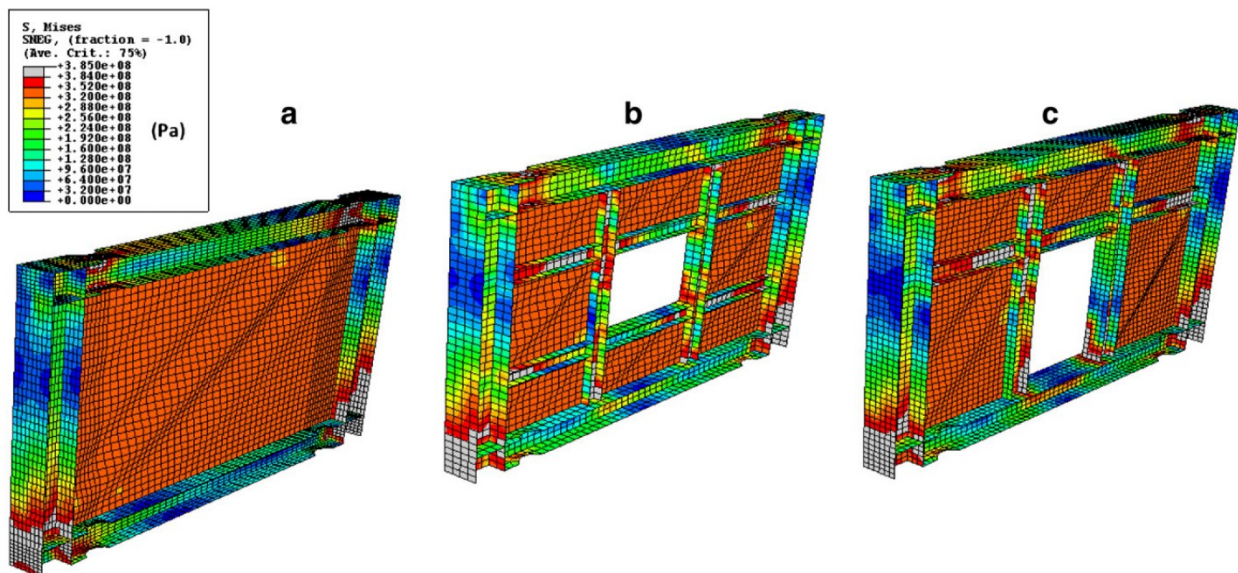
Fig 2.24. Deformed shapes and mises stress distribution of three single-storey models after analysis (Hosseinzadeh and Tehranizadeh 2012)

The results showed that the location or the type of the opening does not affect the strength of the panel but the size of LBEs have a minor effect on the panel strength. Another finding of this study was that since AISC Design Guide 20 does not consider the additional forces imposed on the boundary frame by LBEs, using this procedure may not lead to proper design of the system.

2.7. Use of SPSWs with rectangular openings

As mentioned before, rectangular opening is a feature that is regularly required. Two real world examples of using this feature are reviewed here. The first one is the Sylmar hospital located in Los Angeles, California. The six-storey hospital is a replacement of Olive View hospital which was demolished due to partial collapse during 1971 San Fernando earthquake. The Sylmar hospital uses steel plate shear walls as the lateral load resisting system. In this building, the panels have 7620 mm width and 4724.4 mm height. Two thicknesses are used for the plates which are 15.88 mm and 19.05 mm. Two rectangular openings are placed on the plate as a place for windows. The plates are stiffened somewhat similar to the recommendation by Design Guide 20. This can be seen in Fig 2.25.
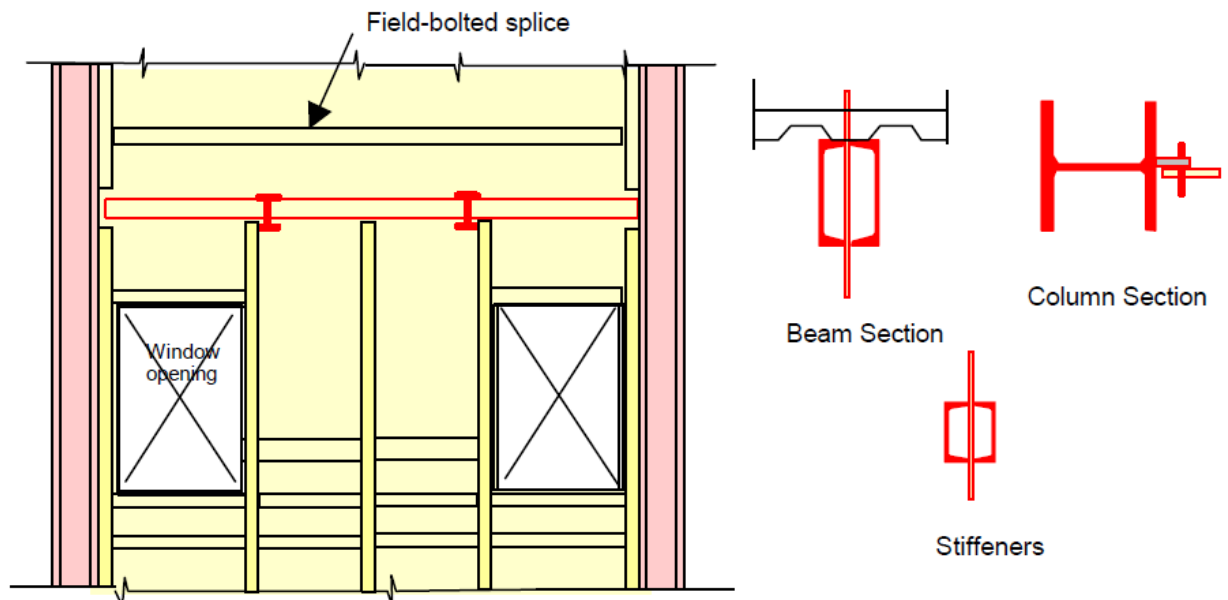
Fig 2.25. Schematics for SPSW system used in Sylmar hospital (Astaneh-Asl 2001)

30

Double channel box sections were welded to the plate as stiffeners to improve the buckling behaviour of the system. Although the designers (Troy 1988) recognized the effect of tension field action on the system, this capacity was not considered in the design of the system. This hospital experienced two ground motions from the 1987 Whittier and the 1994 Northridge earthquakes. Astaneh Asl (Astaneh-Asl 2001) visited this building after the 1994 Northridge earthquake and reported "severe damage to some non-structural elements" of the building. He concluded that these damages were due to the high stiffness of the building.

The second example is a 35-storey building located in Kobe, Japan. This office building is a very important case, because it experienced the well-known 1995 Kobe earthquake, 7 years after the construction was completed. The structure has a dual lateral load resisting system consisting of steel plate shear walls and moment resisting frames. As it can be seen in Fig 2.26, SPSWs in this building have a rectangular opening. A large number of stiffeners are used on the plate that divides the plate into many small subpanels.

Fig 2.26. Damages to 26th floor SPSWs (Fujitani et al. 1996)

Astaneh Asl (Astaneh-Asl 2001) visited this building after the earthquake and reported "no visible damage". Minor damages including local buckling on the SPSWs of the 26th floor of the building was reported by other studies (Fujitani et al. 1996).

2.8. Summary and Conclusions

Some of the key research publications closely related to the objectives of the present research work were reviewed in this chapter. Some of the advantages of using stiffeners were demonstrated thorough these studied. The effects of perforations on SPSWs was also studied in this chapter. The general behaviour of rectangular openings in both stiffened and unstiffened SPSWs was examined. The lack of proper considerations based on dedicated research on the topic of rectangular openings was discussed. Practical use of such system in real world was reviewed and through examples it was shown this system can be very effective against lateral loads. However, this research aims to prove it is possible to design such system more efficiently without using heavily reinforced plates.

CHAPTER 3

Analytical and numerical investigation of stiffened steel plate shear walls[1]

3.1. Abstract

Steel plate shear wall (SPSW) is often required to prevent early buckling of the steel infill plate. This is done by adding horizontal and vertical stiffeners to the infill plate. This paper investigates the effects of stiffeners on SPSWs based on a well-established plate-frame interaction (PFI) analytical model. It is observed from the analytical investigation that stiffeners can increase the shear strength of the infill plate by 15% and the elastic stiffness by 53%. The ability of the PFI method in predicting the behaviour of stiffened SPSWs is also evaluated numerically. A series of SPSW models with a different number of horizontal and vertical stiffeners are analyzed, and their buckling behaviour is studied. A close agreement between the PFI method and the finite element analysis is observed. In addition, a recently proposed design criterion for selecting the size of stiffeners to prevent the global buckling of the infill plate is evaluated. Finally, an improved stiffness criterion for designing stiffeners in stiffened SPSWs is proposed. FE analysis shows that the proposed stiffness criterion is effective in preventing the global buckling of the stiffened infill plates in SPSWs.

Keywords: Steel plate shear wall; Stiffeners; Buckling; Finite element analysis; Pushover analysis.

3.2. Introduction

Steel plate shear walls (SPSWs) are used in buildings as an effective lateral load-resisting system to resist wind and earthquake loads. SPSW system has been shown to have high strength and ductility. Many analytical as well as experimental studies (Berman and Bruneau 2003; Bhowmick, et al. 2009; Choi and Park 2009; Driver et al. 1998; Thorburn et al. 1983; Timler and Kulak 1983) have been conducted on the behaviour of unstiffened SPSW systems. Also, different methods have been proposed for the analysis and design of SPSWs. The most common method for analysing unstiffened SPSWs is the strip model, which was proposed in 1983 by Thorburn et al. (Thorburn et al. 1983). This model simulates the behaviour of the tension field, which is developed once the infill plate buckles, with a series of tension-only strips oriented along the tension field. Using the least work principles, Timler and Kulak (Timler and Kulak 1983) derived an expression to predict the angle of inclination of the tension strips. The current edition of AISC 341-16 (AISC 2016) and CSA S16-19 (CSA, 2019) have both adopted the strip model for analysing unstiffened SPSWs. The strip model was used by Kaveh and Farhadmanesh (Kaveh and Farhadmanesh 2019) to optimize the seismic design of SPSWs by minimizing the weight of the structure. In most unstiffened SPSWs, the infill plate is thin enough and buckles at a relatively small lateral load. To improve the behaviour of the system, horizontal and vertical stiffeners can be attached to the infill plate. The first research on steel plate shear walls with stiffeners was conducted in Japan (Takahashi et al. 1973). Different stiffener configurations were considered in that study and the effectiveness of these configurations in preventing the buckling of the infill plate was studied. Stiffened infill plate has been found to increase the stiffness and energy dissipation capacity of the SPSW system. Sabouri-Ghomi and Sajjadi (Sabouri-Ghomi and Sajjadi 2012) conducted an experimental study to investigate the behaviour of stiffened and unstiffened steel plate shear walls. Their results showed around a 51% increase in stiffness and a 26% increase in energy absorption capacity when using stiffened steel plates. Guo et al. (Guo, Hao, and Liu 2015) studied the effects of cross and diagonal types of stiffeners by conducting an experimental investigation. Their results showed using stiffeners prevented the out-of-plane deformation of the plate effectively. The yield strength in models with cross stiffeners was observed to increase by 20 % and 25% in models with

34

diagonal stiffeners. Sabouri-Ghomi et al. (Sabouri-Ghomi et al. 2012) also studied the behaviour of stiffened and unstiffened steel plate shear walls with openings. Their numerical study showed that in unstiffened plates, the location of the opening affected the reduction in the shear strength of the infill plate. On the other hand, the location of the opening did not affect the shear strength reduction of the infill plate. Farahbakhshtooli and Bhowmick (Farahbakhshtooli and Bhowmick 2019) evaluated the seismic performance of stiffened shear walls. It was observed that the force modification factors currently used in seismic design for unstiffened SPSWs can also be used for stiffened SPSWs. The elastic buckling strength of stiffened plates was recently studied in Japan and a method to estimate the strength was proposed (Ikarashi et al. 2020).

Another well-known design method for SPSWs is the plate-frame interaction (PFI) method (Sabouri-Ghomi and Roberts 1991; Sabouri-Ghomi, Ventura, and Kharrazi 2005). The PFI method is capable of analyzing thin or thick steel plates and also plates with openings. This method considers the shear buckling stress and tension field stress of the plate as well as the interaction between the plate and boundary frame. The ability of this method to closely predict the behaviour of SPSWs has been demonstrated with numerical and experimental studies (Sabouri-Ghomi and Sajjadi 2012; Zirakian and Zhang 2015). Recently, Mamazizi et al. (Mamazizi et al. 2022) proposed a modified PFI method to evaluate the behaviour of SPSWs with beam-connected infill plates. To the best of the authors' knowledge, no research is currently available on the PFI method for the evaluation of the behaviour of stiffened SPSWs. In this research, a theoretical investigation based on the PFI method is conducted to evaluate the behaviour of stiffened SPSWs. This paper also evaluates the accuracy of the PFI method to predict the behaviour of stiffened plate shear walls by conducting non-linear finite element analysis.

Recommendations are provided for engineers to select the number of stiffeners on the plate to benefit from the advantages of stiffened SPSWs. In the end, a design criterion for selecting the size of stiffeners is also investigated. In order to achieve the objectives, a nonlinear FE model is first developed using a finite element analysis program, ABAQUS (ABAQUS, 2014). The FE model is validated against experimental tests by Sabouri-Ghomi and Sajjadi (Sabouri-Ghomi and Sajjadi 2012). With the validated FE model, a series of SPSW models with different stiffener numbers and sizes are analyzed. Based on the results from finite element analyses, an improved stiffness requirement for stiffeners in stiffened SPSWs is provided.

3.3. PFI method for stiffened SPSWs

When a steel plate shear wall is subjected to lateral loads, the general state of post-buckling stresses is determined as shown in Fig 3.1. Assuming the beams and columns surrounding the plate are strong enough to resist loads from the tension field action on the plate, the stresses on the plate during the post-buckling state are a combination of critical buckling stress and tension field action stress. The critical buckling stress of the plate, τ_{cr}, is calculated by

$$\tau_{cr} = \frac{K\pi^2 E}{12(1-\mu^2)}\left(\frac{t}{b}\right)^2 \le \tau_{wy} = \frac{\sigma_0}{\sqrt{3}} \tag{3.1}$$

where E is the modulus of elasticity; K is the plate buckling coefficient; μ is Poisson ratio; σ_0 is the yield stress of the material; t and b are the plate thickness and width respectively.

The plate buckling coefficient, K, is a function of plate geometry and boundary conditions. For plate simply supported on four edges, solutions for K were developed by Timoshenko and Goodier (S. Timoshenko and Goodier 1970) and are as follows:

$$K = 4 + 5.35\left(\frac{b}{d}\right)^2 \quad \text{for } \frac{d}{b} \le 1 \tag{3.2}$$

$$K = 5.35 + 4\left(\frac{b}{d}\right)^2 \quad \text{for } \frac{d}{b} \ge 1 \tag{3.3}$$

where d is the height of the plate.

Maximum value for τ_{cr} is the yield shear stress of the plate τ_{wy}. After buckling of the plate, tension field stresses are developed gradually on the plate with at angle of θ with the horizontal axis. The tension field stress at yielding (σ_{ty}) can be determined using Von Mises yield criterion.

36

$$\sigma_{ty}^2 + 3\tau_{cr}\sigma_{ty}\sin(2\theta) + (3\tau_{cr}^2 - \sigma_0^2) = 0 \tag{3.4}$$

By calculating τ_{cr} and σ_{ty}, the shear strength of the plate (F_{wu}) can be determined as follows:

$$F_{wu} = bt(\tau_{cr} + 0.5.\sigma_{ty}\sin(2\theta)) \tag{3.5}$$

The elastic shear displacement of the infill plate (U_{we}) can also be calculated by adding critical shear displacement and shear displacement due to the post-buckled component of the shear forces. The shear displacement due to the post-buckled component is obtained by equating the tension field's strain energy to the work done by the shear forces' post-buckled component.

$$U_{we} = d\left(\frac{\tau_{cr}}{G} + \frac{2\sigma_{ty}}{E\sin2\theta}\right) \tag{3.6}$$

where G is the shear modulus of the plate.

The relationship between τ_{cr} and σ_{ty} is drawn in Fig 3.2 based on Eq. (3.4). As it is observed in Fig. 2, by increasing τ_{cr}, σ_{ty} decreases. When a plate is very thin (very small value for t/b in Eq. (4.1), the plate will buckle soon after the lateral load is applied and τ_{cr} is very small, therefore it can be neglected. In this situation, practically all of the shear strength of the plate is the result of the tension field action on the plate. For plates that have a considerable thickness, τ_{cr} cannot be neglected and should be considered when calculating the shear strength of the plate. If the plate is very thick, τ_{cr} will be equal to the yield shear stress of the plate and σ_{ty} will be zero. Therefore, in this situation, the elastic buckling of the plate is prevented.
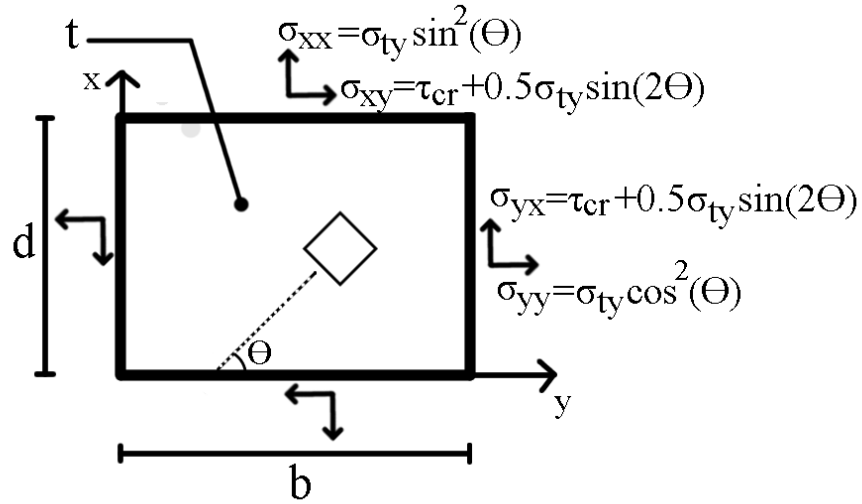
Fig 3.1. State of post-buckling stress on an infill plate
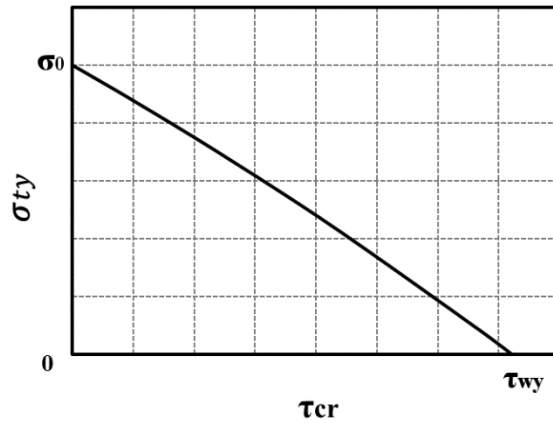
Fig 3.2. Relationship between critical buckling stress and tension field stress

Using a very thick plate is not an efficient solution to prevent the buckling of the plate, therefore stiffened plates are used in practice for this purpose. A stiffened steel plate shear wall is usually constructed by installing vertical and horizontal plate stiffeners on the infill plate. The stiffeners divide the shear panel into rectangular sub-panels. Generally, there are two possible buckling modes that can occur on a stiffened plate. If the stiffeners are not strong enough, the plate will buckle under lateral load, similar to an unstiffened steel plate. This is called global buckling mode and the purpose of properly designed stiffeners is to prevent this buckling mode. The second buckling mode is local bucking mode which occurs when buckling takes place in the sub-panels

38

of the stiffened plate and therefore global buckling of the plate is prevented. The two buckling modes are shown in Fig 3.3.
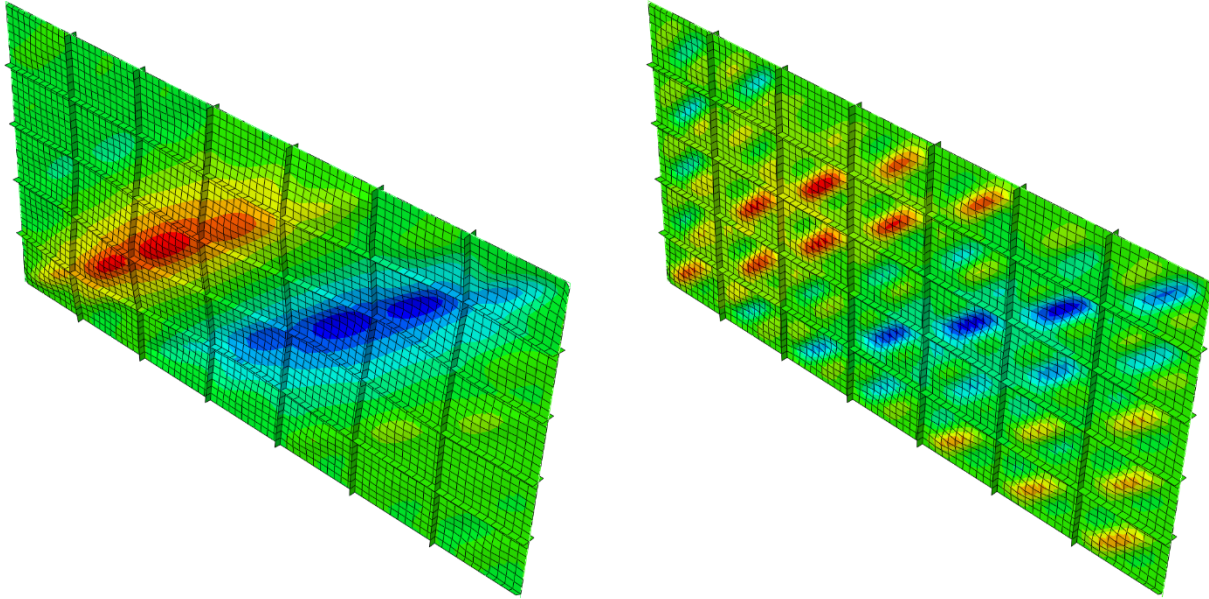
Fig 3.3. Buckling modes of a stiffened plate: Global Buckling (left) and Local Buckling (Right)

The shear strength, stiffness and elastic shear displacement of a stiffened SPSW can be determined using the PFI method. Assuming that the stiffeners are strong enough to prevent global buckling of the infill plate and the spacing between stiffeners is regular, τ_{cr} for a subpanel on the plate can be calculated using Equations (3.1), (3.2) and (3.3) by replacing b and d as the width and height of the subpanels. Since the size of the subpanels are the same, the calculated τ_{cr} is the critical buckling stress of the plate. Therefore, σ_{ty} and subsequently the shear strength of a stiffened plate can be determined using Eq. (3.4) and Eq. (3.5), respectively. Once τ_{cr} and σ_{ty} are known, the elastic shear displacement can be calculated using Eq. (3.6).

3.4. Analytical study to investigate effects of stiffeners in SPSWs

When designing stiffened SPSWs, it is important to determine the number of stiffeners on the infill plate. Increasing the number of stiffeners on the plate reduces the size of the subpanels. As This results in an increase in the critical buckling stress of the plate. However, since τ_{cr} has an upper limit (Eq. (3.1)), increasing the number of stiffeners after a certain point will not increase τ_{cr}. This is shown in Fig 3.4 where a general relationship between τ_{cr} and plate slenderness (b/t) is presented.
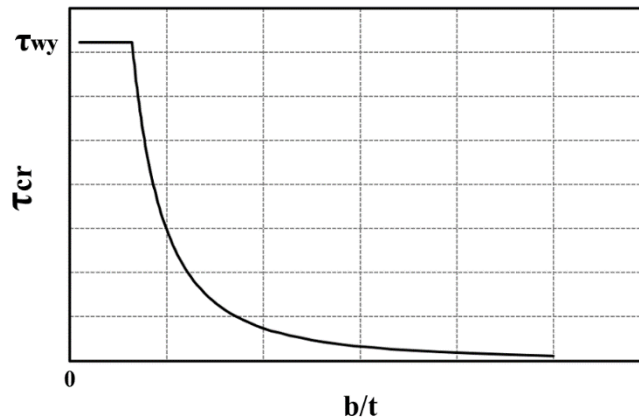
Fig 3.4. General relationship between critical buckling stress and slenderness ratio of a stiffened plate

As discussed earlier, increasing τ_{cr} will result in a reduction of σ_{ty}, and when τ_{cr} reaches the upper limit, σ_{ty} will be zero and local buckling will not take place in the plate before yielding. One of the advantages of using stiffeners is that the value of σ_{ty} becomes small and thus reduces the moment on the boundary members. If the size of the subpanels is very small, τ_{cr} is maximum. In that case, the force from the tension field is completely removed, and no extra bending moment will be imposed on the surrounding members. This type of plate is named here as a fully stiffened plate.

Another benefit of using stiffeners is to increase the shear strength of the plate. For an unstiffened plate, τ_{cr} is negligible and can be assumed as 0 and therefore σ_{ty} will be equal to σ_0. If the angle of tension filed θ is taken as 45 degrees, which is a reasonable assumption according

40

to well-established studies (Shishkin, Driver, and Grondin 2009), the shear strength of an unstiffened plate can be determined by the following equation:

$$(F_{wu})_{\text{unstiffened}} = \frac{1}{2} bt\sigma_0 \tag{3.7}$$

The shear strength of a fully stiffened plate can be determined similarly. Assuming the size of the subpanels are small enough that τ_{cr} is equal to τ_{wy} and therefore σ_{ty} is 0. The shear strength of the stiffened plate can then be calculated by

$$(F_{wu})_{\text{stiffened}} = \frac{bt\sigma_0}{\sqrt{3}} \tag{3.8}$$

From Eq. (3.8) and Eq. (3.7), $\frac{(F_{wu})_{\text{stiffened}}}{(F_{wu})_{\text{unstiffened}}}$ can be obtained as 1.15, which shows that a fully stiffened plate will have around 15% more shear strength than a similar unstiffened plate.

Similarly, the elastic shear displacement of an unstiffened plate can be obtained as:

$$(U_{we})_{\text{unstiffened}} = \frac{2d\sigma_0}{E} \tag{3.9}$$

Assuming the Poisson's ratio of steel as 0.3, the relationship between elastic and shear modulus is $E = 2.6G$. Therefore, the elastic shear displacement of a fully stiffened plate can also be calculated by

41

$$(U_{we})_{\text{stiffened}} = \frac{2.6d\sigma_0}{E\sqrt{3}} \qquad\qquad (3.10)$$

From Eq. (3.10) and Eq. (3.9), the ratio of the elastic shear displacement of fully stiffened plate to the elastic shear displacement of an unstiffened plate is obtained as 0.75. This shows that, theoretically, the elastic shear displacement of a fully stiffened plate is about 25% less than a similar unstiffened plate.

The elastic stiffness of a plate can be calculated by dividing the shear strength by the elastic shear displacement.

$$K = \frac{F_{wu}}{U_{we}} \qquad\qquad (3.11)$$

Since the shear strength of a fully stiffened plate is 15% more than an unstiffened plate, and the elastic shear displacement of a fully stiffened plate is about 25% less than a similar unstiffened plate the elastic stiffness of a fully stiffened plate is increased by about 53% in comparison to a similar unstiffened plate. Thus, by adding stiffeners to the infill plate, the elastic stiffness of the SPSW system can be increased significantly.

3.5. Finite element analysis of stiffened steel plate shear walls

To investigate the accuracy of the PFI method in predicting the strength and stiffness of stiffened infill plates, and also to discuss the benefits of the stiffeners, a series of stiffened SPSWs were analysed using ABAQUS software. The finite element modeling approach adopted in this study was first validated against the experimental study on stiffened SPSWs by Sabouri-Ghomi and Sajjadi (Sabouri-Ghomi and Sajjadi 2012). The infill plate in the experiment had a height of 960 mm and a width of 1410 mm, and the plate thickness was 2 mm. There were four horizontal and four vertical stiffeners attached to the plate. All stiffeners had a thickness of 4 mm and a width of 60 mm. The test specimen was subjected to cyclic loading by two hydraulic jacks at the two ends of the beam. For the finite element model, ABAQUS 4-node general-purpose shell (S4R) element was selected to model the infill plate and the boundary frame. The connection of the infill plate to the frame, and also the connections of beam-to-columns were assumed rigid. The bases of the

columns were considered fixed, and the out-of-plane movement of the beam was also restrained. In order to initiate buckling in the infill plate, an eigenvalue buckling analysis was first conducted. Then, an initial imperfection of 1 mm was applied to the plate corresponding to the first buckling mode of the steel plate. Cyclic analysis was conducted by applying displacements at the two sides of the beam, similar to the experiment. In this study, ABAQUS/Standard was adopted for all FE analyses. ABAQUS/Standard uses an implicit dynamic integration method and automatically adjusts the time increment to achieve convergence in analysis for highly nonlinear problems. Fig 3.5 shows the developed FE model for the specimen tested by Sabouri-Ghomi and Sajjadi (2012). Fig 3.5 also compares the load-displacement curves obtained from the finite element analysis with that obtained from the test. As observed from Fig 3.5, there is a very close agreement between the FE analysis results and results obtained from the test. The analysis also showed local buckling in the FE model, as observed in the test.
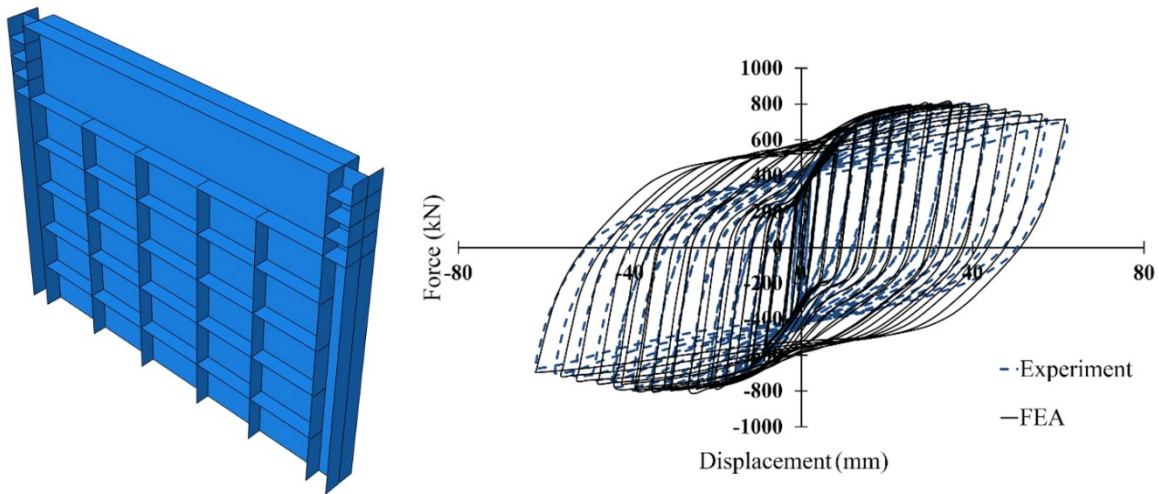
Fig 3.5. Comparison of cyclic analysis with test results of Sabouri-Ghomi and Sajjadi [6]: FE model (left) and load-displacement curve (right)

Using the validated FE modelling approach, a series of SPSW models with different plate widths, heights, and thicknesses were developed and analyzed. Wide flange sections were selected

for columns and beams. These members were designed to withstand the yielding forces from the infill plate yielding. Since the purpose of this study was to investigate the behaviour of the infill plate, for simplicity the boundary frame was modeled using the ABAQUS beam element. Table 3.1 presents the plate and boundary member dimensions. The steel material used for all SPSW models was the same and the material properties for boundary elements, infill plate, and stiffeners are presented in Table 3.2.

For each model in Table 3.1, seven variations with a different number of stiffeners were considered. The number of stiffeners was from one to seven in each direction. Each variation had an equal number of horizontal and vertical stiffeners and the stiffeners in each direction were equally spaced (as shown in Fig 3.6). The purpose of this consideration was to gradually reduce the size of the subpanels until τ_{cr} reached its upper limit and the plate was considered fully stiffened. An unstiffened plate was also modeled for each model. Nonlinear pushover analysis was carried out for all FE models with a target drift of 4 percent. Fig 3.7 shows the deformed shapes of SPSW models M4x3x6 and M5x3x6.

Table 3.1. Plate dimensions and frame sections for the SPSW models

Model Name	Plate Height (m)	Plate Width (m)	Plate Thickness (mm)	Column Section	Beam Section
M3x6x6	3	6	6	W310x226	W610x498
M3x5x6	3	5	6	W310x226	W610x341
M3x4x6	3	4	6	W310x226	W610x140
M3.5x5x6	3.5	5	6	W310x342	W610x341
M3.5x4x6	3.5	4	6	W310x342	W610x140
M3.5x4x4	3	4	4	W310x158	W610x174
M3x4x8	3	4	8	W310x253	W610x285
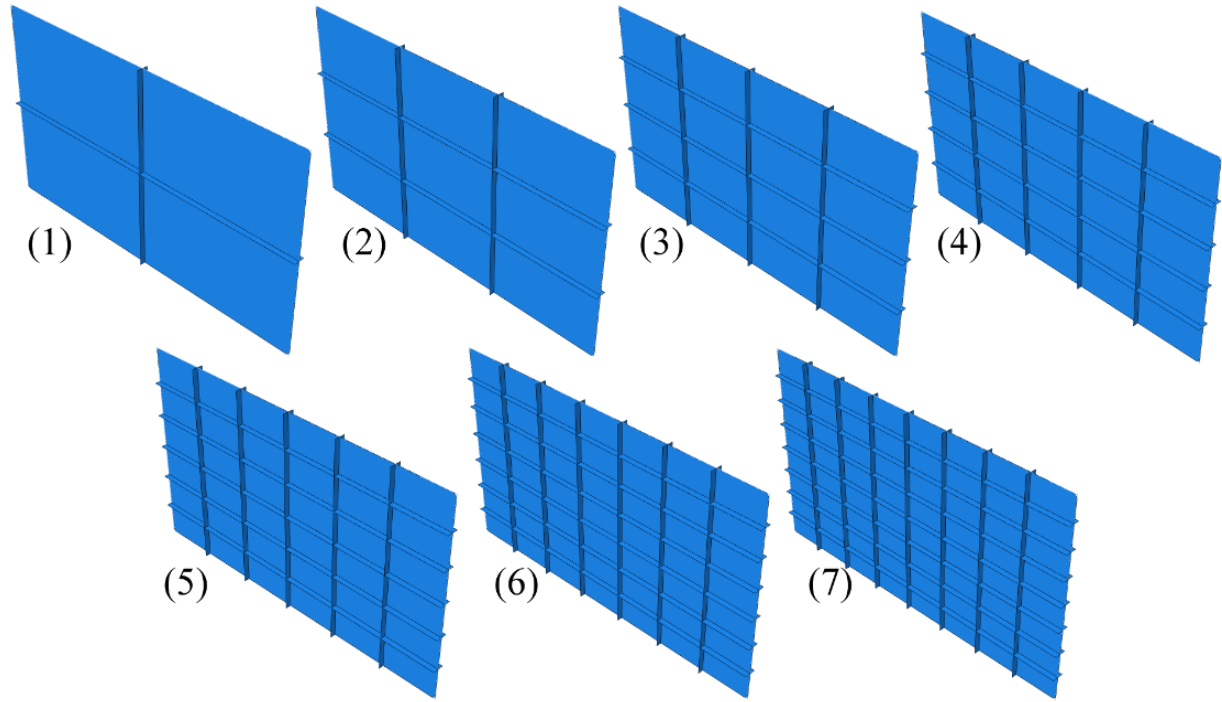
Fig 3.6. Stiffener variations considered for each model

Table 3.2. Material properties for the FE models

Element	Elastic Modulus (MPa)	Yield Stress (MPa)
Infill Plate	200,000	250
Stiffeners	200,000	250
Columns	200,000	350
Beam	200,000	350
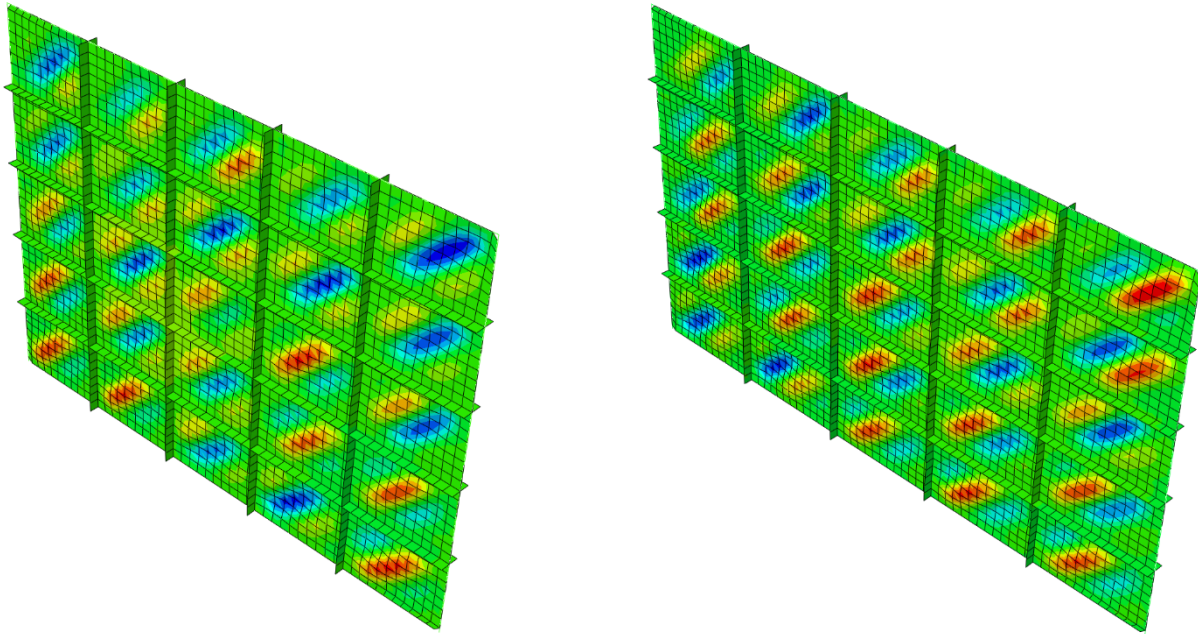
Fig 3.7. Deformed shape of the models M4x3x6 (left) and M5x3x6 (Right)

Since one the of purposes of conducting FEA was to compare the results with theoretical calculations, the displacement and force of the plate at yielding needed to be determined. To determine the yield point of FEA pushover curves, bilinear idealized curves were used. The idealized curve is obtained by equating the area under the pushover curve and the area under the idealized curve. An example of an idealized curve is shown in Fig 3.8. From the bilinear idealized curves, yield displacement and yield strength were obtained for all SPSW models.
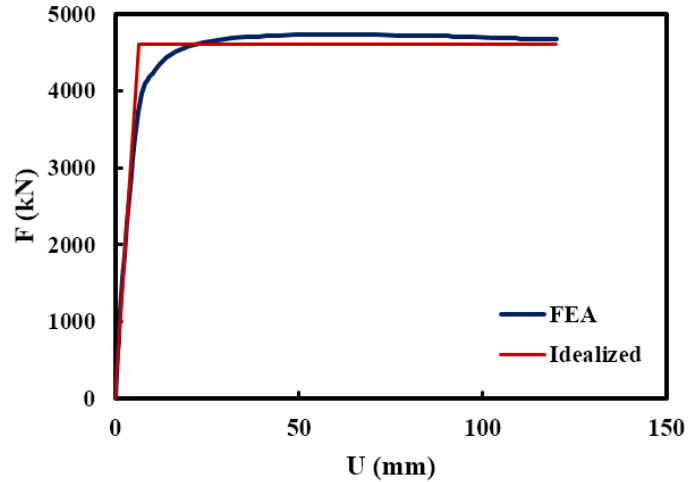
Fig 3.8. Example of an idealized curve drawn from FEA pushover curve

Fig 3.9 shows the yield force against the slenderness ratio of the plate (b/t). For all models, results from FEA are compared with predicted values by the PFI method. As predicted, it is observed that when the slenderness ratio is decreased (when the number of stiffeners is increased), the shear strength of the SPSW models increases. Overall, there is close agreement between the predicted values by the PFI method and finite element analysis results. The predicted shear strength for unstiffened plates and plates with one or two stiffeners in each direction is very close to FEA results. The predicted values when the plate is fully stiffened are also very close to the results from FEA. However, there is a small overestimation of shear strength when there are three to five stiffeners in each direction. This is usually a situation when the value for τ_{cr} is not negligible, but it has not reached its upper limit either. FE analysis results show that most models had around 13% increase in shear strength when the plate was fully stiffened. This value is very close to the 15% predicted by the PFI method. The maximum increase in shear strength was around 14% for the SPSW model M6x3x6 and the minimum increase in shear strength was around 10% for the model M4x3x4.
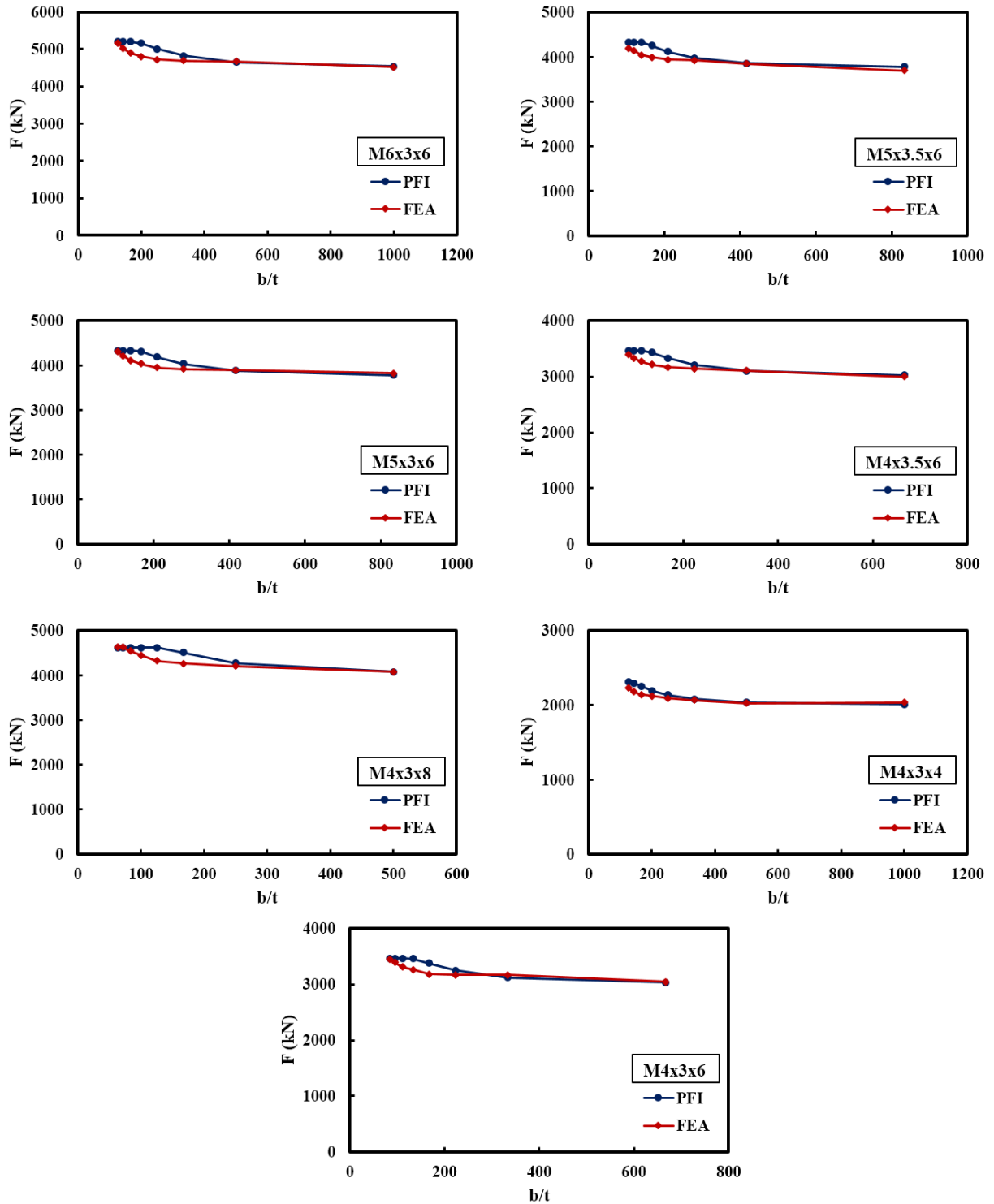
Fig 3.9. Comparison between the yield forces from finite element analysis and PFI method for all SPSW models
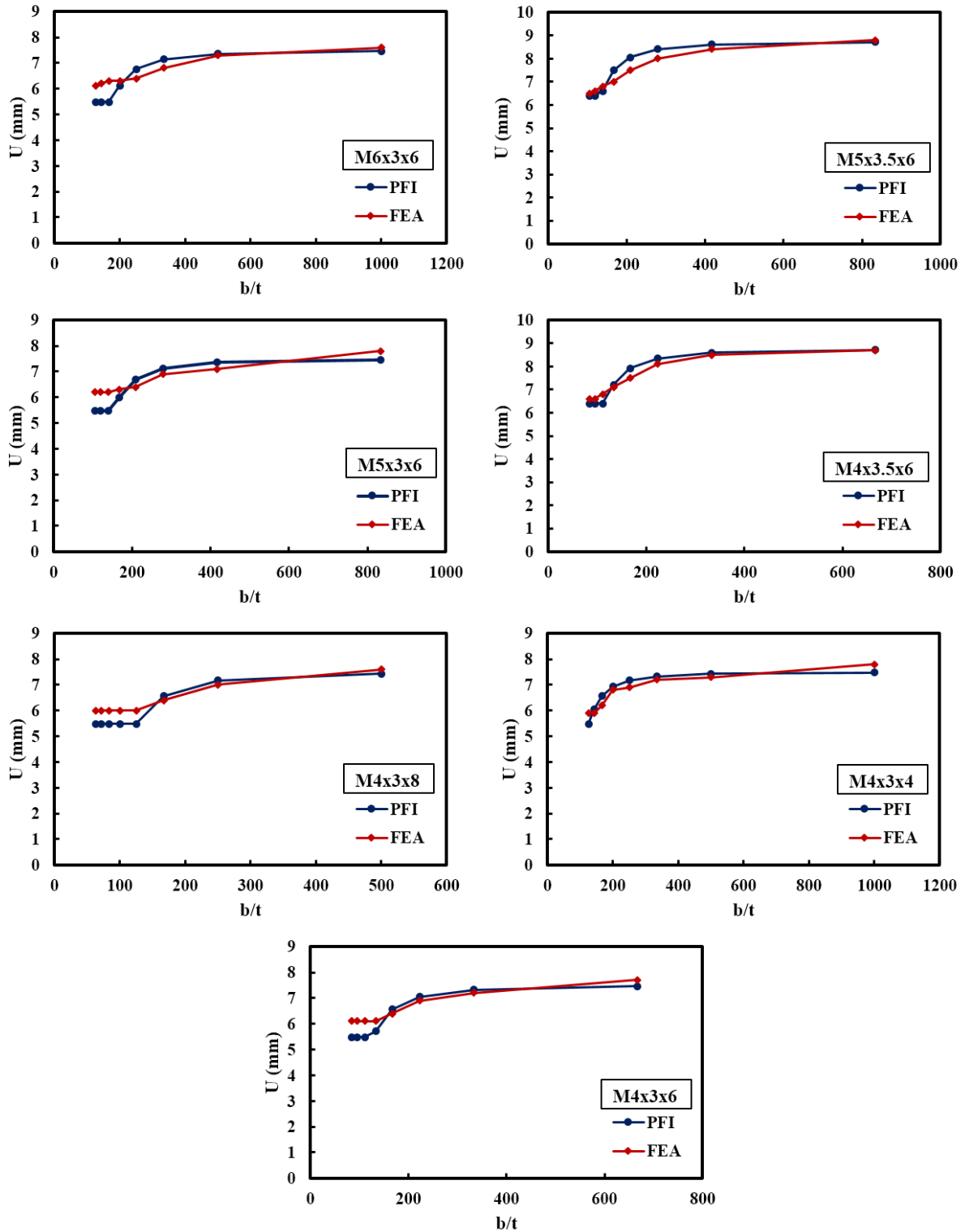
Fig 3.10. Comparison between the yield displacements from FE analysis and PFI method for all SPSW models

49
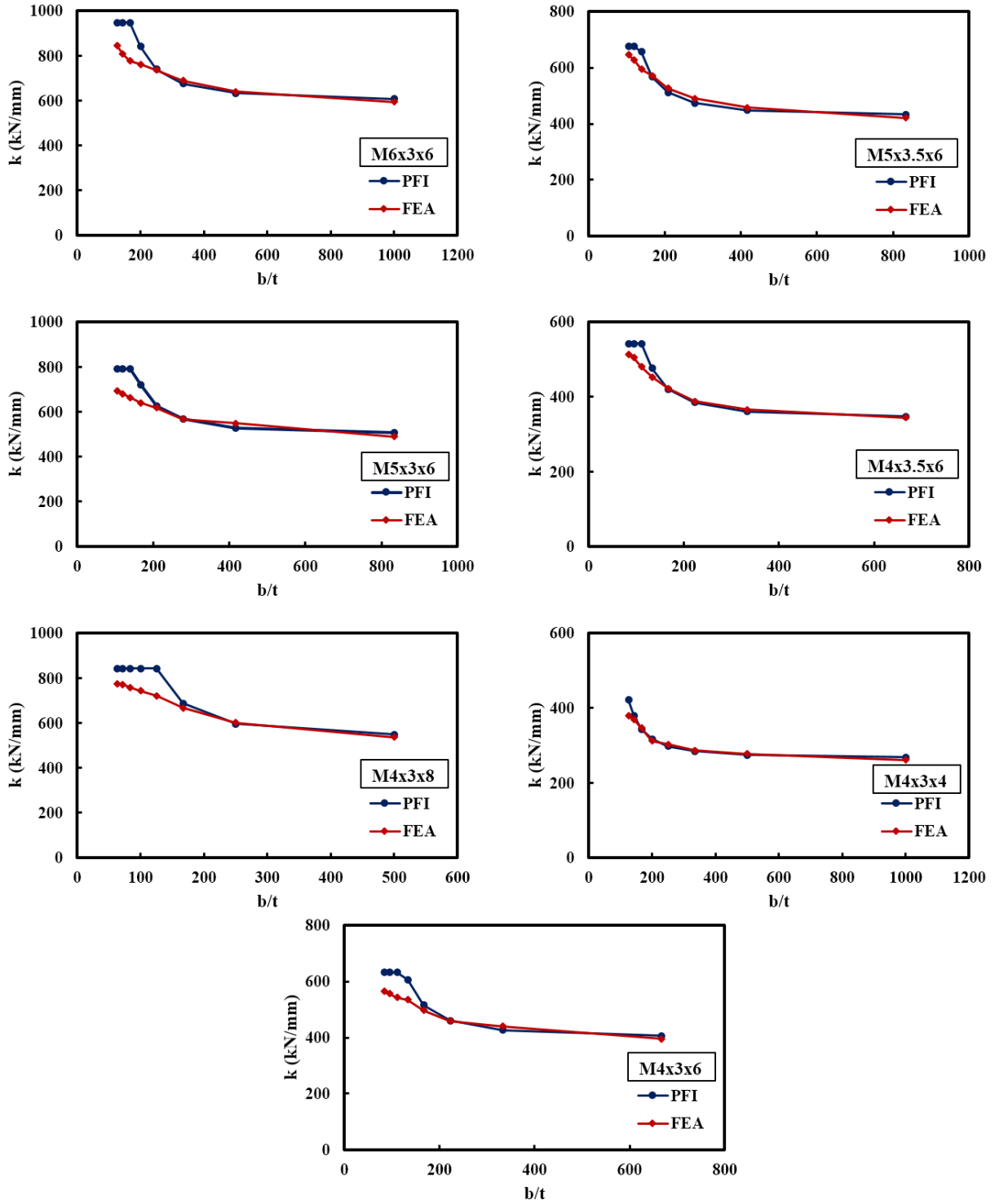
Fig 3.11. Comparison between the stiffness from FE analysis and PFI method for all SPSW models

Fig 3.10 shows the yield displacement against the slenderness ratio of the plate. Similar to the shear strength, predicted values by the PFI method are compared with results from FEA for all SPSW models. A decrease in yield displacement can be observed in SPSW models when the slenderness ratio decreases. There is a good overall agreement between results from FEA and calculated values from the PFI method. From the FEA results, the maximum decrease in yield displacement was found to be 26% for the model M5x3.5x6, which is very close to the 25% predicted by PFI method. The minimum amount of decrease in yield displacement of fully stiffened plates was 20% for the model M6x3x6. This value is predicted by the PFI method to be around 25%.

Using yield displacement and shear strength, the stiffness of the SPSW models was also studied. Fig 3.11 shows the relation between the initial stiffness and the slenderness ratio of the plate. Finite element analysis results showed that for all models, the elastic stiffness of fully stiffened plates increased by at least 41%. The maximum increase in elastic stiffness was 53% for the model M5x3.5x6.

As mentioned before, the selection of the number of the stiffeners on a plate is important when designing stiffened steel plate shear wall. This depends on the required increase in parameters such as shear strength or stiffness of the steel plate shear wall. The results from PFI and FEA showed that using one or two stiffeners in each direction will not add any noticeable benefits to the behaviour of the system, as observed in Fig 3.10, Fig 3.10 and Fig 3.11. This can also be seen in Fig 3.4, which shows for larger values of slenderness ratio, τ_{cr} does not increase noticeably. When the slenderness ratio of the subpanels is 20% of an unstiffened plate (four stiffeners in each direction), noticeable effects are observed. Although at this point, for most of the models, τ_{cr} has not reached its maximum value yet, it is possible to improve the behaviour of the system. More considerable effects are observed when the slenderness ratio of the subpanels is around 16.6% of an unstiffened plate (five stiffeners in each direction). Therefore, if it is intended to increase shear strength or stiffness to their maximum value, the number of stiffeners should be selected so that τ_{cr} is equal to τ_{wy}. However, using fewer stiffeners on the plate can still improve the behaviour of the SPSW system. For example, when the model M5x3.5x6 had five stiffeners in each direction, τ_{cr} for the subpanels did not reach τ_{wy}, and FE analysis results showed a 10% increase in shear strength and a 45% increase in stiffness. It is important to note that adding more

stiffeners after τ_{cr} has reached its maximum value will not improve the behaviour of the SPSW system anymore.

3.6. Selection of size of stiffeners in SPSW

When using stiffened steel plate shear walls, it is necessary for the stiffeners to be strong enough to prevent global buckling on the plate. For this purpose, a design criterion that was proposed by Sabouri-Ghomi et al (Sabouri-Ghomi et al. 2008) was implemented in this study. Based on this criterion, the moment of inertia of stiffeners can be calculated to prevent the global buckling of the infill plate. Therefore, if the following criterion is satisfied, local buckling will take place on the plate.

$$\left(\frac{I_y}{S_y} + \frac{t^3}{12(1-\upsilon^2)}\right)^{0.25} \left(\frac{I_x}{S_x} + \frac{t^3}{12(1-\upsilon^2)}\right)^{0.75} > 0.0916 \frac{t^3}{S_x^2}\left(\frac{k_l}{k_g}\right)d^2 \tag{3.12}$$

where I_x and I_y are moment of inertia of vertical and horizontal stiffeners, respectively; S_x and S_y are spacing between vertical and horizontal stiffeners, respectively (shown in Fig 3.12); t is the infill plate thickness; d is the infill plate height; k_g is the global shear buckling coefficient. The value for k_g depends on the boundary connection of the plate and it can be assumed as 3.64 for simple connections or 6.9 for rigid connections. k_l is the local shear buckling coefficient and can be calculated from Eq. (3.2) and Eq. (3.3).
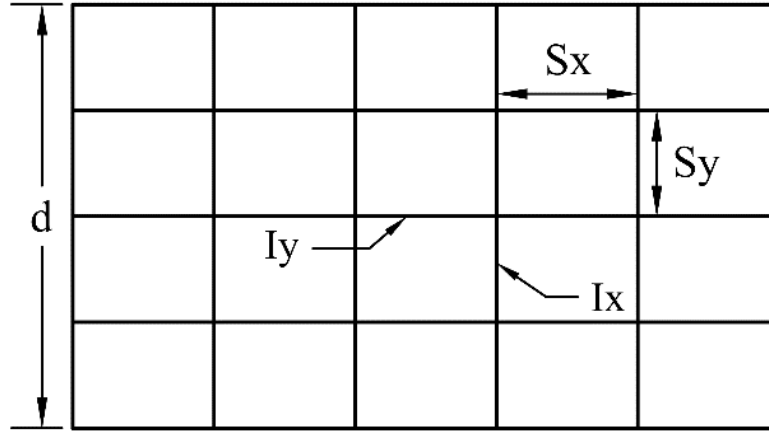
Fig 3.12. Horizontal and vertical stiffeners in a stiffened infill plate

This criterion is based on the concept that in order to force the plate into local buckling, the global critical shear buckling stress of the plate should be greater than the local critical shear buckling stress. When spacing between the vertical stiffeners is equal to spacing between the horizontal stiffeners and the stiffeners have the same moment of inertia, the following simplified equation is suggested [18]:

$$I > 0.0916 \left(\frac{d^2}{S} \left(\frac{k_l}{k_g} \right) - S \right) \cdot t^3 \tag{3.13}$$

For the FE models, the initial size of the stiffeners was selected according to this criterion. FE analysis showed that when there were five or more stiffeners in each direction, the selected size of stiffeners was capable of preventing global buckling. However, for models with less than five stiffeners in each direction global buckling occurred on the plate. Therefore, for these models, the size of the stiffeners was gradually increased until local buckling was observed. Stiffeners details calculated from Eq. (3.12) and finite element analysis results for the model M6x3x6 are shown in Table 3.1 as an example.

Since it was showed before that most of the advantages of using stiffeners take place when the slenderness ratio of the subpanels is 16.6% of an unstiffened plate, using Eq. (3.12) to design

the stiffeners, in this case, is correct. However, if larger slenderness ratios are used for the plates, using Eq. (3.12) may not lead to correct results. In this case, required moment of inertia of the stiffeners for local buckling is larger than the value calculated from Eq. (3.12).

Table 3.3. Details of stiffeners and finite element analysis results for the model M6x3x6

Stiffener thickness (mm)	Stiffener width (mm) (on each side)	Number of stiffeners		Stiffeners spacing (mm)		FE analysis result
		Vertical	Horizontal	S_x	S_y	Buckling mode
6	69	7	7	750	375	Local
6	66	6	6	857	420	Local
6	63	5	5	1000	500	Local
6	59	4	4	1200	600	Global
6	54	3	3	1500	750	Global
6	50	2	2	2000	1000	Global
6	42	1	1	3000	1500	Global

3.7. Modification to the current stiffness requirement for stiffeners in stiffened SPSWs

Since the results in the previous section showed that the accuracy of the current stiffness requirement for stiffeners may be related to the number of stiffeners on the infill plate, a series of stiffened SPSW models were considered to quantify the relation between the number of stiffeners and the buckling mode. For the selected models, the plate and frame properties are same as the M3x6x6 model in Table 3.1. A total number of 70 models were considered for this part of the study. The models had 1 to 10 vertical stiffeners and 1 to 7 horizontal stiffeners. Therefore, a diverse range of possible configurations of stiffeners for the SPSW system was studied. To find the minimum required moment of inertia to prevent the global buckling, each model was analyzed

several times. For each model, the moment of inertia was calculated according to Eq. (3.12) and the model was analyzed. Then, based on the obtained results, whether local or global buckling occurred on the plate, the moment of inertia was increased or decreased by changing the width of the stiffeners with an increment of 1 mm, and the model was analyzed again. This process was repeated until the minimum required moment of inertia for local buckling of the plate was found for each model.

For each model, the ratio of the left side to the right side of Eq. (3.12) was calculated using the obtained required moment of inertia for local buckling. This ratio is named "R" here. Since the right side of the equation determines the limit at which the switch between buckling modes happens, multiplying it by the calculated ratio R will adjust this limit according to the obtained results from finite element analysis.

The results of the analyses and details of the models such as the number of stiffeners and their sizes as well as the calculated R ratios are shown in Table 4. As expected, it is observed from Table 4 that for plates with a smaller number of stiffeners, R is a number greater than 1. This means that the given limit by the stiffness criterion for shifting the buckling mode of the plate is not accurate and the correct value for the limit is a larger number. Therefore, stiffeners that are designed using this limit are not strong enough to prevent global buckling of the plate. On the other hand, the value of R for the plates with a large number of stiffeners is less than 1. This shows that when the plate is extensively stiffened, using the stiffener design criterion in Eq. (3.12) will lead to overdesigned stiffened SPSW. However, this is not critical since the stiffeners will fulfill their main objective which is preventing the global buckling of the plate.

FE analysis results in this section and the previous section showed that the current stiffness requirement (Eq. (3.12)) for stiffener design needs modification. It is observed that using the current stiffness criterion for design of stiffeners of SPSWs will not always lead to the desired outcome and the accuracy depends on the number of stiffeners. Therefore, the calculated values for R are used to modify the current stiffness criterion for stiffeners of SPSWs.

Table 3.4. Stiffener details and calculated values of R

55

Model Name	Stiffener Thickness (mm)	Stiffener Width (mm) (on each side)	Number of Stiffeners		Stiffeners Spacing (mm)		
			Vertical	Horizontal	Sx	Sy	R
P6x3-S10x7	6	56	10	7	545	375	0.66
P6x3-S10x6	6	58	10	6	545	429	0.86
P6x3-S10x5	6	59	10	5	545	500	1.06
P6x3-S10x4	6	58	10	4	545	600	1.16
P6x3-S10x3	6	58	10	3	545	750	1.27
P6x3-S10x2	6	57	10	2	545	1000	1.28
P6x3-S10x1	6	62	10	1	545	1500	1.64
P6x3-S9x7	6	56	9	7	600	375	0.65
P6x3-S9x6	6	58	9	6	600	429	0.85
P6x3-S9x5	6	60	9	5	600	500	1.11
P6x3-S9x4	6	62	9	4	600	600	1.46
P6x3-S9x3	6	61	9	3	600	750	1.56
P6x3-S9x2	6	63	9	2	600	1000	1.85
P6x3-S9x1	6	64	9	1	600	1500	1.98
P6x3-S8x7	6	57	8	7	667	375	0.66
P6x3-S8x6	6	59	8	6	667	429	0.87
P6x3-S8x5	6	61	8	5	667	500	1.15
P6x3-S8x4	6	64	8	4	667	600	1.60
P6x3-S8x3	6	66	8	3	667	750	2.06
P6x3-S8x2	6	65	8	2	667	1000	2.20
P6x3-S8x1	6	66	8	1	667	1500	2.41
P6x3-S7x7	6	58	7	7	750	375	0.66
P6x3-S7x6	6	59	7	6	750	429	0.84
P6x3-S7x5	6	62	7	5	750	500	1.18
P6x3-S7x4	6	65	7	4	750	600	1.67
P6x3-S7x3	6	69	7	3	750	750	2.47
P6x3-S7x2	6	68	7	2	750	1000	2.72

P6x3-S7x1	6	72	7	1	750	1500	3.46
P6x3-S6x7	6	59	6	7	857	375	0.65
P6x3-S6x6	6	61	6	6	857	429	0.87
P6x3-S6x5	6	62	6	5	857	500	1.13
P6x3-S6x4	6	66	6	4	857	600	1.71
P6x3-S6x3	6	70	6	3	857	750	2.59
P6x3-S6x2	6	70	6	2	857	1000	3.20
P6x3-S6x1	6	80	6	1	857	1500	5.28
P6x3-S5x7	6	63	5	7	1000	375	0.72
P6x3-S5x6	6	63	5	6	1000	429	0.89
P6x3-S5x5	6	63	5	5	1000	500	1.12
P6x3-S5x4	6	67	5	4	1000	600	1.71
P6x3-S5x3	6	72	5	3	1000	750	2.77
P6x3-S5x2	6	75	5	2	1000	1000	4.19
P6x3-S5x1	6	77	5	1	1000	1500	5.36
P6x3-S4x7	6	69	4	7	1200	375	0.84
P6x3-S4x6	6	70	4	6	1200	429	1.09
P6x3-S4x5	6	71	4	5	1200	500	1.44
P6x3-S4x4	6	69	4	4	1200	600	1.74
P6x3-S4x3	6	73	4	3	1200	750	2.77
P6x3-S4x2	6	80	4	2	1200	1000	5.07
P6x3-S4x1	6	79	4	1	1200	1500	6.54
P6x3-S3x7	6	72	3	7	1500	375	0.83
P6x3-S3x6	6	75	3	6	1500	429	1.16
P6x3-S3x5	6	76	3	5	1500	500	1.54
P6x3-S3x4	6	83	3	4	1500	600	2.65
P6x3-S3x3	6	77	3	3	1500	750	2.98
P6x3-S3x2	6	83	3	2	1500	1000	5.44
P6x3-S3x1	6	76	3	1	1500	1500	6.56
P6x3-S2x7	6	80	2	7	2000	375	0.92

P6x3-S2x6	6	82	2	6	2000	429	1.24
P6x3-S2x5	6	82	2	5	2000	500	1.61
P6x3-S2x4	6	86	2	4	2000	600	2.48
P6x3-S2x3	6	80	2	3	2000	750	2.88
P6x3-S2x2	6	88	2	2	2000	1000	5.83
P6x3-S2x1	6	86	2	1	2000	1500	9.29
P6x3-S1x7	6	96	1	7	3000	375	1.17
P6x3-S1x6	6	94	1	6	3000	429	1.39
P6x3-S1x5	6	98	1	5	3000	500	2.03
P6x3-S1x4	6	93	1	4	3000	600	2.39
P6x3-S1x3	6	86	1	3	3000	750	2.77
P6x3-S1x2	6	89	1	2	3000	1000	4.89
P6x3-S1x1	6	89	1	1	3000	1500	9.09

Careful examination of the calculated values shows a generally predictable pattern for R that is related to the number of vertical and horizontal stiffeners. It can also be observed that R is influenced by the number of vertical and horizontal stiffeners individually and considering only the total number of stiffeners to predict R will not lead to correct results. For example, according to Table 4, both of the models P6x3-S6x3 and P6x3-S3x6 have a total number of 9 stiffeners, but R is not the same for the two models. This is because P6x3-S3x6 has 6 horizontal and 3 vertical stiffeners and the P6x3-S6x3 model has 3 horizontal and 6 vertical stiffeners.
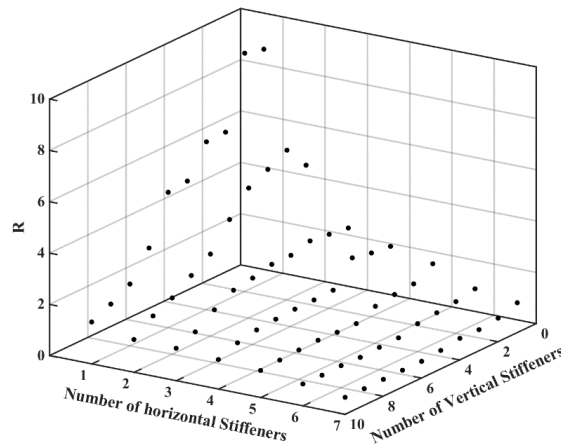
Fig 3.13. Relation between the numbers of horizontal stiffeners, vertical stiffeners and R

The relation between the numbers of horizontal stiffeners, vertical stiffeners, and R is shown in Fig 3.13. It is observed that reducing the number of stiffeners in any direction will increase R, as expected. To find a correlation between R and the number of vertical and horizontal stiffeners, multiple regression analysis was carried out with help of MATLAB. The goal was to find an equation that can be used to predict the value for R according to the number of vertical and horizontal stiffeners. Different types of multiple regression were tried to find the best results. For this study, the main consideration was that the equation should be relatively simple and easy to use but also accurate.

Based on the regression analysis, an inverse paraboloid function was found to have an excellent representation for the analysis data. As it is can be seen in Fig 3.14, the overall shape of this function has a very good agreement with the data trend in all areas, and most of the data points are below or very close to the surface. Thus, the equation of this surface was accepted as the result of the regression analysis.
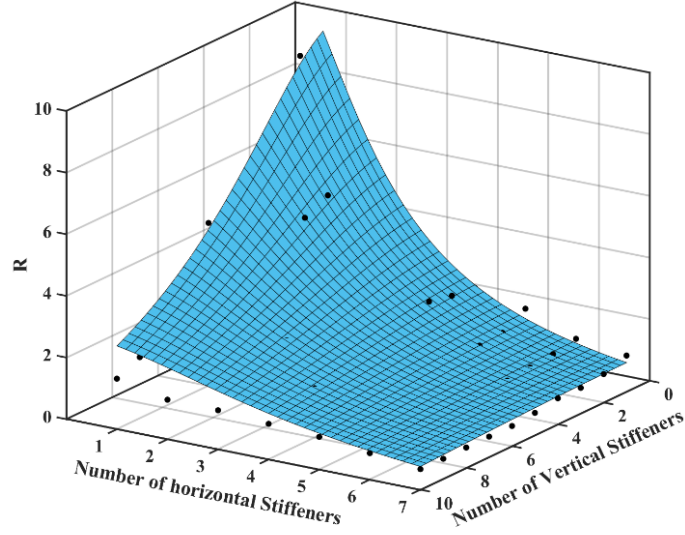
Fig 3.14. Inverse paraboloid function considered for R

Eq. (3.14) represents the surface in Fig 3.14, which is the result of the regression analysis. In this equation N_V and N_H are the numbers of vertical and horizontal stiffeners, respectively. The result from this equation is applied to the right side of Eq. (3.12) as calibration factor (β). Thus, Eq. (3.12) can be modified as Eq. (3.15).

$$\beta = \frac{1}{0.0027\left(N_V{}^2\right) + 0.02\left(N_H{}^2\right) + 0.08} \tag{3.14}$$

$$\left(\frac{I_y}{S_y} + \frac{t^3}{12(1 - \upsilon^2)}\right)^{0.25} \left(\frac{I_x}{S_x} + \frac{t^3}{12(1 - \upsilon^2)}\right)^{0.75} > 0.0916 \frac{t^3}{S_x^2}\left(\frac{k_l}{k_g}\right) d^2 \cdot \beta \tag{3.15}$$

If the spacing between stiffeners and moment of inertias are identical for vertical and horizontal stiffeners, Eq. (3.15) can be simplified to Eq. (3.16).

$$I > 0.0916 \left(\frac{d^2}{S} \left(\frac{k_l}{k_g} \right) \cdot \beta - S \right) \cdot t^3 \tag{3.16}$$

As mentioned before, R is a value obtained for each specific model to adjust the stiffness criterion for stiffeners. The value of β obtained from Eq. (3.14) is not exactly equal to R, but it is a close prediction of R. Therefore, by applying β to Eq. (3.12), the stiffness criterion is calibrated according to the obtained results from finite element analysis. Using the calibrated design criterion for stiffeners should lead to local buckling of stiffened plates, even with a low number of horizontal and vertical stiffeners.

3.8. Validation of the proposed calibration factor for improved stiffness criterion

The proposed calibration factor is based on results from series of finite element analyses on a steel plate shear wall with certain dimensions. To evaluate the effectiveness of the calibration factor developed for improved stiffness criterion, the models presented in Table 3.1 were considered.

In order to validate the outcome for all the different stiffener configurations considered in the previous section, 70 stiffener variations were considered for each of model, with similar stiffener numbers and arrangements as before. Thus, in total 420 FE models were developed to investigate the effectiveness of the proposed calibration factor, β. For each model, the stiffener size was calculated using Eq. (3.15). The buckling behaviour of each model was studied after analysis to assess the accuracy and the effect of the proposed calibration factor.

The results of the analyses showed that all models experienced local buckling, even the models with very small numbers of stiffeners. Two examples for deformed shapes of SPSW models with four horizontal and vertical stiffeners are shown in Fig 3.15. Also, the difference between the deformed shapes of the SPSW model with two horizontal and vertical stiffeners (model P5x3-S2x2 in Table 4) before and after use of the calibrated design criterion is presented in Fig 3.16. Since FE analysis of all of the models displayed the intended outcome, which was the prevention of global buckling of the infill plate, the effectiveness of using Eq. (3.15) in the design of the stiffeners is established.
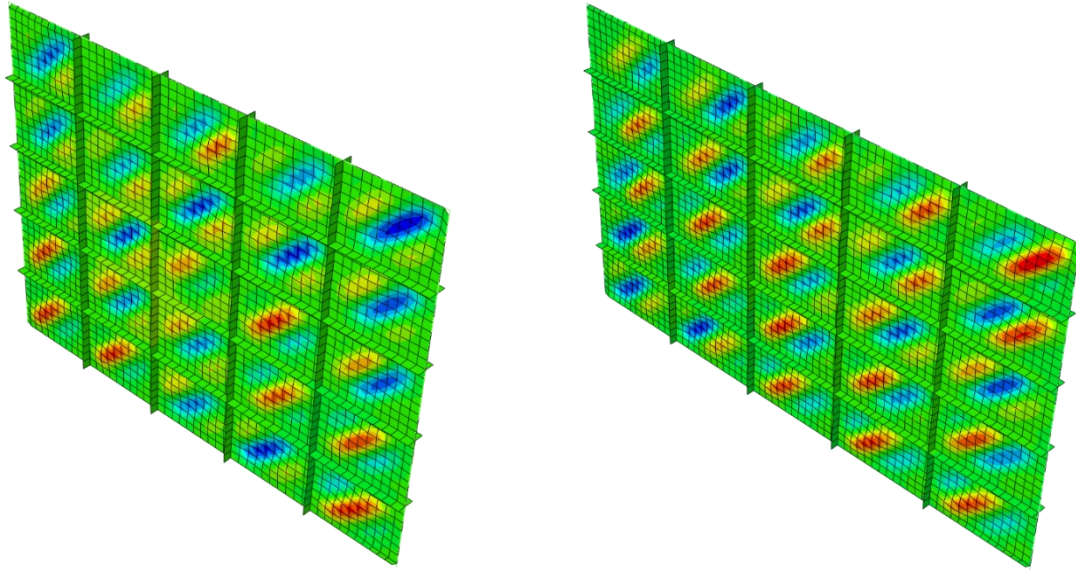
Fig 3.15. Validation of the proposed improved design criterion: plates with 4 m width (left) and 5 m width (right) both experienced local buckling
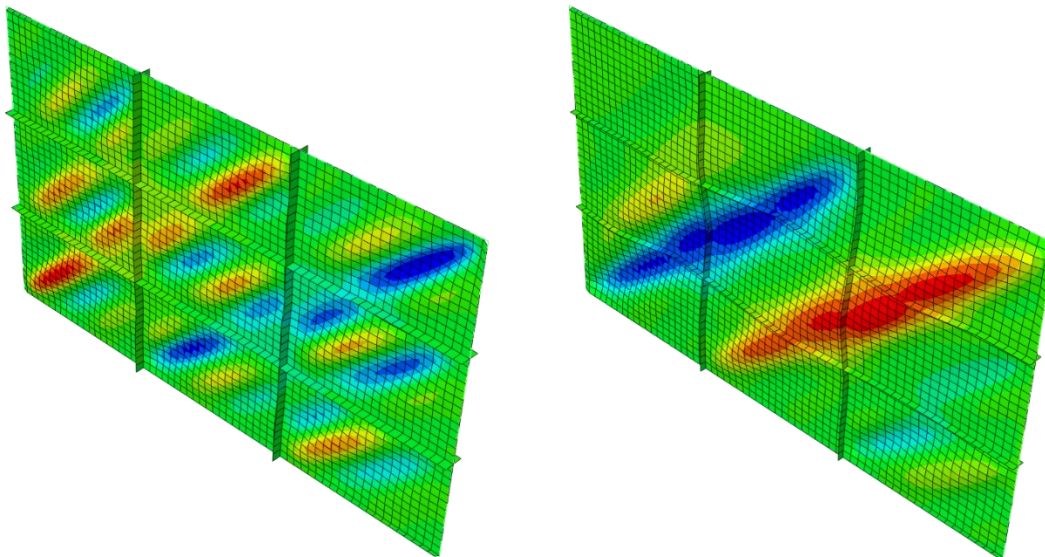
Fig 3.16. Validation of the proposed improved design criterion: stiffeners designed using improved (left) and original (right) design criteria

3.9. Discussions for practical design of stiffeners

It was observed from detailed FE analyses that when there were a large number of stiffeners attached to the infill plate, the calculated value of the proposed calibration factor (β) was below 1. Although the results of validation models proved that using calculated β values that were lower than 1.0 would lead to local buckling of the infill plates in stiffened SPSWs, as a conservative measure the calculated β values that are less than 1.0 are recommended to be assumed as 1.0. Therefore, in those cases, Eq. (3.15) will be the same as Eq. (3.12).

Also, while a wide range of numbers of stiffeners on the infill plates is examined in this study, it is recognized that not all of these stiffener configurations are possibly useful when it comes to the practical design of steel plate shear walls for buildings. For example, in the analyzed models, some cases have only a few vertical stiffeners and a large number of horizontal stiffeners or vice versa. The reason for considering these cases was to investigate the effect of the number of stiffeners on the calibration factor more accurately and completely. With these considerations, the final proposed equation for calibration factor is more inclusive and is reliable for a wider range of possible scenarios. The SPSW dimensions considered in this study are close to what are commonly used in real life design and construction of SPSW systems. Thus, the proposed improved stiffness criterion for design of stiffeners is aimed to assist practicing engineers for reliable and practical design of the stiffened SPSW system.

3.10. Conclusions

The behaviour and design of stiffened steel plate shear walls were investigated in this study. The PFI method for designing the system and prediction key parameters such as shear strength and stiffness was studied. Then finite element models with different plate sizes were developed and the effects of the number of stiffeners on different parameters was investigated. The results from finite element analysis were also compared to prediction from the PFI method to evaluate the PFI method accuracy. A design criterion for selecting the size of the stiffeners to prevent global buckling of the plate was also studied. The results showed that the PFI method is a reliable tool to

predict the behaviour of stiffened SPSW systems. This method can be used to design the system and also decide how much a plate should be stiffened. Conclusions from this study can be summarized as follow:

- Theoretical investigation showed that stiffeners can increase the shear strength and shear stiffness of the plate up to 15% and 53%, respectively. The yield displacement of the plate was reduced as much as 25%. Also, it was observed that adding more stiffeners after the critical buckling stress of the subpanels reached its upper limit was not beneficial.

- FE analysis results showed that the PFI method reasonably predict shear strength, stiffness and yield displacement of a stiffened plate. The predictions were more accurate for fully stiffened plates or plates with only a few stiffeners.

- FE analysis results also confirmed that an increase in shear strength and stiffness and a decrease in yield displacement. The increase in shear strength was 10-14% and the decreases in yield displacement was found to be between 20-26%. The elastic stiffness was found to increase between 41 and 53%. These values were close to the theoretical predictions by the PFI method. Both finite element analysis and the PFI method showed that using one or two stiffeners in each direction did not have any noticeable benefits for the SPSW system. The advantages of using stiffeners became noticeable when the slenderness ratio of the plate was about 20% to 16%.

- Using the design criterion, (Eq. (3.12), for stiffeners to force the plate into local buckling, was found to be effective when there are five or more stiffeners in each direction. In this case, local buckling was observed in all FE models. For plates with less number of stiffeners, Eq. (3.12) was found inadequate to prevent the global buckling of the plate.

- A calibration factor was proposed to improve the currently used stiffness criterion, Eq. (3.12), for horizontal and vertical stiffeners of SPSW systems. The proposed calibration factor, which is a function of the number of horizontal and vertical stiffeners, is simple and easy for design engineers to use. It was observed that the proposed improved stiffness criterion was effective in ensuring local buckling of infill plates with any (low to high) number of stiffeners.

CHAPTER 4

Numerical analysis of steel plate shear walls with rectangular openings[2]

4.1. Abstract

Rectangular openings are often required on the infill plate of steel plate shear walls (SPSWs). However, research on the behaviour of SPSWs with rectangular openings is limited. In this paper, the behaviour of steel plate shear walls with a rectangular opening is studied. Finite element analyses are carried out on unstiffened plates with different sizes of rectangular openings. A decrease in the shear strength of the plate and also large out-of-plane deformations around the openings are observed in all models. As a solution to these problems, stiffeners are attached to the infill plate and the models are analyzed again. Different numbers and arrangements of stiffeners are considered and the effectiveness of each arrangement in preventing the deformation of the opening is studied. Results show that stiffeners can effectively limit the out-of-plane deformation of the opening of the infill plate. It is also observed that the use of stiffeners increases the shear strength of the infill plate with a rectangular opening. Based on the study, an effective stiffener layout around the rectangular opening is proposed. The proposed stiffener layout is found to improve the behaviour of SPSWs with rectangular openings. Models with different opening locations and different opening aspect ratios are also analyzed and the results show that the location and aspect ratio of the opening has a very minor effect on the strength of the infill plate. Finally, an equation is proposed for the shear strength of the infill plate with a rectangular opening with the proposed stiffener layout.

Keywords: Steel plate shear wall; Stiffeners; Rectangular opening; Finite element analysis.

4.2. Introduction

Steel plate shear wall (SPSW) has been established as an effective lateral load resisting system against earthquakes. The system is currently used in moderate-to-high seismic regions and both American (ANSI/AISC 2016) and Canadian steel design standards (CSA 2014) have adopted the SPSW system. It has been shown by many studies that the SPSW system has many advantages such as high strength and stiffness and large energy dissipation capacity (Thorburn et al. 1983; Driver et al. 1998b; Bhowmick, Driver and Grondin 2009; Dhar and Bhowmick 2016). The option to provide openings with different sizes and arbitrary locations on the infill plate is also available for the SPSW system

The first study on the effects of an opening on the infill plate was conducted in 1992 by Roberts and Sabouri-Ghomi (Roberts and Sabouri-Ghomi 1992). A series of cyclic loading experimental tests were carried out on unstiffened steel plate shear walls with a circular opening at the center of the plate. Their results showed a reduction in both shear stiffness and strength of the infill plates. A conservative linear reduction factor, as presented in equation [1]], was proposed to calculate the shear strength and stiffness of perforated SPSWs.

$$V_{op} = V_p \left(1 - \frac{D}{b}\right)$$
(4.1)

where V_p is the strength of the panel without opening and V_{op} is the strength of the panel with opening, b is the length of the panel and D is the diameter of the opening..

Reduction in strength and stiffness was also confirmed by numerical studies on perforated SPSWs. Purba and Bruneau (Purba and Bruneau 2009) studied a 4000 mm by 2000 mm single-storey SPSW with a series of small identical circular perforations. Their study showed the same effect on the shear strength of the system and the linear reduction factor for the specific form of perforations was calibrated. Experimental and numerical investigations on the specific type of regularly placed perforations were also conducted in other studies (Vian et al. 2009; Vian, Bruneau, and Purba 2009; Farahbakhshtooli and Bhowmick 2021; Barua and Bhowmick 2019) and more design recommendations were provided for this type of special perforation.

66

Investigations by Bhowmick (Bhowmick 2014) and Bhowmick et al. (Bhowmick, Grondin, and Driver 2014) on a series of single and multi-storey finite element models with circular perforations also suggested a reduction factor that can approximately predict the strength of the plate with circular perforations. Rectangular openings are often required to place nonstructural elements such as windows. However, very limited research is currently available on SPSWs with rectangular openings. Sabouri-Ghomi and Mamazizi (Sabouri-Ghomi and Mamazizi 2015) conducted an experimental study to investigate the effect of rectangular openings on SPSWs. Two rectangular openings placed at different locations of the infill plate were considered. Three stiffened SPSW specimens were tested under quasi-static cyclic loading and the results showed an equal reduction in strength and stiffness regardless of the distance between the two openings.

Since thin steel infill plates of SPSWs have a large load-bearing capacity even after buckling due to the formation of tension field, unstiffened SPSWs with thin infill plates are commonly used by engineers. Plate buckling and the resulting deformations may not necessarily be an issue for a solid infill plate; however, for infill plates with rectangular openings, these deformations may raise serious concerns. Especially, relatively large out-of-plane deformations are a major concern for any nonstructural element placed in the opening. A recognized method to improve the behaviour of SPSWs is attaching stiffeners to the steel infill plate. Using Vertical and horizontal stiffeners divides the plate into subpanels and can prevent the global buckling of the plate. Stiffened steel plate shear walls are proven to have higher shear strength, stiffness, and energy dissipation capacity. This was observed in the experimental tests by Sabouri-Ghomi and Sajjadi (Sabouri-Ghomi and Sajjadi 2012). A design criterion for stiffeners to prevent the global buckling of the plate and force the buckling into subpanels was proposed by the same authors (Sabouri-Ghomi et al. 2008). An experimental study by Guo et al. (Guo, Hao, and Liu 2015) on the cross and diagonal types of stiffeners showed a 20% increase in yield load in models with cross stiffeners and 5% more in models with diagonal stiffeners. Seismic performance of stiffened SPSWs was studied by Farahbakhshtooli and Bhowmick (Farahbakhshtooli and Bhowmick 2019) and their results revealed that the currently used force modification factors in seismic design for unstiffened SPSWs can also be used for stiffened SPSWs.

Design guidelines for steel plate shear walls with regularly distributed circular perforations are currently available in the current Canadian steel design standard (CSA S16-19), and no

guidelines are available for rectangular openings. This is mainly due to a lack of research on SPSWs with rectangular openings. This paper presents the behaviour of steel plate shear walls with rectangular openings. Nonlinear finite element (FE) analyses are carried out on unstiffened SPSWs with different sizes of rectangular openings. In addition, different arrangements of stiffeners around the rectangular openings are considered and the effectiveness of each stiffener layout in preventing the deformation around the opening is studied using FE analysis. Also, an effective stiffener layout around the rectangular opening is proposed. Finally, an equation is proposed for the shear strength of the infill plate with a rectangular opening stiffened with the proposed stiffener layout.

4.3. Finite element model for steel plate shear walls

In this research, a series of SPSW models with rectangular openings and different stiffener layouts around the openings are analyzed using ABAQUS software (ABAQUS 2014). In all FE models, the frame, infill plate, and stiffeners were modeled using 4-node general-purpose shell element (ABAQUS element S4R). The element S4R has six degrees of freedom (three translations and three rotations) per node. For all the pushover analyses, a non-linear isotropic hardening model was used and for quasi-static cyclic loading, a kinematic hardening model available in ABAQUS was considered.

Before conducting the analysis, the FE modeling approach was validated against a published experimental study on stiffened SPSW (Sabouri-Ghomi and Sajjadi 2012). The length, height, and thickness of the infill plate in the experimental study were 1410 mm, 960 mm, and 2 mm, respectively. The infill plate had four identical stiffeners in each direction with a width of 60 mm and a thickness of 4 mm. The test specimen was subjected to quasi-static cyclic loading.

In the FE model, the frame, the infill plate, and the stiffeners were modeled by using 4-node general-purpose shell (S4R) element. Similar to the experiment, the top beam was restrained against out-of-plane movement and the base of the model was fixed. The beam-to-column connections were rigid. Cyclic loading was applied at the two ends of the top beam following the loading pattern of the experiment. Since the geometry of the model is not complex, a structured mesh control was assigned to the model. A mesh sensitivity study was conducted and based on the

study, a global mesh size of 40 mm was selected for the FE model. To initiate the buckling of the infill plate, an initial imperfection was applied to the model corresponding to the first buckling mode of the plate. Fig 4.1 shows the FE mesh of the tested specimen. Hysteresis curves obtained from the finite element analysis are compared with the test results in Fig 4.2. As shown in Fig 4.2, in general, there is a good agreement between the FE analysis and the test results. Both strength and stiffness of the SPSW obtained from FE analysis are very close (less than 5% difference) to the corresponding values obtained from the test.
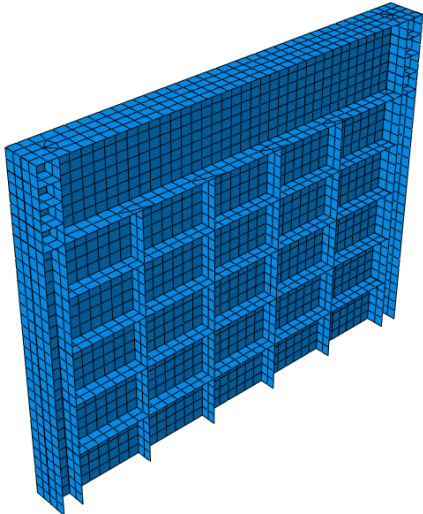
Fig 4.1. Finite element mesh for specimen tested by Sabouri-Ghomi and Sajjadi
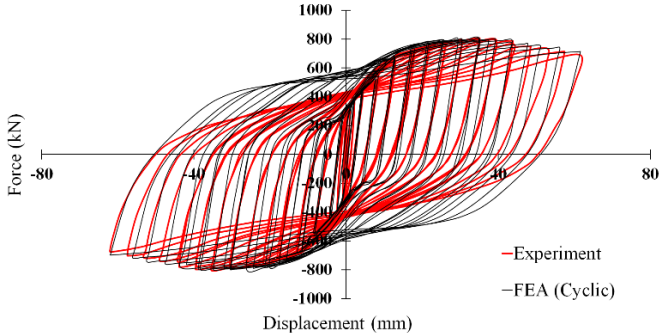
Fig 4.2. Comparison of cyclic analysis with test results of Sabouri-Ghomi and Sajjadi

4.4. Analysis of unstiffened SPSWs with a centrally placed rectangular opening

In order to understand the fundamental behaviour of steel plate shear walls with rectangular openings, five single-storey finite element models with different opening sizes were analyzed. The height and length of the openings were selected as 10, 20, 30, 40, and 50 percent of the height and length of the infill plate.

4.4.1. Selection of the shear walls

The SPSW models selected in this study were part of a hypothetical office building located in Vancouver, Canada. As shown in Fig 4.3, the building is considered to have a symmetrical plan with an equal bay width of 6 m. To resist lateral loads, the building was provided with two SPSWs in each direction. The building foundation was assumed to be on soft rock or dense soil, corresponding to site class C in NBCC 2015 (NBCC 2015). The snow load at the roof level was calculated as 1.64 kPa and the dead load was considered 3 kPa for the roof. All members were designed according to NBC 2015 (NBCC 2015) and CSA S16-14 (CSA 2014). The equivalent static force procedure of the National Building Code of Canada (NBCC 2015) was adopted to calculate the seismic forces. For the calculations, the importance factor (I), ductility-related force modification factor (R_d), and overstrength-related force modification factor (R_o) were assumed as 1.0, 5.0, and 1.6 respectively. A storey height of 3.8 m was considered for the SPSW building.

To design the SPSW system, the angle of inclination of the tension field (α), needs to be determined. It has been shown by Shishkin et al. (Shishkin, Driver, and Grondin 2009) that the angle of inclination in SPSW varies between 38° and 50° and the effect of this variation on the ultimate capacity of the system is very little. Thus, in this study, the angle of inclination (α) was assumed as 45°. Based on practical welding and handling considerations, an infill plate thickness of 3.0 mm was selected for all SPSWs. The boundary frames for SPSWs were designed for the resulting forces from the infill plate yielding. Based on the capacity design method for SPSWs (Berman and Bruneau 2008), the infill plate is the element that dissipates the energy during an earthquake and undergoes extensive plastic deformations while the surrounding boundary elements remain essentially elastic. Plastic hinges are also allowed at the two ends of the beam and at the base of the columns. To ensure that a uniform tension field can develop in the infill plate,

70

the boundary columns of the SPSW must have minimum stiffness. CAN/CSA-S16-14 provides a flexibility parameter to ensure that the boundary columns have the required minimum stiffness. The column flexibility parameter, (ω_h) is given as:

$$\omega_h = 0.7h(\frac{w}{2LI_c})^{0.25} \tag{4.2}$$
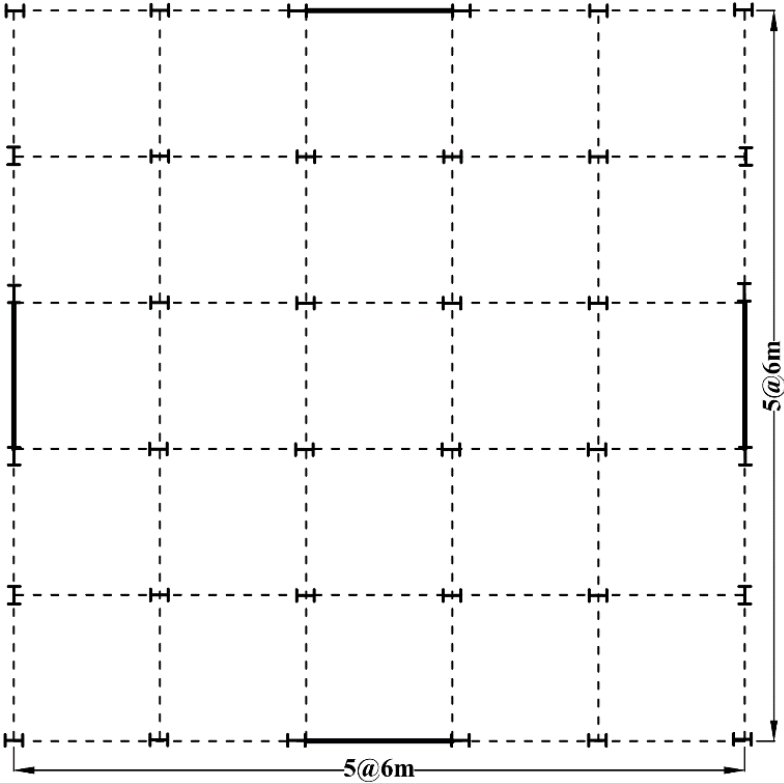
Fig 4.3. Plan view of the hypothetical building with SPSWs

In Eq. (4.2), w, h, and L are thickness, height, and length of the infill plate, respectively; I_c is the moment of inertia of the columns. The final designed beam and column sections for the selected SPSWs are presented in Table 4.1.

Table 4.1. Summary of plate dimensions and frame sections

Plate Height (m)	Plate Width (m)	Plate Thickness (mm)	Column Section	Beam Section
3.8	6	3	W360x262	W460x193

4.4.2. Finite element models and pushover analysis results

The infill plates in the five selected models are unstiffened and a rectangular opening is considered at the center of the plate. The material properties for the plate and boundary elements are shown in Table 4.2.

Table 4.2. Plate dimensions and frame sections for the finite element models.

Element	Yield Stress (MPa)
Infill Plate	250
Stiffeners	250
Columns	350
Beam	350

Nonlinear pushover analysis was carried out for each model with a target drift of 4%. In addition to the five models, a model without an opening was also analyzed for comparison purposes. The results of FE analyses are presented in Table 4.3 and Fig 4.4. Table 4.3 shows the name, opening dimensions, and the maximum value of out-of-plane displacement (U3) around the opening obtained from the FE analysis of each model. The comparison of the obtained pushover

curves for the five selected SPSW models is also shown in Fig 4.4. As expected, a decrease in initial stiffness and shear strength can be observed in all models compared to the solid plate. The decrease in strength and stiffness of the SPSW is more with an increase in opening size. In the model with the smaller opening size (Unstf-Op10%), the shear strength is about 94% of the shear strength of infill plate without opening. In the model with the larger opening (Unstf-Op50%), shear strength drops to about 41% of that of the solid model. The reduction factor mentioned in Eq. (4.1) for Unstf-Op50%, by assuming D as the diameter of the rectangular opening, is also calculated 0.41. This shows that using Eq. (4.1) (with D as the equivalent diameter of the rectangular opening) will lead to correct results for SPSWs with rectangular openings.

As is observed in Table 4.3, due to the early buckling of the infill plate, large out-of-plane deformations take place around the opening. Fig 4.5 shows the out-of-plane deformations in model Unstf-Op40%. The amount of out-of-plane deformation increased as the size of the opening increased. This shows that plates with larger rectangular openings are prone to larger out-of-plane deformations.

Table 4.3. Opening dimensions and the obtained maximum value of out-of-plane displacement around the opening of the unstiffened models

Model Name	Opening Length (mm)	Opening Height (mm)	Maximum out-of-plane deformation (U3) around the opening (mm)
Unstf-Op10%	600	380	120
Unstf-Op20%	1200	760	125
Unstf-Op30%	1800	1140	176
Unstf-Op40%	2400	1520	191
Unstf-Op50%	3000	1900	209
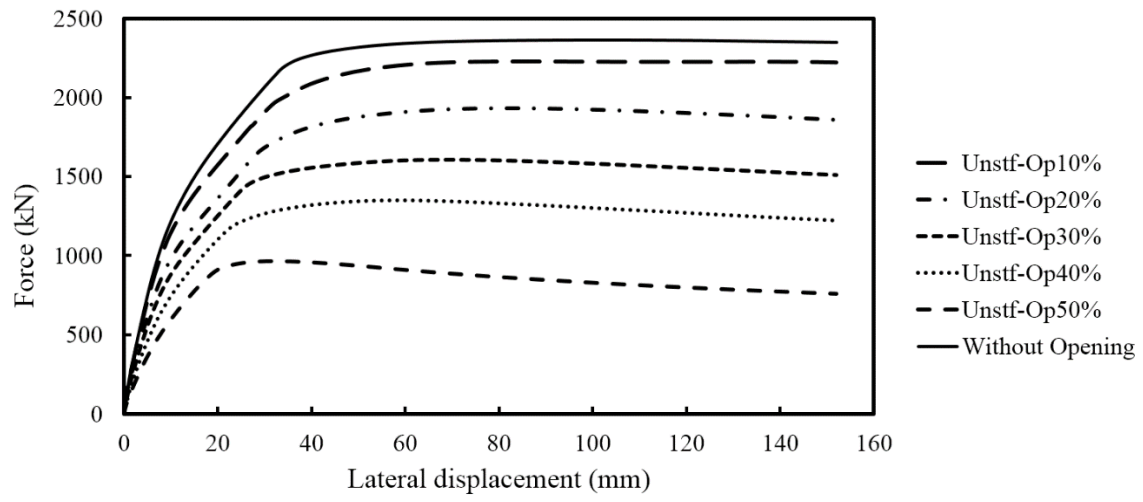
Fig 4.4. Comparison of pushover curves for unstiffened plates with different opening sizes
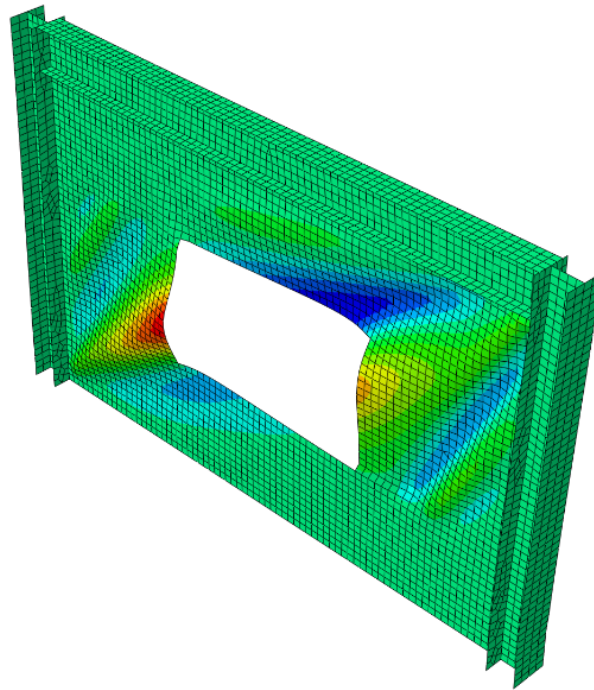
Fig 4.5. Deformed shape of model Unstf-Op40%

4.5. Analysis of stiffened SPSWs with a centrally placed rectangular opening

One of the objectives of this paper was to prevent the deformation around the opening as much as possible and improve the behaviour of the system. As mentioned before, using stiffeners is a recognized method to prevent the global buckling of the plate; therefore, attaching stiffeners to the infill plate was selected as the solution to minimize out-of-plane deformation around the opening.

4.5.1. Stiffeners arrangements

Stiffened SPSWs are usually heavily stiffened. The objective of this study was to find the number of required stiffeners and their arrangement around the opening to effectively prevent or minimize the deformation. While one can achieve this objective by using a lot of stiffeners, the objective here was to use as few stiffeners as possible and improve the behaviour of the SPSW without heavily reinforcing it. Four different stiffener arrangements were tested for this purpose. These arrangements are shown in Fig 4.6.

Stiffeners were attached to both sides of the infill plate in all of the arrangements. For each type of stiffener arrangement, five FE models with opening sizes similar to before (10%, 20%, 30%, 40%, and 50% of the height and length of the infill plate) were analyzed. For all the models, the width and thickness of the stiffeners on each side were 120 mm and 7 mm, respectively. The dimension of the stiffeners was obtained by selecting an initial size and then gradually increasing it until global buckling of the plate was prevented and only local buckling occurred. Fig 4.7 shows FE models for each type of stiffener arrangement. The results of the analyses are presented in Table 4.4. Since the results of the analyses include the shear strength of the infill plates and frame, a model with only the rigid frame was also analyzed to obtain the pushover curves for the infill plates only.

The effect of attaching stiffeners on the out-of-plane deformation around the opening can be observed from the results in Table 4.4. In all models, the out-of-plane deformation significantly decreased compared to the unstiffened models. In almost all models, the amount of out-of-plane deformation is limited to under 10 mm. Fig 4.8 shows deformation around the opening for each type of stiffener layout.

Among the considered stiffener arrangements, Type-4 was found to provide the overall best results. This arrangement has two full vertical and two full horizontal stiffeners covering the four sides of the opening and four short stiffeners placed in the middle of each side of the opening. In the model with the largest opening, the out-of-plane deformation was reduced from 209 mm (for Unstf-Op50%) to less than 5 mm (for Type4-Op50%). It was also observed that adding the middle stiffeners resulted in limiting the in-plane deformation around the opening. The tension field developed in the larger subpanels in type1 to 3, caused larger in-plane deformations to take place around the opening. Adding the middle stiffeners in Type-4 stiffener layout reduced these deformations.
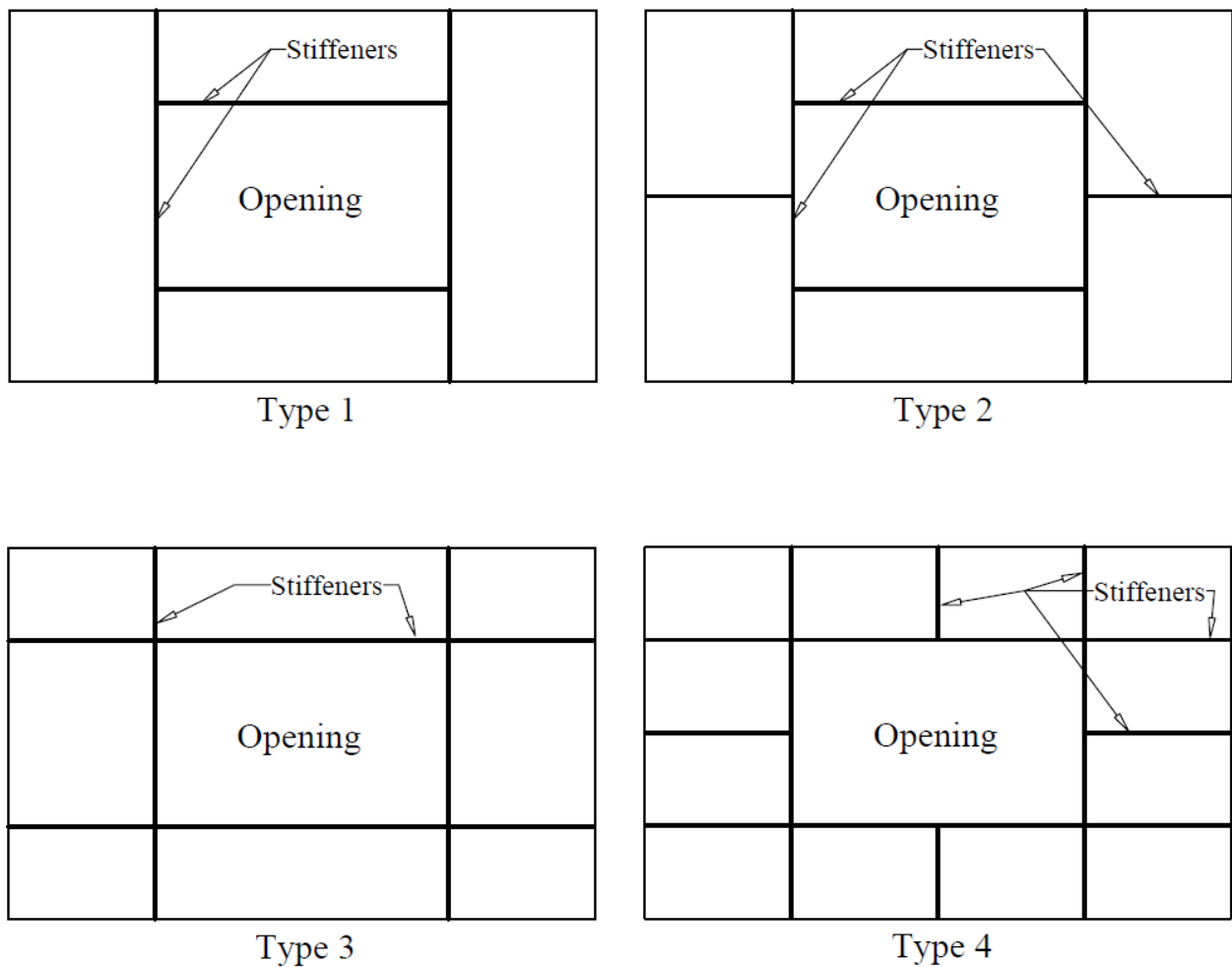
Fig 4.6. Four different types of stiffener arrangements considered for the study
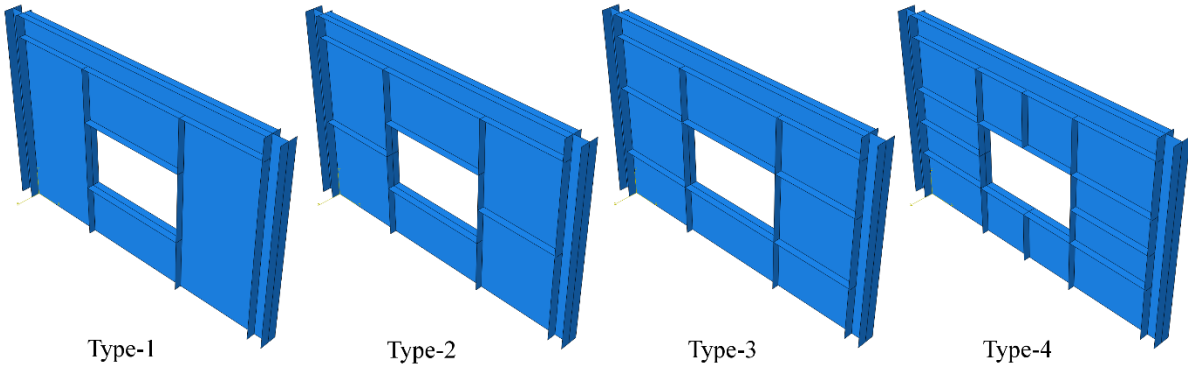
Fig 4.7. Example of FE models created for each type of arrangement

Table 4.4. Opening dimensions and maximum out-of-plane displacement obtained around the opening of the stiffened models

Model Name	Opening Length (mm)	Opening Height (mm)	Maximum U3 around the opening (mm)
Type1-Op10%	600	380	4.6
Type1-Op20%	1200	760	1.9
Type1-Op30%	1800	1140	1.3
Type1-Op40%	2400	1520	2.6
Type1-Op50%	3000	1900	6.4
Type2-Op10%	600	380	1.1
Type2-Op20%	1200	760	1.2
Type2-Op30%	1800	1140	3.5
Type2-Op40%	2400	1520	2.3
Type2-Op50%	3000	1900	4.8

Type3-Op10%	600	380	1.2
Type3-Op20%	1200	760	0.4
Type3-Op30%	1800	1140	5.1
Type3-Op40%	2400	1520	0.2
Type3-Op50%	3000	1900	3
Type4-Op10%	600	380	0.2
Type4-Op20%	1200	760	2.7
Type4-Op30%	1800	1140	2.3
Type4-Op40%	2400	1520	0
Type4-Op50%	3000	1900	4.2

Type1-Op30%   Type2-Op30%   Type3-Op30%   Type4-Op30%
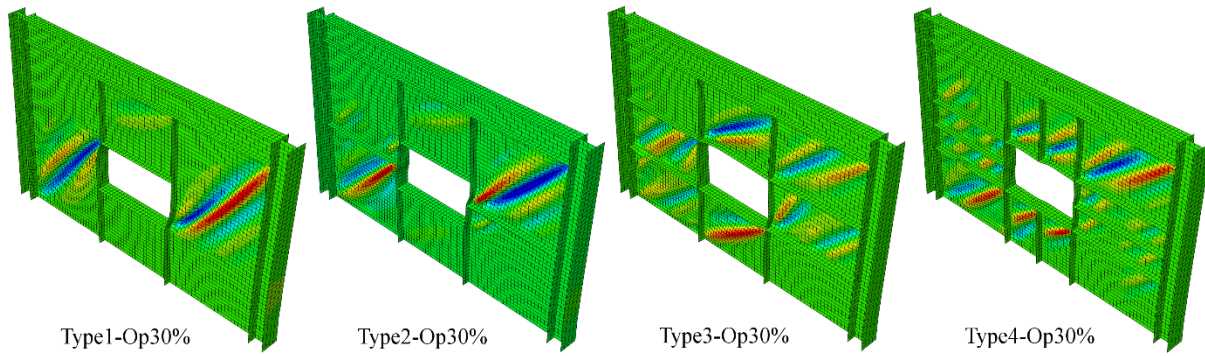
Fig 4.8. Deformed shape of each of the considered stiffener arrangement
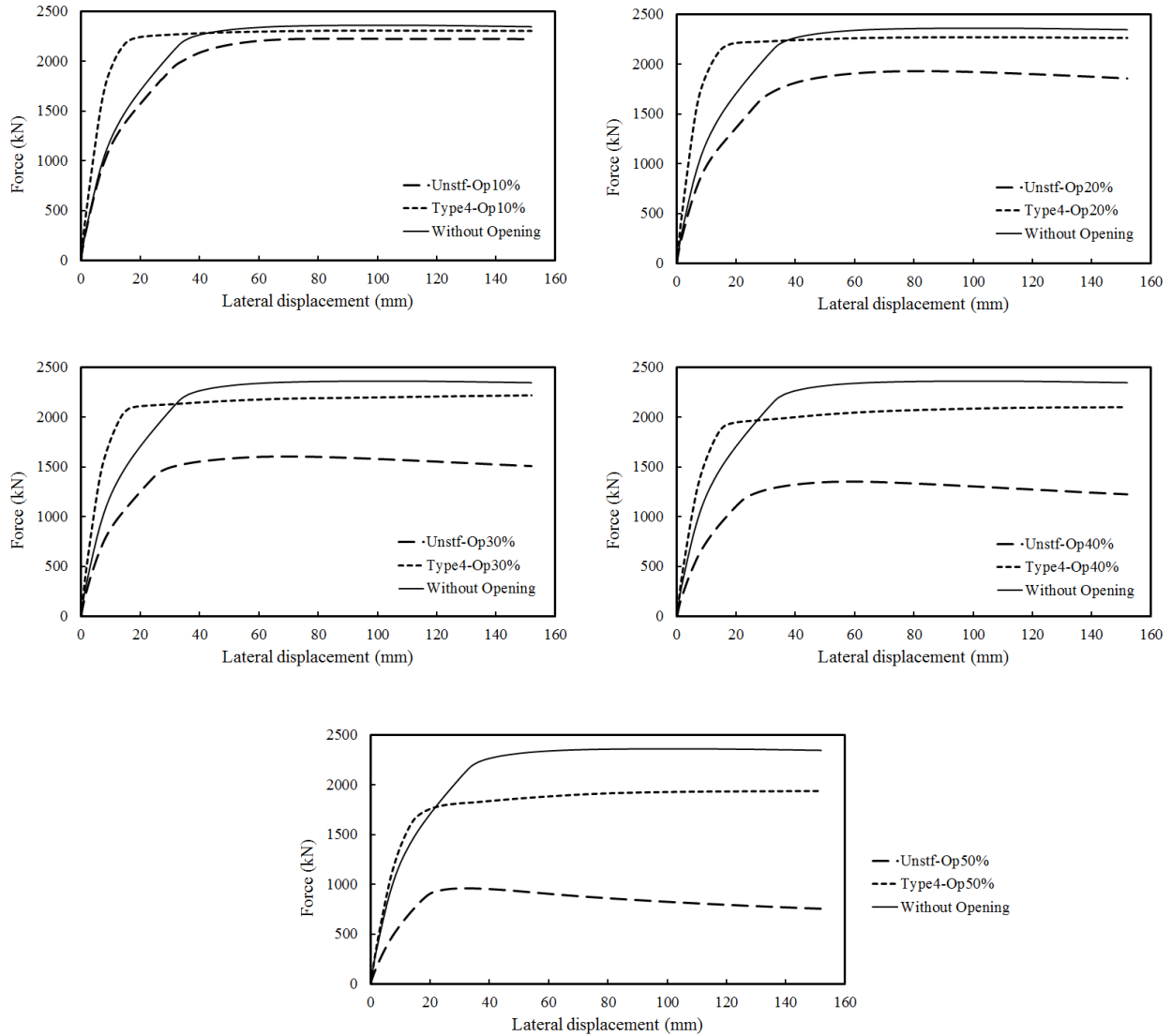
Fig 4.9. Comparison between the pushover curves for the stiffened (Type 4 only) and unstiffened plate for the same opening size

Thus, the Type-4 arrangement was found as the best stiffener arrangement. Fig 4.9 shows the comparison between the pushover curves for the Type-4 arrangement, unstiffened plates with opening, and the plate without opening. As observed in this Figure, the stiffeners improved the behaviour of the system significantly. In comparison to unstiffened plates, the amount of shear strength and stiffness is higher in stiffened plates. The values of these parameters are closer to the solid plate. Therefore, the negative effects due to placing an opening on the plate are reduced when

79

a Type-4 stiffener arrangement is considered on the infill plate. This effect becomes much more apparent as the size of the opening increases. In the plate with the largest opening considered in this study (rectangular opening with 50% of the height and length of the infill plate), attaching the Type-4 stiffener layout increased the shear strength of the plate from 41% of the solid plate to around 82% of the solid infill plate.

4.6. Analysis of stiffened Plates with a rectangular opening in different locations

To evaluate the performance of the selected arrangement when the opening is not placed at the center, a series of models with different opening locations were analyzed. Four opening locations near the corners of the plate were considered for this purpose as shown in Fig 4.10. At each location, five models with opening sizes similar to before were considered. In addition, the Type-4 stiffener arrangement around the opening is considered. Therefore, a total number of 20 models were analyzed in this part. Other properties of the models remained the same as before. The result of the analyses showed that in all 20 models, out-of-plane deformation was under 10 mm. This value was under 5 mm for 17 models. The maximum out-of-plane deformation was 6.8 mm which was for the model C4-OP50%, where C4 indicates the location of the opening which is near the top left corner of the plate. The deformed shape of model C1-OP40% is shown in Fig 4.11.
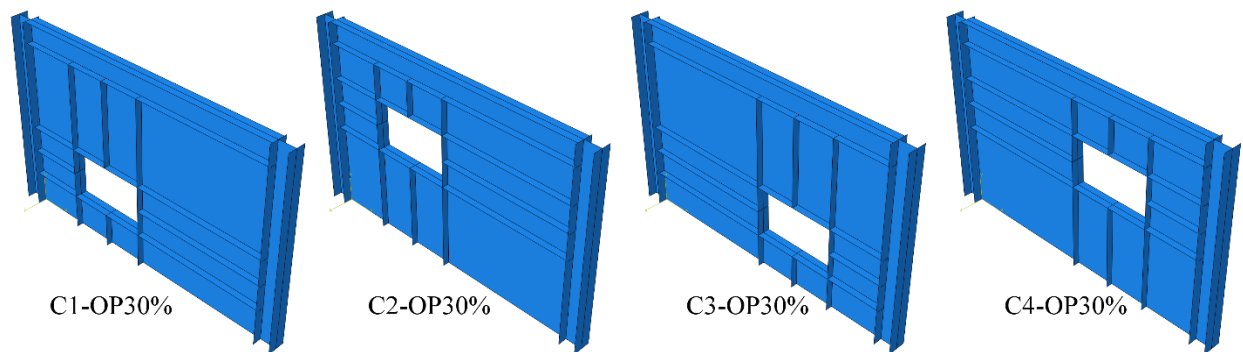
Fig 4.10. SPSW models with rectangular openings in different locations

In addition to the deformation of the plates, their pushover curves and shear strengths were also examined. It was observed that the location of the opening had very little effect on the ultimate shear strength of the panel. As shown in Fig 4.12, for each considered opening size, the shear strength of the stiffened plate is much higher in comparison to the shear strength of unstiffened plate. Also, the shear strength of infill plate with the centrally placed opening is close to the shear strength of plate with openings in other locations.
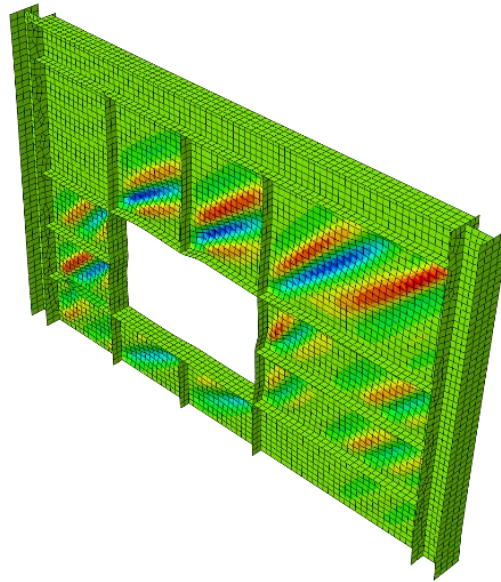
Fig 4.11. Deformed shape of model C1-OP40%
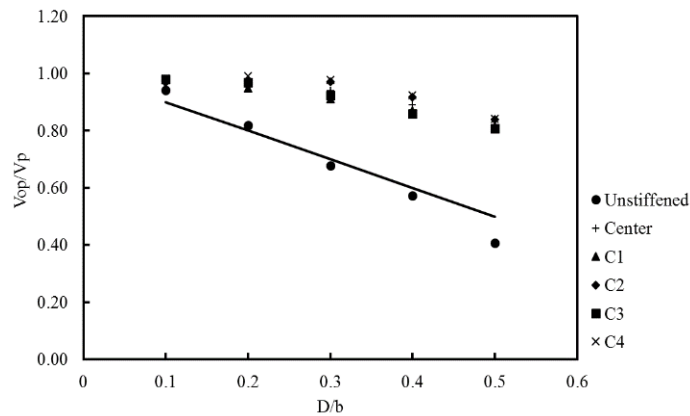
Fig 4.12. Strength ratios of plates with openings to solid plate for different opening sizes and locations

4.7. Development of shear strength equation for stiffened SPSW with rectangular opening

It can be observed from Fig 4.12 that similar to unstiffened plates, there is a correlation between the opening ratio and the strength of the stiffened infill plate with opening. In Fig 4.12, V_{op}/V_P is the ratio of strength of infill plate with rectangular opening to strength of solid infill plate. Earlier research suggested that for SPSWs with rectangular opening, Eq. (4.1) can be used to calculate shear strength of the infill plate with rectangular opening where D can be considered as the length of the rectangular opening. Thus, in Fig 4.12, the solid line is obtained using Eq. (4.1) with D as the length of the rectangular opening. As observed from Fig 4.12, the points for larger openings in unstiffened plates are below the line, meaning that use of D as the length of rectangular opening will lead to incorrect results. However, if D is taken as the diameter of the opening instead of its length, a better correlation is obtained for unstiffened infill plate, as shown in Fig 4.13. The diameter, D, can be obtained by equating the area of the rectangular opening to an equivalent circle.

It is observed from Fig 4.12 that for Type-4 stiffened plate arrangement around the rectangular opening, using Eq. (4.1) results in very conservative estimates, even with the assumption of D as the length of the opening. As shown in Fig 4.12, for larger opening sizes, the calculated shear strength of the plate using Eq. (4.1) is much lower than the values obtained from FE analysis. Thus, it was believed that the shear strength of infill plate with rectangular opening might be function of both length and height of the opening.

To investigate whether the shear strength of the infill plate is affected by both length and height of the opening or only by its length, more FE models were developed. In the developed models, a rectangular opening was placed at the center of the infill plate with a constant height of 0.6×plate height (h). In the new FE models, the length ratios of the rectangular openings (length of the opening/length of the infill plate) were kept same as earlier (i.e. 10%, 20%, 30%, 40%, and 50%).
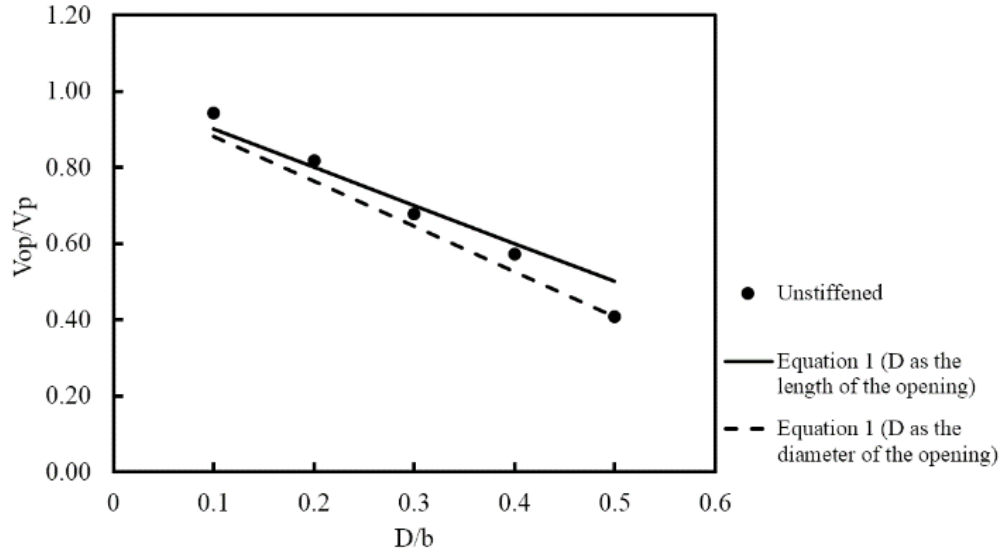
Fig 4.13. Strength ratios of unstiffened infill plates with openings to solid plate

Results from analyses of the new FE models are shown in Fig 4.15. In this figure, the results of the new models (rectangular openings with height of 0.6h) are compared to the results from previous models (original length and height of the rectangular openings). The comparison showed that the two values are very close and changing the height of the opening from h to 0.6h had a negligible effect on the infill plate's strength. This validates that in stiffened plates, strength is solely affected by the length of the rectangular opening. In Fig 4.15, the solid line was obtained using Eq. (4.1), where D was assumed as the length of the rectangular opening. Considering the underestimation of the strength when using Eq. (4.1) for stiffened plates, a calibration factor was applied to the equation based on the results. The dashed line in Fig 4.15 shows the line resulted from the calibration. This line shows that using Eq. (4.3) will result in much more accurate predictions for shear strength of the infill plate with rectangular opening and Type 4 stiffener layout.

$$V_{op} = V_p \left(1 - 0.5\frac{D}{b}\right) \tag{4.3}$$

Eq. (4.3) was also checked for plates with different opening locations. The dashed line in Fig 4.16 represents the calibrated equation. In this figure all points are located above the line,

83

which shows that Eq. (4.3) can predict the shear strength of the infill plate when the rectangular opening is placed at other locations of the infill plate.
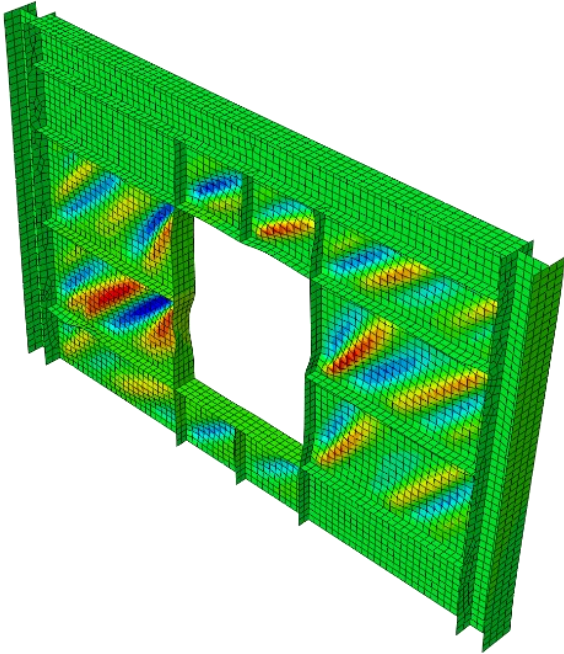
Fig 4.14. Deformed shape of model with 0.3b for opening length and 0.6h for opening height.
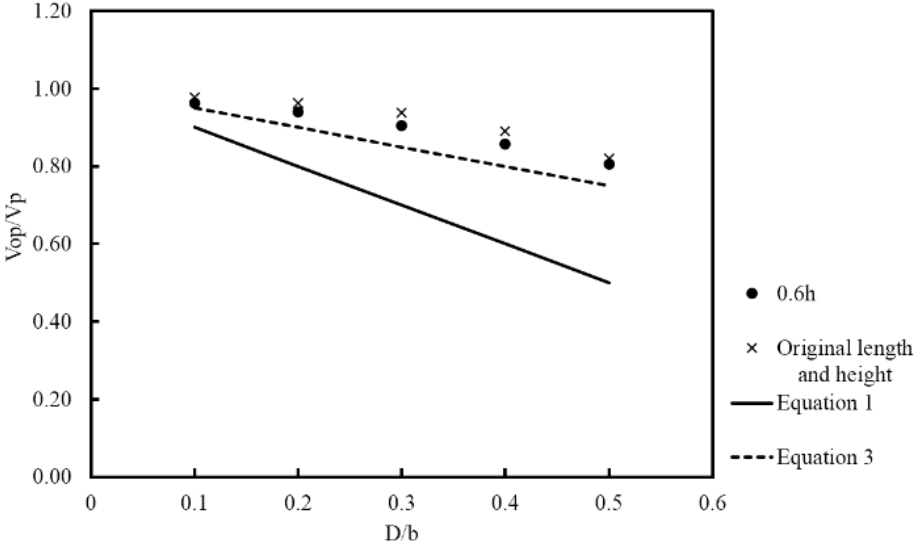
Fig 4.15. Strength ratios of plates with openings to solid plate for openings with constant height
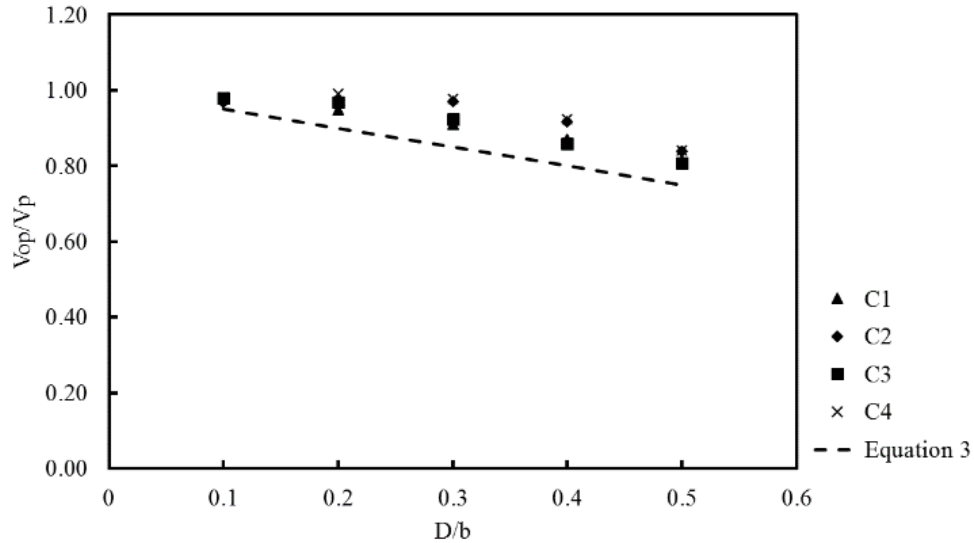
Fig 4.16. Strength ratios of plates with openings to solid plate for different opening locations

It should be noted that Eq. (4.3) is specific to the Type 4 stiffener arrangement and for other type of stiffener arrangement, different shear strength equation might be needed.

4.8. Conclusions

A series of finite element analyses were performed on unstiffened and stiffened steel plate shear walls with rectangular openings. Different sizes, locations, and aspect ratios for openings were considered. Results from analyses of the unstiffened SPSWs showed a decrease in shear strength and stiffness, especially in models with larger openings. In addition, due to the buckling of the infill plates, large out-of-plane deformations were observed around the openings.

To reduce the negative effects of rectangular openings, stiffened infill plate around the opening was proposed as a solution. Four different configurations of stiffeners were studied and the one providing the best results was found. The proposed solution uses four full stiffeners and four short stiffeners to prevent the buckling of the plate. Results showed that stiffened plates using the proposed stiffener arrangement limit the out-of-plane deformation around the opening, lower than 5 mm. Additionally, it increased the shear strength and stiffness of infill plates with

85

rectangular openings significantly. These effects were also confirmed for different opening locations. The effect of changing the opening location was observed to be minor.

Results for stiffened plates with varying opening sizes and locations showed that using Eq. (4.1) will lead to very conservative results. FE models with different opening aspect ratios showed that the shear strength of the stiffened infill plate depended only on the length of the opening. Finally, a newly revised equation was developed for the shear strength of stiffened SPSW with a rectangular opening with the recommended stiffener layout. FE analysis results showed that using the proposed equation provided much more accurate results for the recommended stiffener layout proposed in this study even when the rectangular openings were placed at other locations of the infill plate.

CHAPTER 5

Experimental and numerical study of stiffened steel plate shear walls with rectangular openings[3]

5.1. Abstract

Steel plate shear walls (SPSWs) often need to accommodate rectangular openings on the infill plate. When the SPSW, if unstiffened, is subjected to lateral loadings, such as earthquakes, large deformations may take place around the opening as a result of the thin plate buckling. This paper presents a stiffener layout to limit the deformations around the rectangular opening in the SPSW system. The effectiveness of the proposed layout is investigated by conducting experimental tests on two one-third-scale single-storey SPSWs with openings. Both specimens have a rectangular opening at the center of the plate with different sizes. To prevent deformation around the opening, the plates for the two test specimens are stiffened around the opening without making the system heavily reinforced. Quasi-static cyclic loading tests are performed on the specimens and the deformations around the openings are measured at different stages. Tests show that the proposed stiffener layout can successfully restrain the deformations around the opening. The specimens also show stable hysteresis curves and good energy dissipation capacity. Seismic analyses are also performed on 4-storey stiffened and unstiffened SPSWs with rectangular openings to investigate the seismic response of SPSW with the proposed stiffener layout around the openings. Seismic analyses show that the proposed stiffener layout around the rectangular opening can prevent out-of-plane deformation around the opening in the SPSW system.

---

[3] A revised version of this chapter has been submitted and is under review in *ASCE Journal of Structural Engineering*

5.2. Introduction

Steel plate shear wall (SPSW) has been recognized as an effective lateral load resisting system. Large energy dissipation capacity, high shear strength, and stiffness are some of the main advantages of this system. Various experimental and numerical studies have shown these advantages and the benefits of using SPSWs (Thorburn et al. 1983; Driver et al. 1998a; Bhowmick, et al. 2009; Berman and Bruneau 2005; Lubell et al. 2000; Purba and Bruneau 2015; Astaneh-Asl and Zhao 2002). Therefore, many buildings around the world, especially in North America, have employed this system (Bruneau and Sabelli 2006). Openings in SPSWs are sometimes required by architectural design or to accommodate utilities through the SPSW system.

A number of studies have been conducted on perforated SPSWs. In 1992 the first study on this type of system was carried out by Roberts and Sabouri-Ghomi (Roberts and Sabouri-Ghomi 1992). Sixteen unstiffened steel plate shear walls with a centrally placed circular opening were tested under quasi-static cyclic loading. The results of the experiments showed a reduction in shear stiffness and strength of the SPSW system with centrally placed circular opening. Based on the results, an equation was proposed to estimate the shear strength and stiffness of perforated SPSWs. Vian and Bruneau (Vian and Bruneau ; Vian et al. 2009) conducted an experimental and analytical investigation on SPSWs with a series of small regularly-spaced circular perforations. This specific form of perforations was also studied by Purba and Bruneau (Purba and Bruneau 2009) and a formula to calculate the shear strength of SPSW with regularly spaced circular perforations was proposed. Other numerical studies (Bhowmick et al. 2014; Barua and Bhowmick 2019; Farahbakhshtooli and Bhowmick 2021) on the seismic performance of plates with single or multiple circular openings were conducted and more design recommendations were proposed. While several experimental and numerical studies on SPSWs with circular openings are available, research on SPSWs with rectangular openings is limited. Rectangular openings are often required by architectural design for nonstructural elements such as windows or doors. Sabouri-Ghomi and Mamazizi (Sabouri-Ghomi and Mamazizi 2015) conducted three experimental tests on the effects of rectangular openings on SPSWs. The single storey one-third test specimens had two rectangular openings and they were tested under quasi-static cyclic loading. The difference between the three specimens was the distance between the two rectangular openings. Results from these tests showed a reduction in the strength and stiffness of the SPSW, and there was no difference found in the strength, stiffness, and energy dissipation capacity between the three specimens.

When a rectangular opening is placed on the infill plate, one of the main concerns is the deformation around the opening, especially the out-of-plane deformation due to the early buckling of thin steel plates. One of the known methods to improve the behaviour of the SPSW system and prevent the global buckling of the infill plate is using stiffened plates. It was first proven by Takahashi et al in an experimental study (Takahashi et al. 1973) that attaching stiffeners can change the shear buckling mode of a thin steel plate from global to local. Later, various experimental and numerical studies (Sabouri-Ghomi and Sajjadi 2012; Guo, Hao, and Liu 2015; Farahbakhshtooli and Bhowmick 2019) show the same effects and benefits of using stiffeners. The objective of this research is to limit the deformation around the rectangular opening by using stiffeners and at the same time without heavily reinforcing the infill plate. A recent finite element study by the authors (Sabouri-Ghomi et al. 2022), proposed a simple stiffener configuration around the rectangular opening to achieve this objective. In this layout, four long stiffeners are attached to each side of the rectangular opening. The long vertical stiffeners are extended the full storey height and the long horizontal stiffeners are extended the full bay width. In addition, four short stiffeners are attached at the middle of each side of the opening, perpendicular to the long sides. The current Canadian standard [23] does not provide any provisions for steel plate shear walls with rectangular openings. American steel design standard, AISC 2016 [24], allows the placement of rectangular openings on the infill plate of SPSWs and requires adding local boundary elements (W-shape sections) around the opening. This paper studies an alternative solution to the AISC recommendations that do not use heavy reinforcements such as W-shape local boundary elements around the openings. The proposed alternative is simpler to construct, uses less material, and reduces the weight of the SPSW system. In this study, the proposed stiffener layout around the rectangular opening is investigated by conducting experimental tests on two one-third-scale single-storey SPSW specimens with different opening sizes. In addition, nonlinear seismic analyses of a 4-storey SPSW with a rectangular opening stiffened with the proposed stiffener layout are conducted to investigate the effectiveness of the proposed stiffener layout.

5.3. SPSW specimens' characteristics

For this study, two one-third-scale single-storey specimens were considered. The two specimens were named SPSW-OP50% and SPSW-OP35%. The specimens had a rectangular opening placed

at the center of the infill plate. The length and height of the opening for the SPSW-OP50% specimen were 50% of the plate's length and height. For the SPSW-OP35% specimen, these values were 35% of the plate's length and height. Both specimens had four full stiffeners covering four sides of the opening and four short stiffeners at the middle of each opening side. All the other elements were identical for the two specimens and they were designed according to the Canadian and American steel design standards (ANSI/AISC 2016; CSA 2014). The details for the specimens can be seen in Fig 5.1. The height, length and thickness of the plate of the specimens were 960 mm, 1410 mm, and 2 mm, respectively.

In SPSW systems, the infill plate is usually attached to the boundary members by using fishplates. Here, an angle with a size of 60x60x6 mm was used as the fishplate. The infill plate was overlapped with the fishplate and connected to it by using continuous welding to the fishplate. A strong beam at the bottom of the specimens was used to connect the specimen to the strong floor of the laboratory by using high-strength bolts.
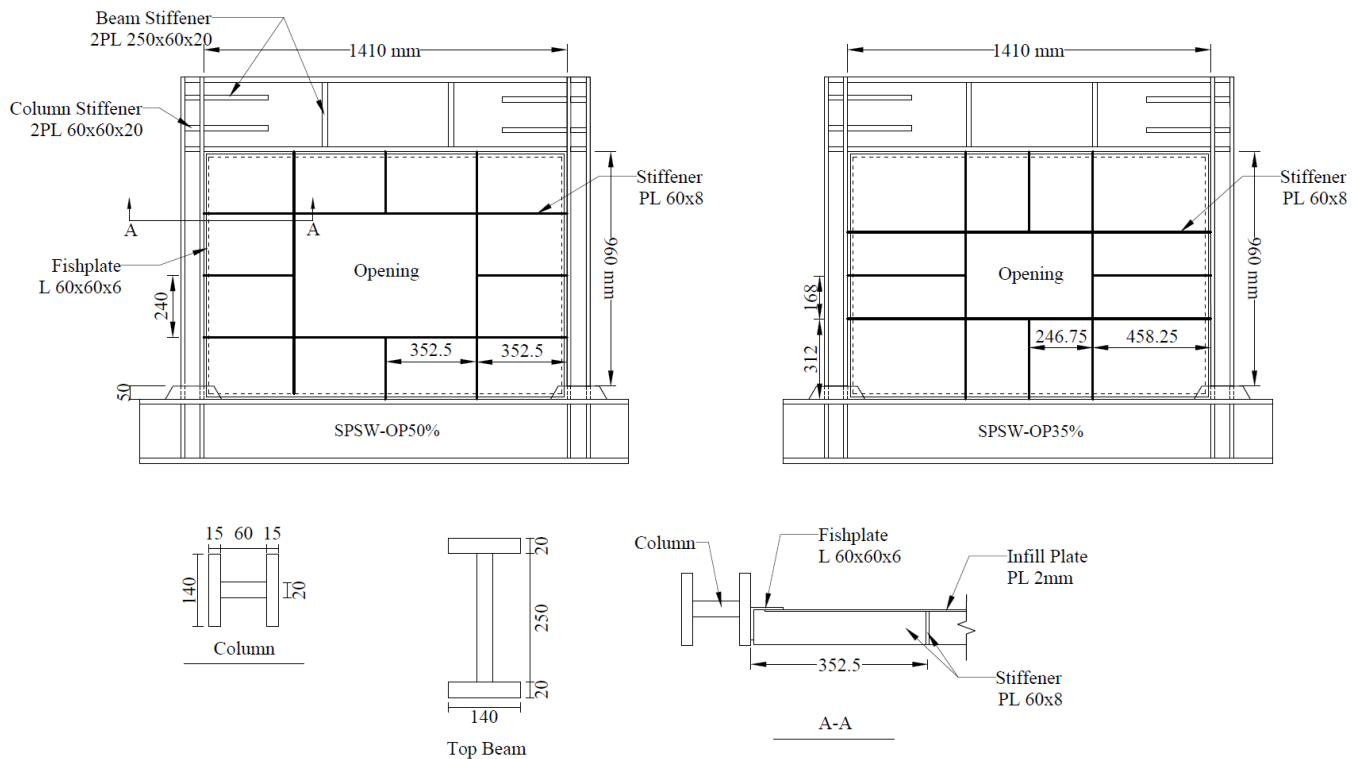
Fig 5.1. Specifications of the two specimens

As explained before, the reason behind using stiffeners was to prevent the global buckling of the plate and reduce the deformation around the opening. In order to achieve this, stiffeners must be strong enough to force the plate into local buckling. The plate stiffeners in this study had a thickness of 8 mm and depth of 60 mm and were attached to one side of the infill plate. The size of the stiffeners was obtained by conducting finite element analysis and gradually increasing the size until local buckling was achieved. FE analysis also helped predict the overall behaviour of the specimens before conducting the experiments. In order to attach the stiffeners to the plate, two different approaches were used. For the SPSW-OP50% specimen, continuous welding on one side of the stiffeners was used. For the SPSW-OP35% specimen, staggered intermittent welding was used.

Table 5.1 presents a summary of the properties of the steel materials used in the tests. Testing for the materials was conducted by preparing tensile test coupons. High-strength steel was used for the surrounding beams and columns, and lower-yield point steel was used for the infill plate.

Table 5.1. Material properties for the specimens

Element	Yield stress (Mpa)	Ultimate stress (Mpa)	Modulus of elasticity (Gpa)
Infill Plate	173	283	201
Beam and columns	395	542	210

5.4. Test setup

The tests were carried out at K. N. Toosi University of Technology structures laboratory. Various methods and instruments were employed to measure and record important parameters and actively monitor the behaviour of the specimens during the experiment. In this section the methods and instruments are described.

5.4.1. Whitewash and grid

The first step in preparing the test setup was applying whitewash (mixture of water and lime) to the specimens. Whitewash is a simple but helpful tool to visualize and observe yielding on test

specimens. During loading, white wash gradually flakes off in regions of yielding and reveals the yielding pattern in different areas of the specimens. Whitewash was applied a day before each test and prior to applying the whitewash, the models were cleaned.

Buckling of the infill plate was also a key event for this experiment. Detecting the buckling mode of the infill plate was very crucial for evaluating the specimens' performances. In the late stages of the experiment, it was expected to clearly observe the buckling; however, in the early stages, minor deformations on the infill plate can be difficult to detect by observation. Thus, a grid with an approximate size of 50 by 50 mm was drawn on the infill plates for better visualization of the buckling of the plate.

5.4.2. Instruments

The stiffeners divided the infill plates into a total number of 12 subpanels. Depending on their size and location, these subpanels can be categorized in three types: top or bottom subpanels, side subpanels and corner subpanels. To measure the strains on the subpanels, plastic strain gauges were installed on one subpanel of each type of subpanels. Plastic strain gauges were also installed on the exterior flanges of both columns near the top and bottom, where yielding was expected to take place.

In order to measure the storey drift of the specimens, two linear variable displacement transducers (LVDTs) were installed on the bottom flange of the top beam. LVDTs were also used to measure in-plane and out-of-plane displacements of the opening. For in-plane deformation measurement, four LVDTs were placed vertically or horizontally at the top and right sides of the opening. For out-of-plane deformation measurement, four LVDTs were placed perpendicular to the plane of the plate on different locations around the opening. The locations of all the instruments are shown in Fig 5.2.

All of the strain gauges and LVDTs were connected to a 32 channel data logger which logged data at 1 second time intervals. During the tests, all the data from the data logger was actively being recorded and monitored.
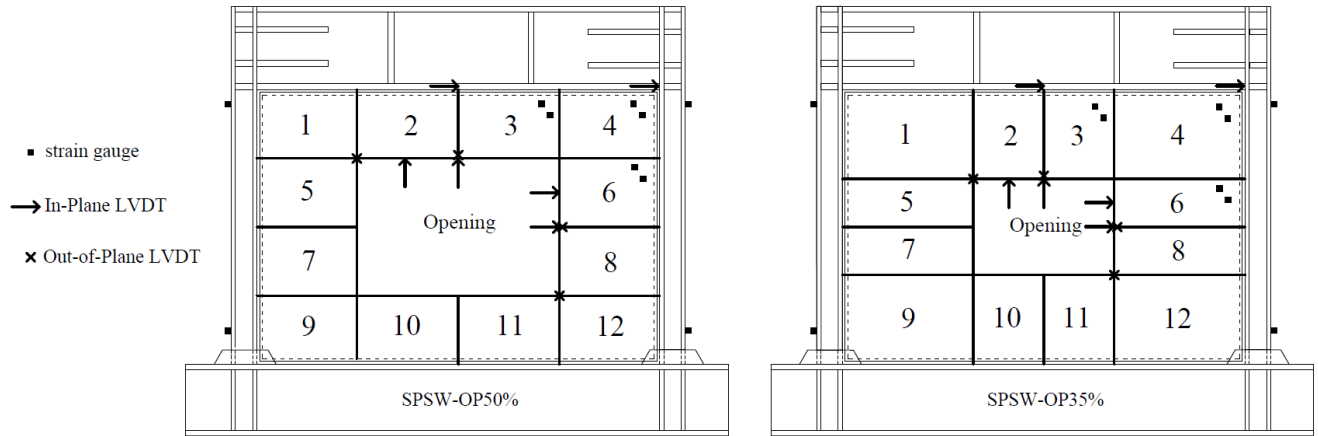
Fig 5.2. Installed instruments' locations and subpanels numbering

5.4.3. Photogrammetry

Although a few LVDTs were installed to measure the deformations around the opening, the number of points to collect data for the purpose of this experiment was not nearly enough. Due to the limited space around the opening, it was not practically possible to install more than a few LVDTs in that area. This fact was recognized before designing the experiment and photogrammetry was selected as a better approach.

Close-range photogrammetry is a powerful tool that can be used to determine three-dimensional coordinates and measure displacements of points on an object. This approach allowed for the measurement of the displacements of many more points around the opening. The drawback of this approach is that it is not continues. The test has to be paused for a few minutes to take the required photos which can be time consuming. Therefore, the procedure was done at four stages during each experiment: at the beginning, at plate yielding, at 2% drift, and at the end of the experiment.

The photogrammetry procedure has two main steps. The first step is done by taking a set of photos of a subject at different angles. In the second step, the photos are processed in an image processing software. In this study Agisoft Metashape (Agisoft 2021) was used for the image processing. For the first step, the photos can be taken using a digital camera and Metashape recommends using camera with a reasonably high resolution (at least 5 megapixels). In this study,

a Canon G7 X Mark II camera with a 24–100 mm focal length, F1.8–2.8 maximum aperture lens and 20 megapixels resolution was used. In order to obtain high quality data for image processing, the following guidelines were followed while taking photos:

- Taking photos using the maximum resolution provided by the camera.

- Setting the focal length to its minimum value and keeping it consistent during all shooting sessions.

- Avoiding high ISOs to reduce the image noise.

- Using a high enough aperture to maintain sufficient focal depth and avoid blurry images.

- Removing any obstructions in the line of photo.

- Filling most of the image frame with the main subject of the photo (the specimen).

- Taking photos at a variety of directions.

- Taking a least three photos at each direction to ensure high clarity in at least one of the images.

Although the software does not require a minimum number of photos for close-range photogrammetry, it states that "more than required is better than not enough". In this study, considering the placement of the specimens and space limitations, the angles shown in Fig 5.3 were used to take the photos. The software does not require for the full object to be visible in all images. If a part of the object is missing in a taken photo it can be reconstructed by the software as long as it is visible in at least two other photos.

The software provides coded and non-coded markers that can be detected by the software during the image processing. These markers were attached to the specimens in different locations. The non-coded markers were attached around the opening. Four coded markers were attached to the corners of the opening. A set of six coded markers were also attached on a plate to the bottom left of the specimen. In the image processing, when the set of photos are imported in the software, coded markers are first detected by the software. The taken photos are then aligned by searching for feature points on the photos and matching them across images into tie points. The camera position for each photo is also found and camera calibration parameters are refined. As the result,

94

a tie point cloud model is visualized by the software. At this point, non-coded markers can also be detected by the software. In order to find out the coordinates of each point, known coordinates should be introduced to the software. For this purpose, the distances between a few of the markers were measured before each test.

Vertical directions   Horizontal directions
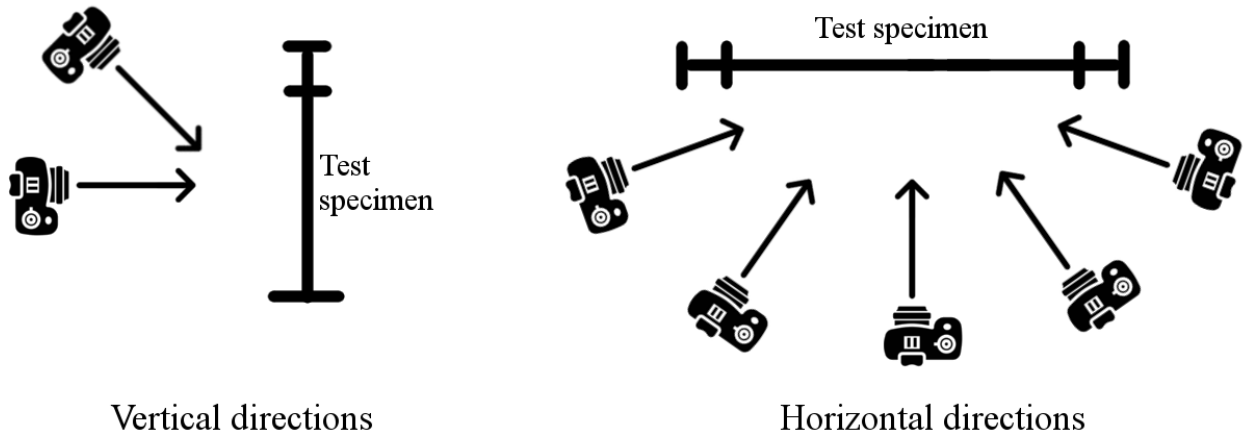
Fig 5.3. Camera angles for the photogrammetry

5.4.4. Loading

Quasi-static cycling loading was applied horizontally to the specimens at one side of the top beam by a hydraulic actuator with a capacity of 2000 kN. To prevent torsional and out-of-plane deflections of the specimens, the top beam was braced at the top against out-of-plane movement. The test setup before the experiment is shown in Fig 5.4. The Applied Technology Council, ATC-24, guidelines (ATC-24 1992) were adopted for the cyclic load pattern. According to the recommendations of ATC-24, at least six cycles with a peak amplitude less than yielding deformation (δ_y) should be carried out. Peak deformation of δ_y and the next two target displacements should all have at least three cycles. The rest of the target displacements can have two cycles. The general loading procedure used in the experiments is shown in Fig 5.5. Based on

the ATC-24 guidelines, the test before any significant yielding was carried out under load controlled condition, and after yielding, displacement controlled test was implemented.
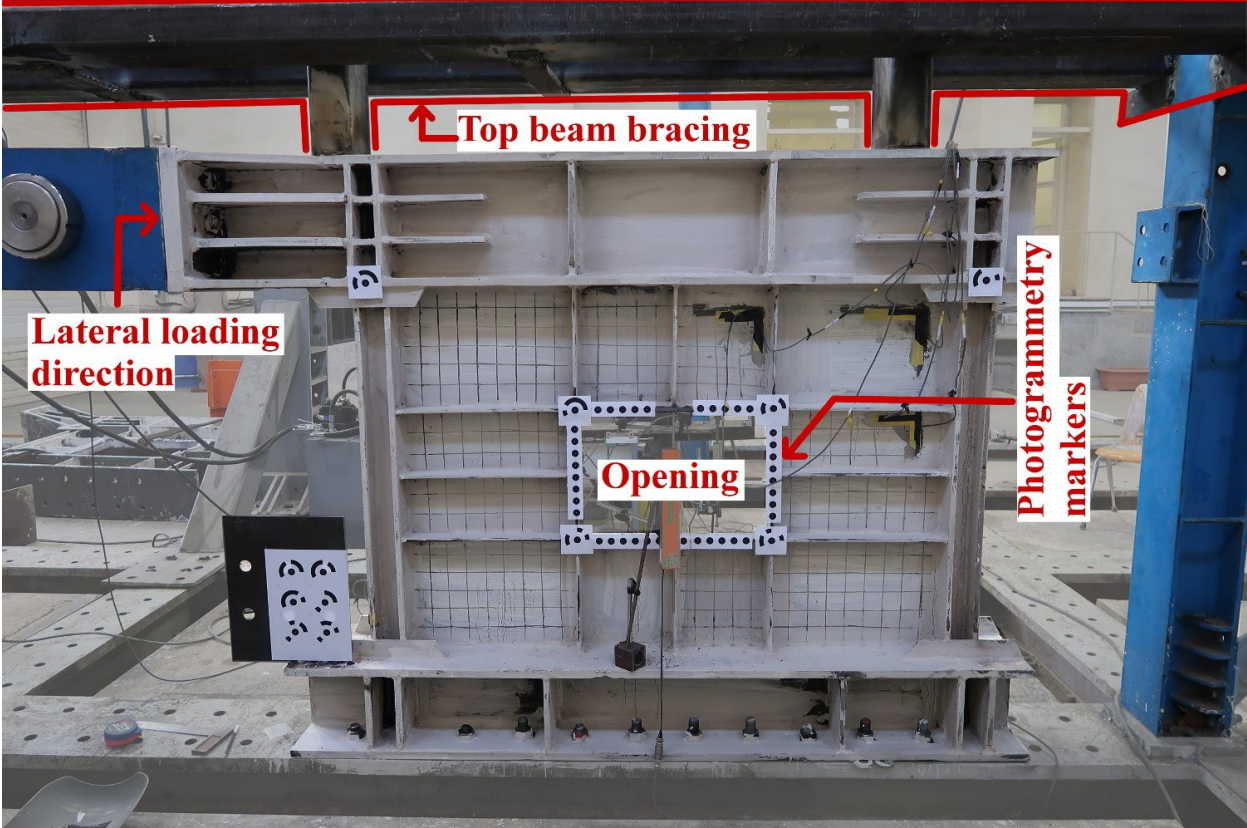
Fig 5.4. Test Setup before the experiment
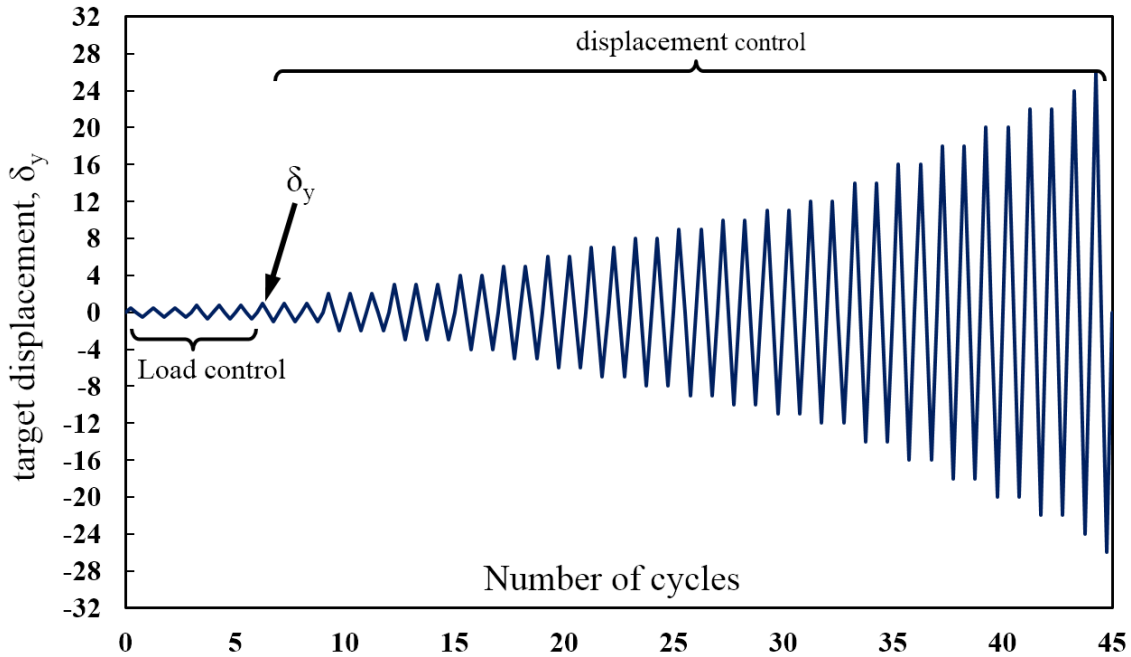
Fig 5.5. Lateral load history based on ATC-24

5.5. Tests descriptions and events

5.5.1. SPSW-OP50% specimen

At the first six cycles of loading, no yielding or buckling was observed in the specimen. The first major yielding in the plate happened at the seventh cycle of the test at around 1.7 mm displacement (0.18% drift). The first yielding was identified from the data from the strain gauges installed on the plate and also from the load-displacement curves of the specimens, which were actively monitored during the tests. Since FE analysis was conducted before the test, an estimation of the first yielding was also available. Thus, all the data was carefully studied around the expected first yielding point during the test. At the tenth cycle, very slight buckling was observed in subpanels 5, 6, 7, and 8. The buckling in these subpanels became more visible by the thirteenth cycle. At this point, whitewashing was also visibly flaked off in some of the subpanels. During the next six cycles, buckling became visible in all of the subpanels, and it became apparent that local buckling was taking place in the infill plate. Fig 5.6 shows the state of a subpanel on the right side of the opening at cycle seventeen. The first tearing happened near the center of subpanel number 6 at cycle twenty-seven. This event was at 15.3 mm displacement (1.6% drift) and the length of the

97

tearing was no more than 2 mm. Whitewash was also visibly flacked off all of the in subpanels. In subpanels 5, 7, 8, and 9 Whitewash was flacked of in an X-shape. Fig 5.7 shows the state of the subpanels 5, 8, and 12 in cycle 27. At 2% drift, small tearing was visible, in an X-shape, in subpanels 5, 6, 7, and 8. A small tear was also observed at the top left corner of the plate. Despite the tearing in the subpanels, the plate still held its continuity, and no major effect on the strength of the specimen was observed. Fig 5.9 shows the specimen at 2% drift. As the cyclic loading continued and larger lateral displacements were imposed on the specimen, tearing occurred in all subpanels, and the length of the tearing increased. An example of one of the subpanels is shown in Fig 5.8.
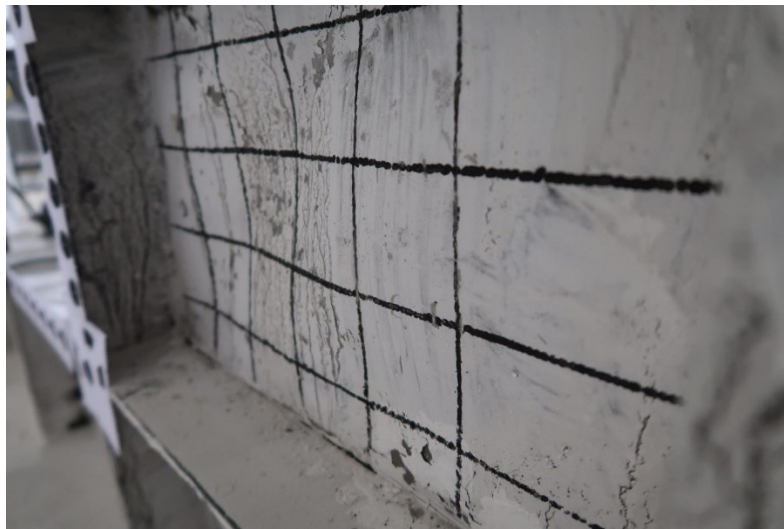
Fig 5.6. A subpanel of SPSW-OP50% in cycle 17 showing local buckling and flaked off whitewashing

Fig 5.7. Subpanels 5, 8, and 12 of SPSW-OP50% in cycle 27 showing local buckling and flaked off whitewashing
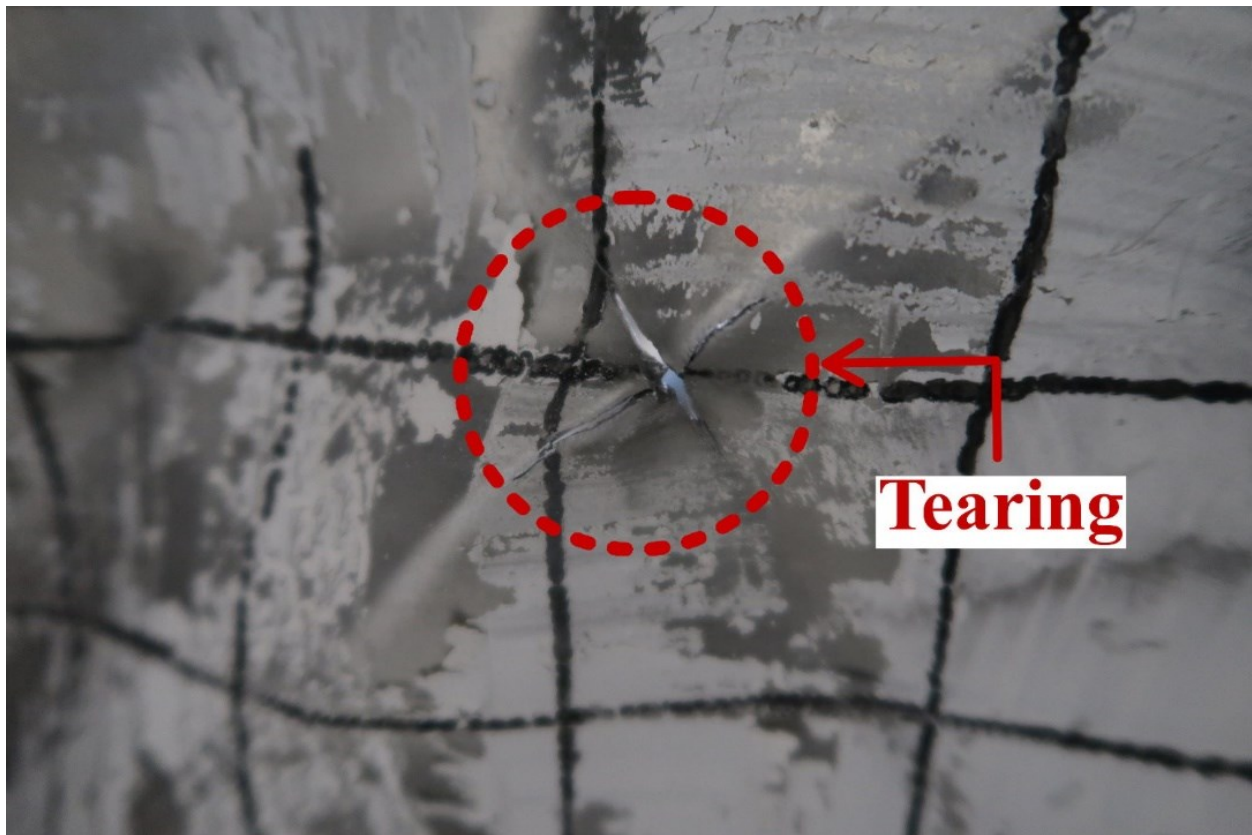
Fig 5.8. Tearing on the subpanels of SPSW-OP50% specimen

The test was stopped after 46 cycles when load bearing capacity of the specimen dropped to around 80% of its maximum capacity. The displacement at the last cycle was 57.8 mm (6% drift), and the ultimate strength of the specimen was around 647 kN. At the end of the experiment, all of the subpanels were severely deformed due to local buckling. Also, tearing was observed in the subpanels, mostly in X-shaped patterns. In-plane deformation was also visible for the stiffeners around the opening. Yielding was observed near the top and bottom of both columns. Fig 5.10 shows the specimen at the end of the experiment.

Fig 5.9. The deformed shape of SPSW-OP50% at 2% drift
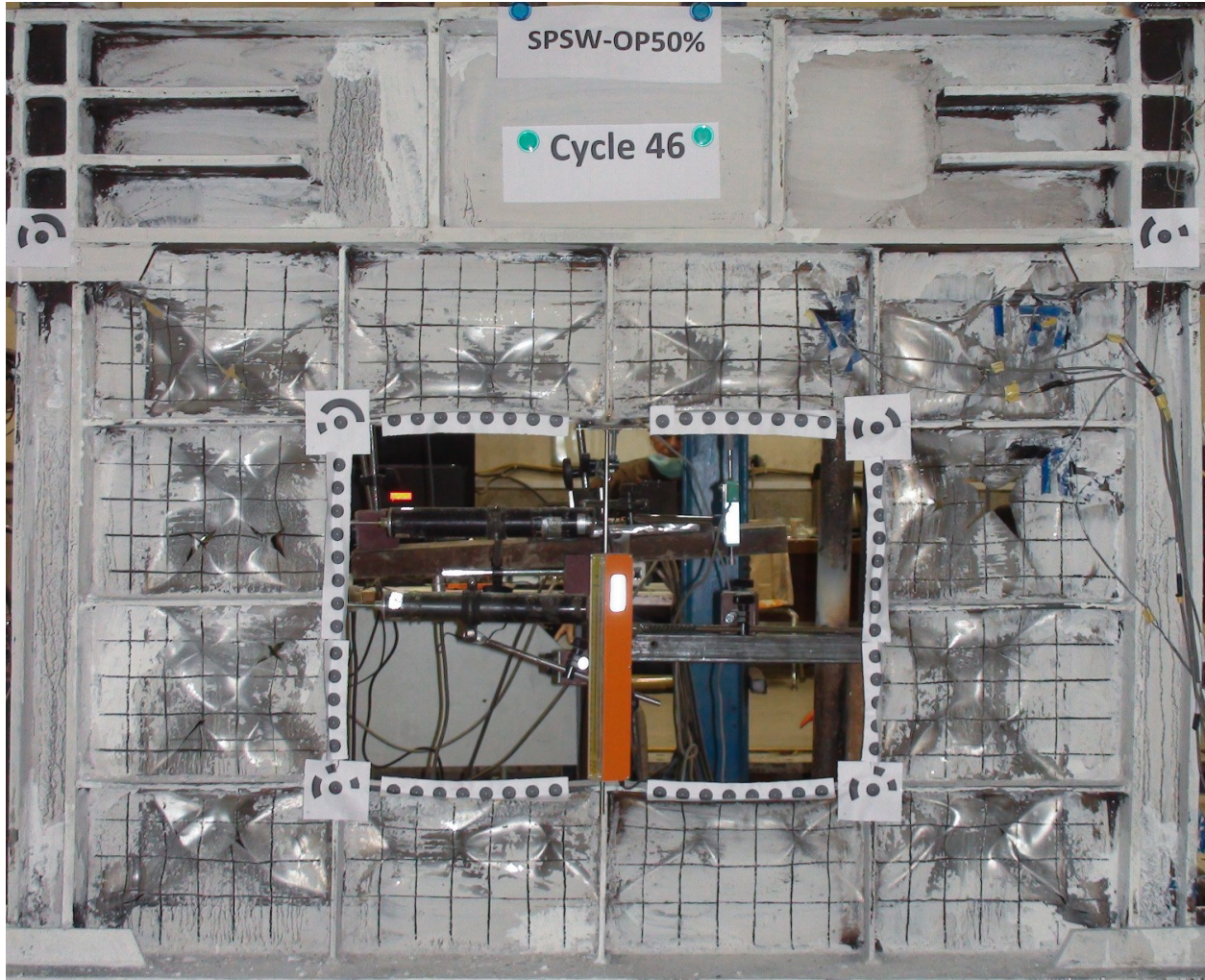
Fig 5.10. The deformed shape of SPSW-OP50% at the end of the experiment

5.5.2. SPSW-OP35% specimen

The first significant yielding in the infill plate happened after six cycles of loading at around 1.6 mm displacement (0.17% drift). Before this, no significant yielding or buckling was observed in the specimen. Minor buckling started to become visible in all four corner subpanels at the eleventh cycle. At the end of the fourteenth cycle, local buckling was developed in all of the subpanels. At cycle eighteenth, buckling was more visible and whitewash was flacked of in some parts of the subpanels. The first tearing happened at cycle twenty-six in subpanel number 9. The length of the tearing was very small and at this point, the applied displacement to the specimen was 14.4 mm (1.5% drift). At cycle thirty whitewash was more visible flacked off on the subpanels. In subpanels

2, 3, 5, 7, 8, 10, 11, and 12 an X-shape pattern was visible were whitewash was flacked off. Fig 5.11 shows the state of the subpanels 1, 9, and 12 in cycle 30. At 2% drift, small tearing was starting to develop in all subpanels except subpanels 10, 11, and 3. The tearing in the subpanels was generally small and had no noticeable effect on the shear strength of the specimen. At cycle forty, tearing happened in all subpanels.
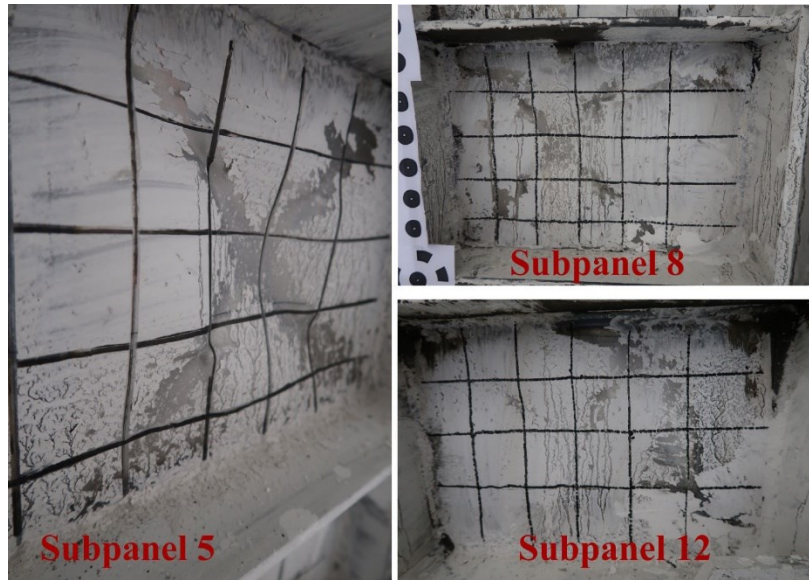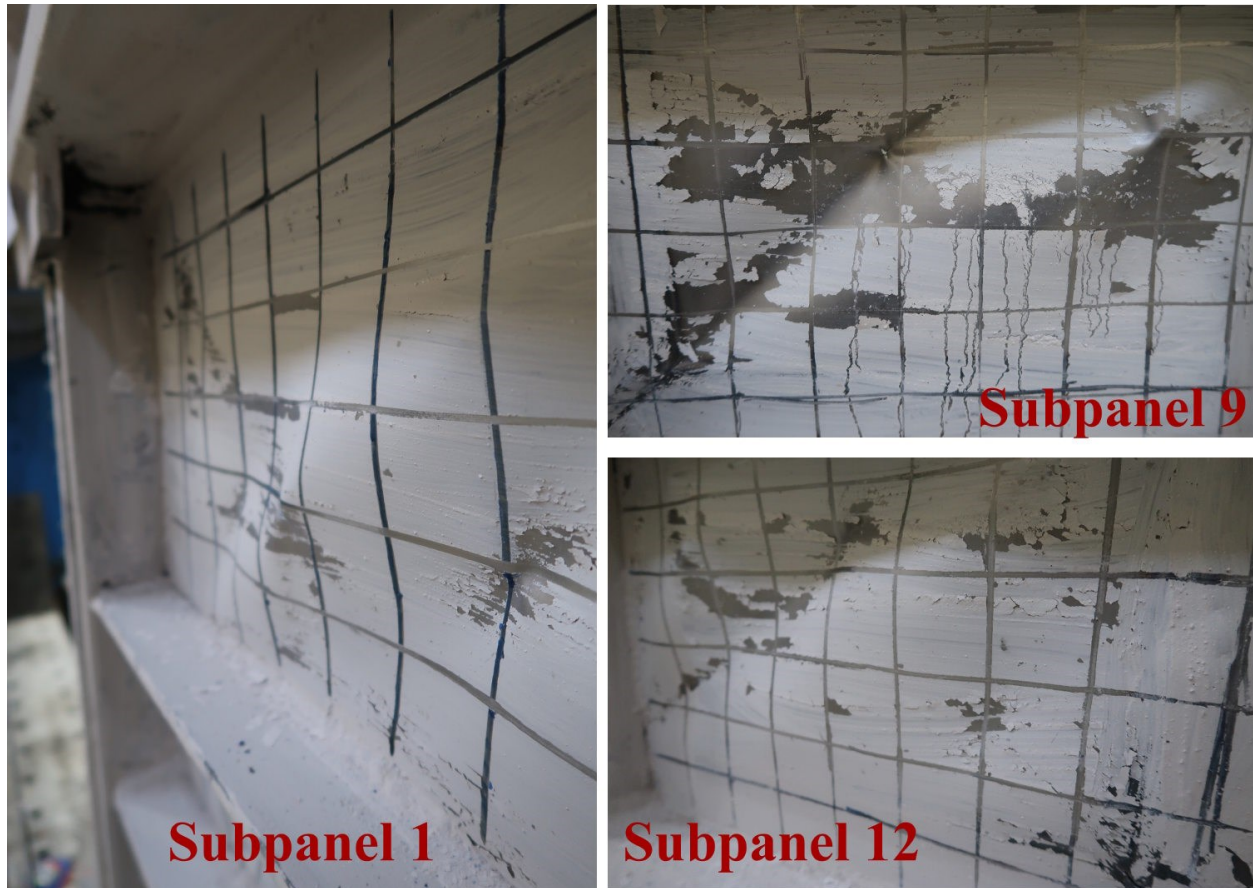

Fig 5.11. Subpanels 1, 9, and 12 of SPSW-OP50% in cycle 27 showing local buckling and flaked off whitewashing
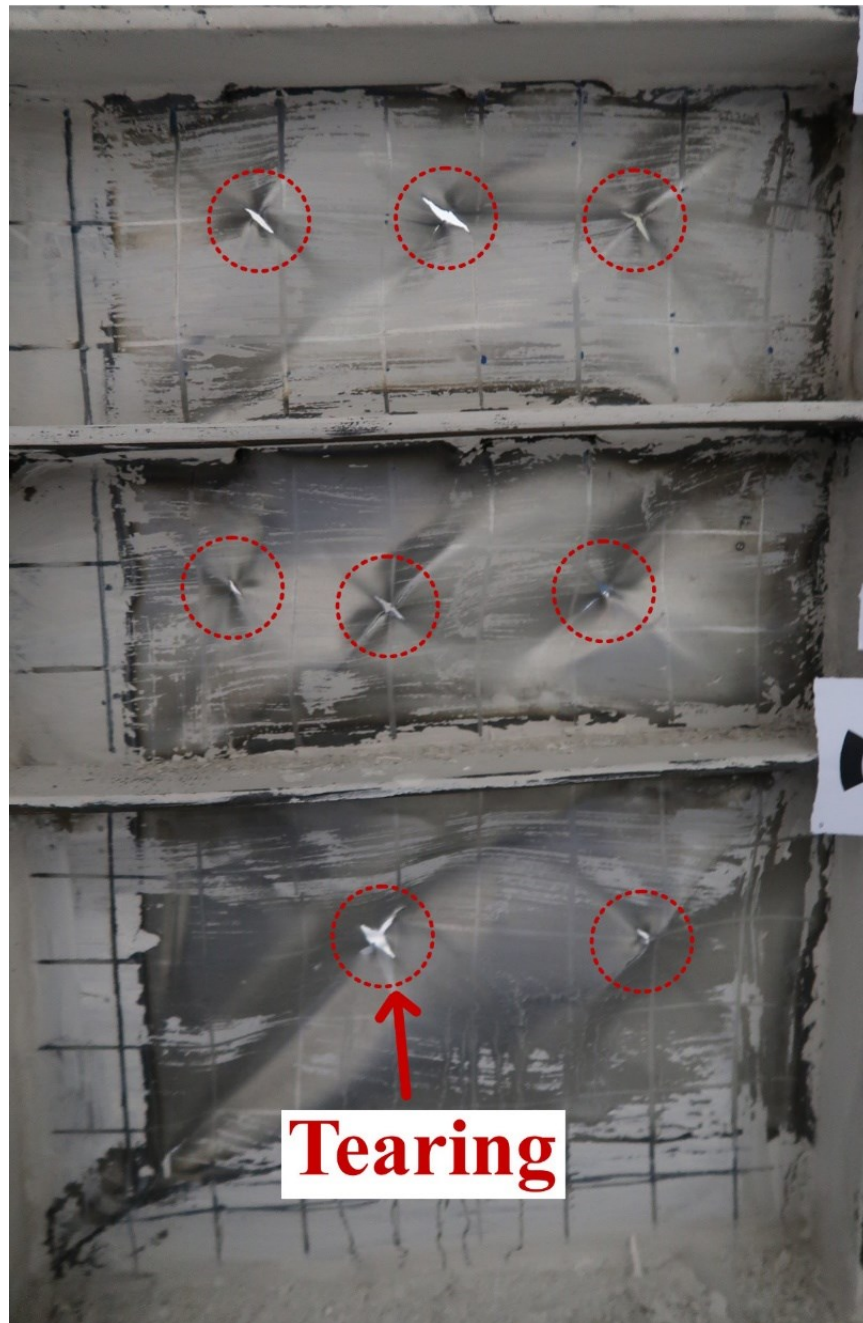
Fig 5.12. Three of the subpanel of SPSW-OP35% in cycle 40 showing tearing

Fig 5.12 shows deformed shapes of three of the subpanels of the left side of the specimen at load cycle forty. The length of the tearing on the corner subpanels was larger than the other subpanels. On these subpanels, tearing happened in one or multiple places, usually in the shape of an X, and also near the corners where the plate was connected to the boundary members.

After 45 cycles, the load-bearing capacity of the specimen dropped below 80% of its maximum capacity, and the test was terminated. The last applied displacement was 41.6 mm (4.3% drift), and the maximum recorded shear strength of the specimen was around 659 kN. At the end of the test, in-plane deformation was visible around the opening. Local buckling caused severe deformations in all subpanels and large tearing occurred in them in different places. Similar to the first experiment, yielding happened in the columns at the top and bottom. The specimen at 2% drift is shown in Fig 5.13. The deformed shape of the specimen at the end of the test is shown in Fig 5.14.
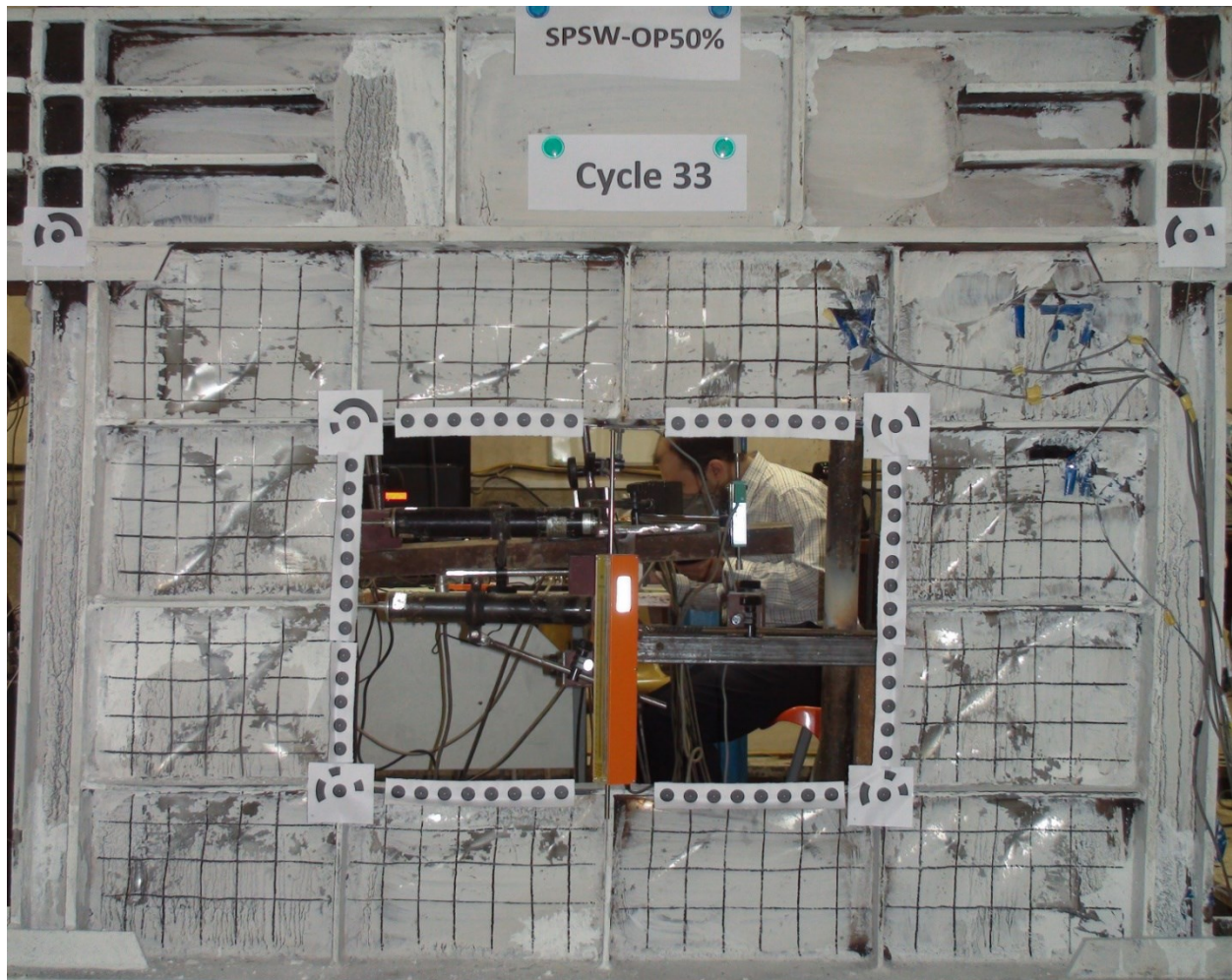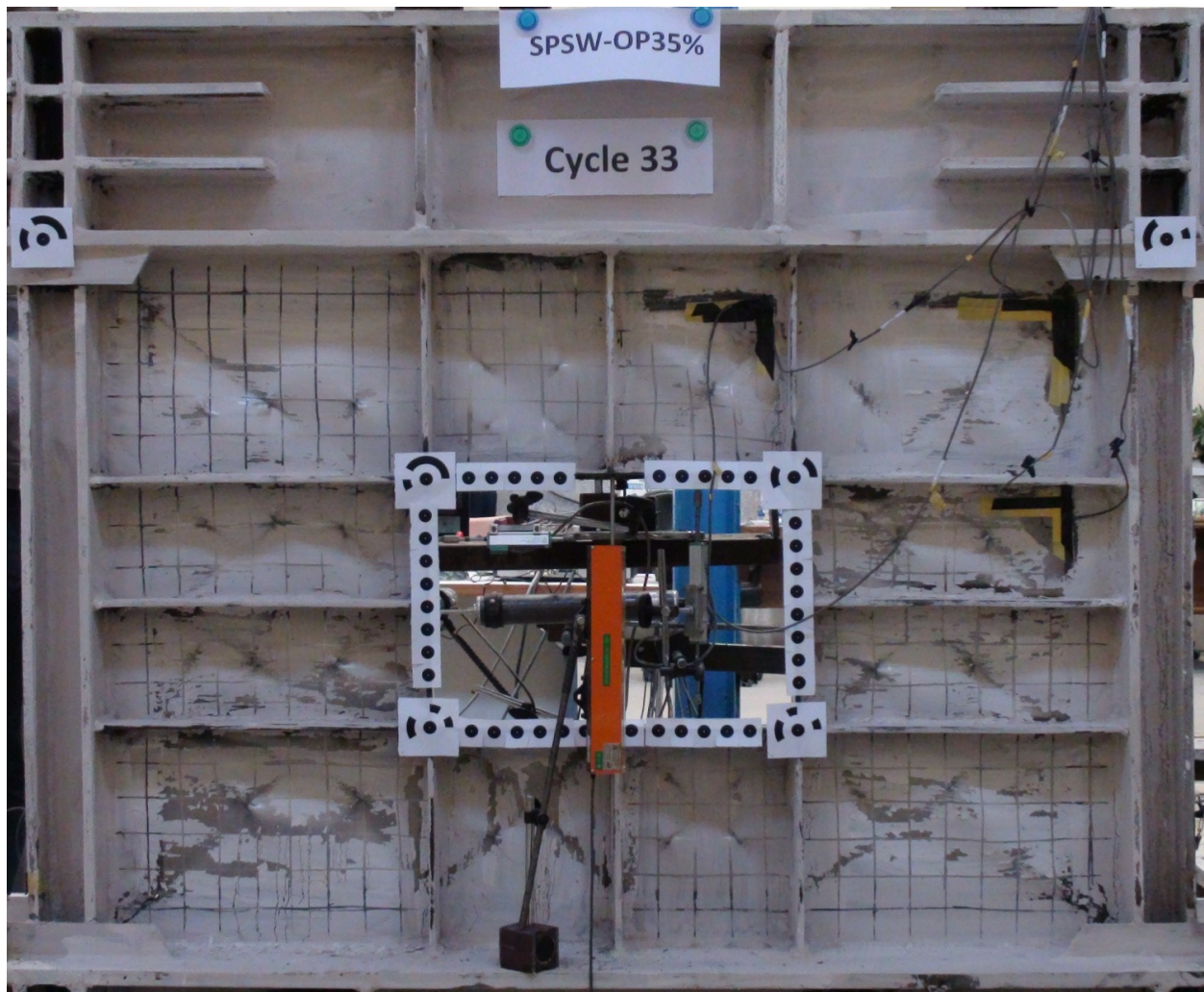

Fig 5.13. The deformed shape of SPSW-OP35% at 2% drift
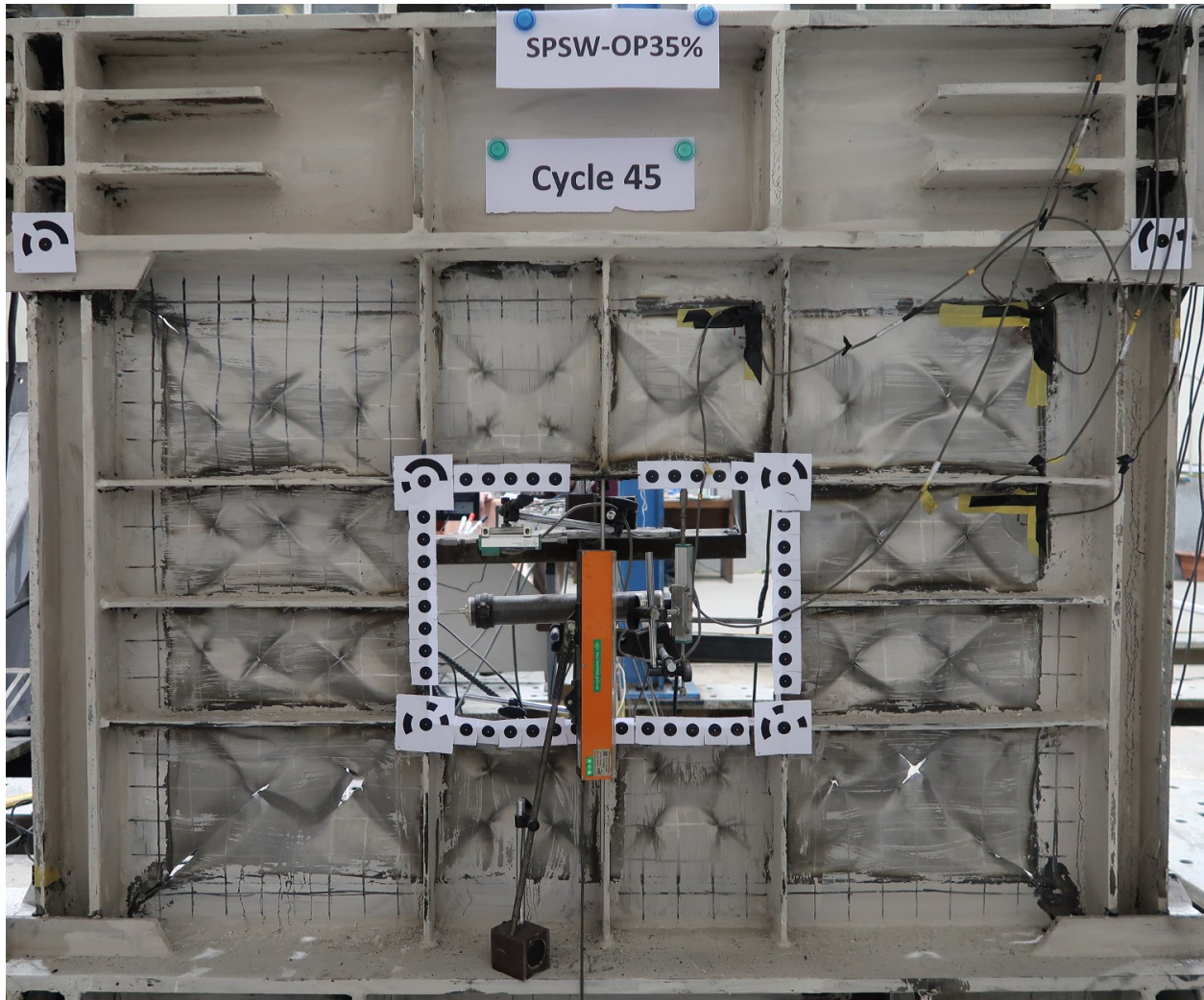
Fig 5.14. The deformed shape of SPSW-OP35% at the end of the experiment

5.6. Hysteresis curves obtained from tests

Hysteresis curves in terms of lateral displacement versus lateral load were obtained from the quasi-static cyclic loading tests. Various important parameters, such as ultimate strength and its corresponding displacement or energy dissipation capacity of the system can be calculated from hysteresis curves. Fig 5.15 and Fig 5.16 show the hysteresis curves for the two tested specimens. It is observed that both specimens have stable hysteresis loops. For the SPSW-OP35% specimen, the maximum shear strength occurred at 22.4 mm displacement (2.3% drift) and the load-bearing capacity of the specimen started to gradually decrease from that point. The SPSW-OP50%

specimen reached its ultimate strength at 27.1 mm displacement (2.8% drift) and the ultimate strength remained constant until the last cycle of the loading. Although the specimen with the smaller opening has a larger maximum shear strength, the difference between the maximum shear strength of the two specimens is very small. Another observation is the difference between the shapes of the two specimens. Hysteresis curves of SPSW-OP50% are more of a spindle shape in comparison to SPSW-OP35%. In the SPSW-OP35% specimen, pinching can be seen in the later cycles of the hysteresis curves, which is usually associated with the buckling of unstiffened thin SPSWs. The reason behind this is the difference between the sizes of the subpanels in the specimens. Due to the larger opening, SPSW-OP50% has smaller subpanels and less distance between the stiffeners. The sizes of the subpanels for SPSW-OP35% are larger, especially for the corner subpanels. These larger subpanels caused the hysteresis behaviour of the specimen to be more similar to an unstiffened steel plate shear wall. This is a well-known effect shown in early investigations of stiffened SPSWs (Takahashi et al. 1973).
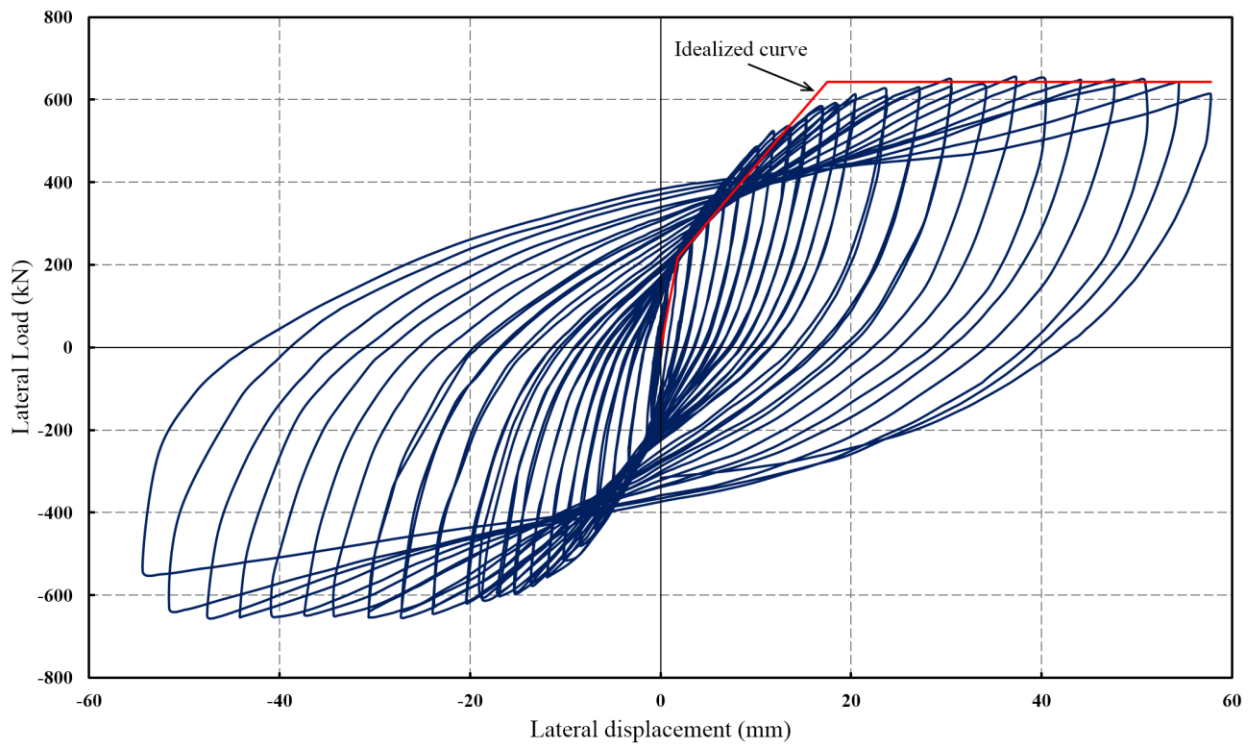
Fig 5.15. Hysteresis and idealized curves of SPSW-OP50%
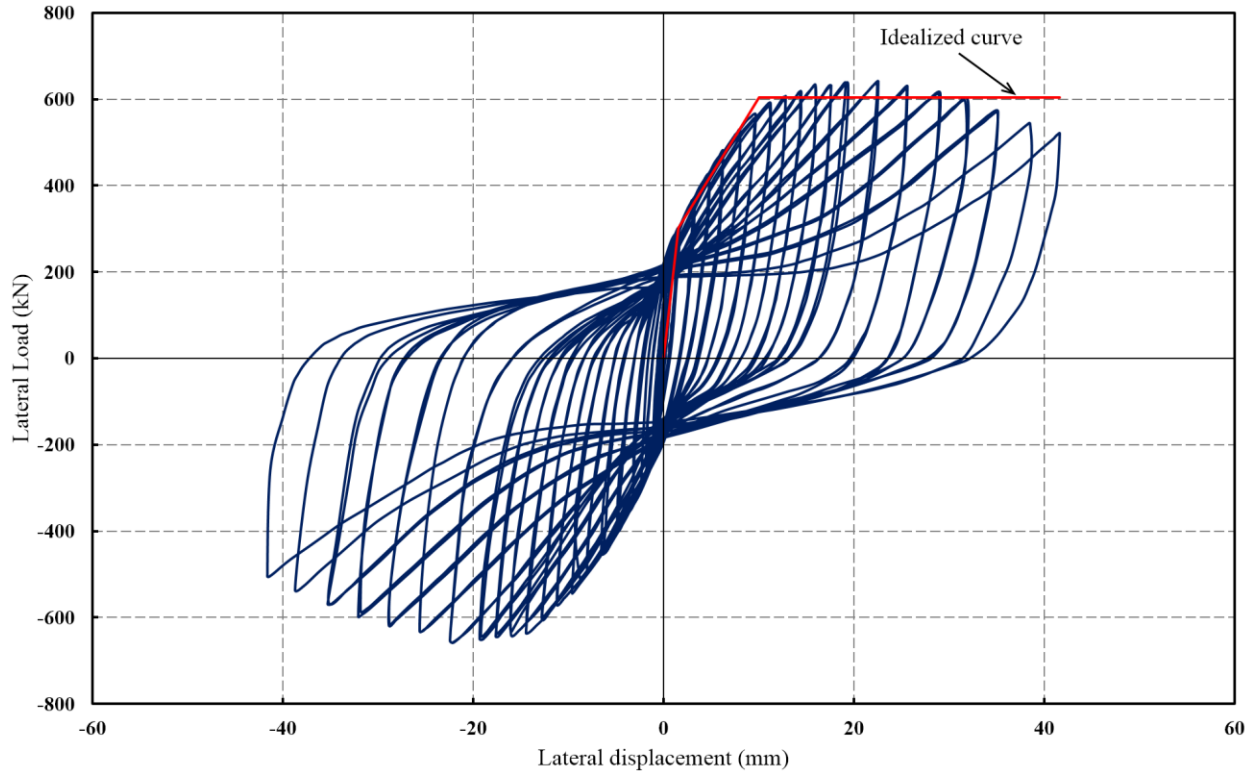
Fig 5.16. Hysteresis and idealized curves of SPSW-OP35%

Idealized curves were also obtained from hysteresis loops. Idealized curves are usually used to indicate key parameters such as yielding point and stiffness. As SPSWs are made of two main elements, an infill plate and boundary frame, two main yield points should be identified on the curves. Thus, the idealized curve for the SPSW system is tri-linear. Since the SPSW system is designed based on the capacity design approach, the yielding of the infill plate should occur before the yielding of the boundary members (yielding at the end of the beams or yielding at the base of the columns). To draw the idealized curves, the first line is traced from the origin to the point where the installed instruments show significant yielding in the infill plate. The second line is drawn from there to the point that significant yielding on the columns is identified. The third line which is drawn horizontally and is obtained by equating the area under the idealized curves and the hysteresis loops. The idealized curves for the two specimens can be seen in Fig 5.15 and Fig 5.16. As it was expected, using lower yield point steel for the infill plate in this experiment caused the infill plate to become inelastic earlier and start absorbing energy at smaller displacements. This phenomenon can be very beneficial as the infill plate can act as a fuse and keep the columns relatively safer from damage. The yield displacements for the infill plate of both models were very

107

close; however, at this same displacement, SPSW-OP35% specimen has higher shear strength. Also, the initial stiffness for SPSW-OP35% was 35% higher than SPSW-OP50%.

Energy dissipation capacity was also calculated from the hysteresis loops. In each full cycle, the area under the enclosed loop is equal to the energy dissipated. The total energy dissipated by each specimen at different displacements during the experiment is shown in Fig 5.17. As is observed, SPSW-OP35% specimen has generally more energy dissipation capacity than the SPSW-OP50% specimen at the same displacements, but the difference is not significant. In both specimens, the amount of dissipated energy becomes larger as yielding develops on the specimens and the area under each cycle of the hysteresis curves becomes larger.
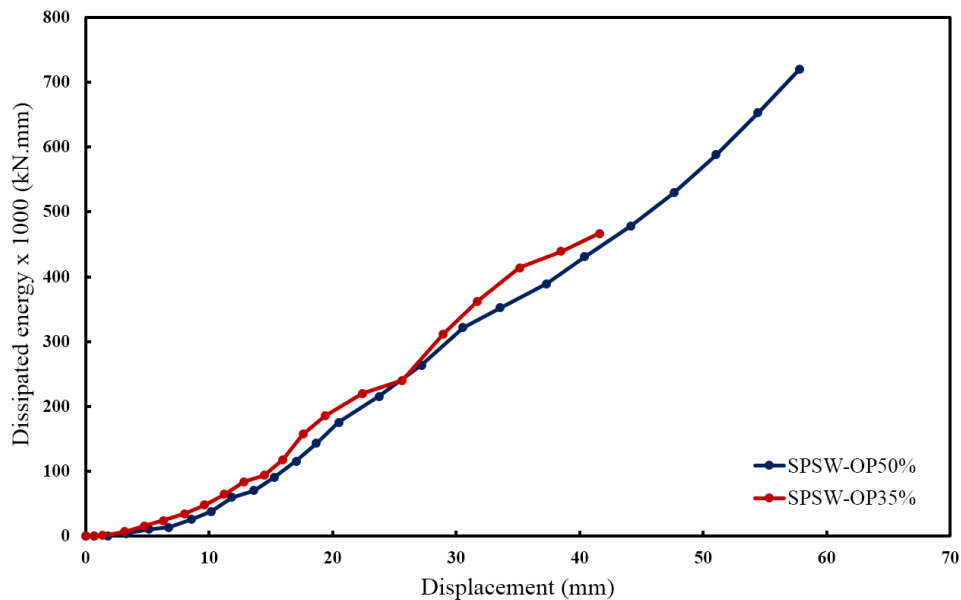
Fig 5.17. The amount of dissipated energy from the specimens

5.7. Deformation around the opening

The main purpose of using stiffeners in this study was to restrain the large deformations that commonly take place around the opening. For both specimens, global buckling of the plate was successfully prevented by the stiffeners. As mentioned before, photogrammetry was conducted to measure deformations around the openings. At different stages of the experiments, three-

dimensional coordinates of several points around the openings were acquired from photogrammetry. The data obtained from photogrammetry was processed using the Agisoft Metashape software (Agisoft 2021), and the highest accuracy setting was selected for the process. Deformations of a total of 62 points for OP50 and 43 points for OP35 around the opening were studied during different stages of the experiments.

The deformation around the opening at yielding for both specimens was negligible. The shape of SPSW-OP35% opening before loading and at yielding are shown in Fig 5.18 and Fig 5.19 respectively. Fig 5.20 shows the deformed shape of SPSW-OP35% opening at 2% drift and Fig 5.21 at the end of the experiment. At 2% drift, the horizontal deflections for all points were less than 1 mm. The maximum vertical deflection was 3.2 mm and it was observed at the left half of the bottom side of the opening. At this drift, out-of-plane deformation for all points remained under 1 mm. At the end of the experiment, the maximum horizontal and vertical deflections were 1.7 mm and 5.7 mm, respectively. The out-of-plane deformation remained under 1 mm for all points.
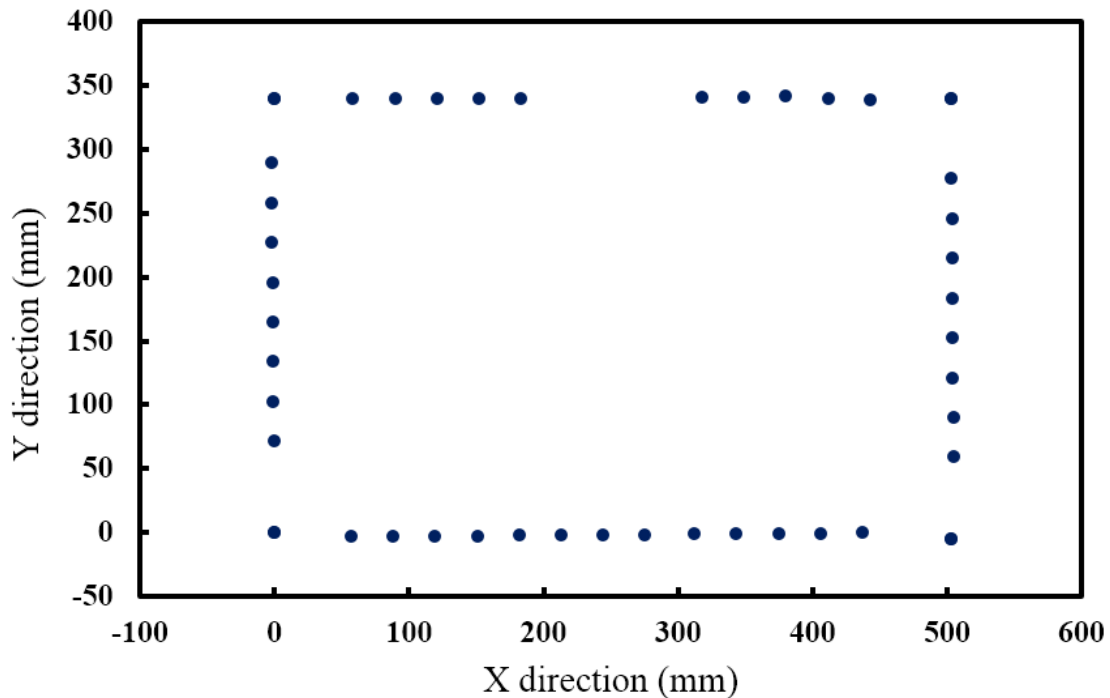
Fig 5.18. Shape of SPSW-OP35% opening before loading
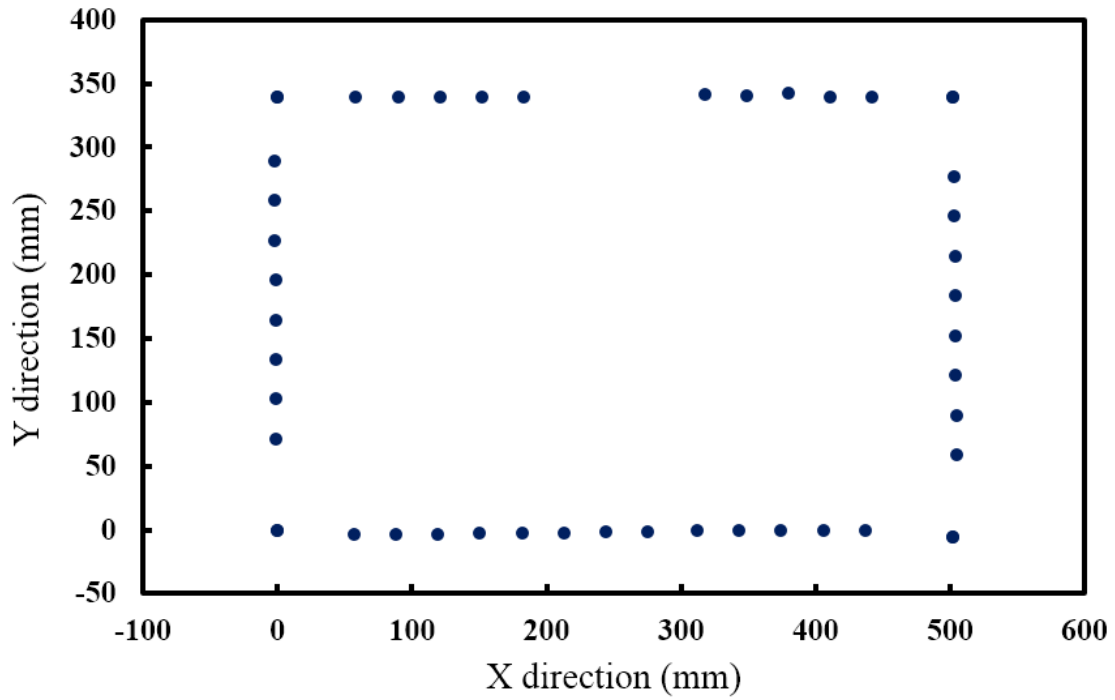
Fig 5.19. Deformed shape of SPSW-OP35% opening at yielding
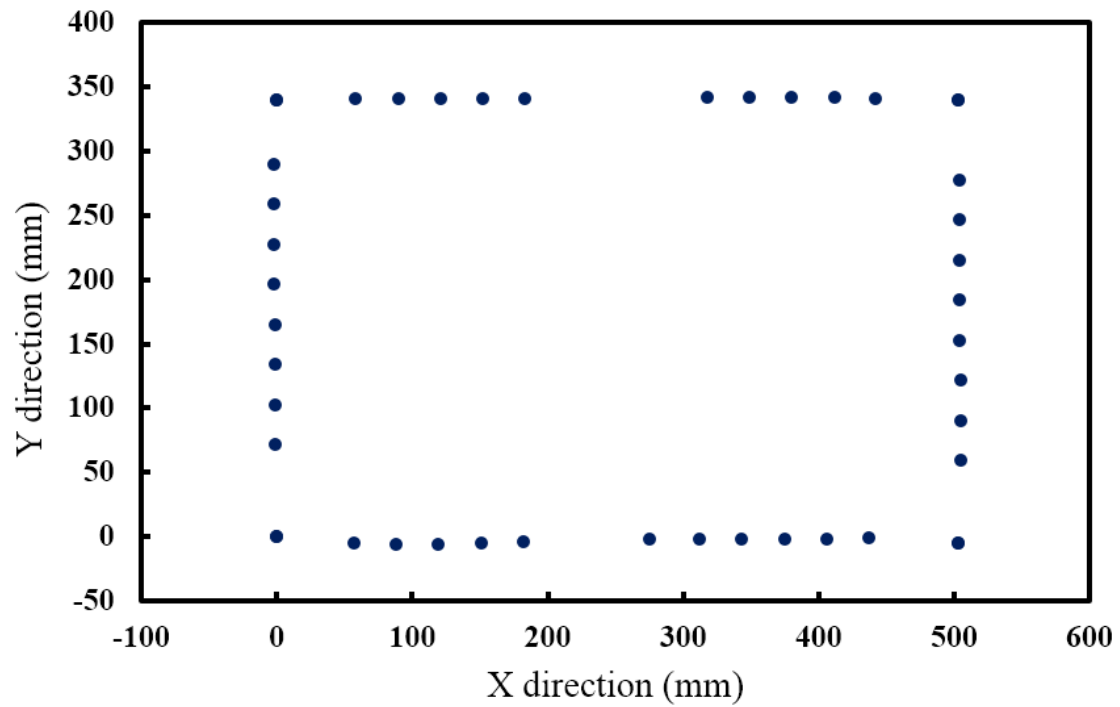
Fig 5.20. Deformed shape of SPSW-OP35% opening at 2% drift
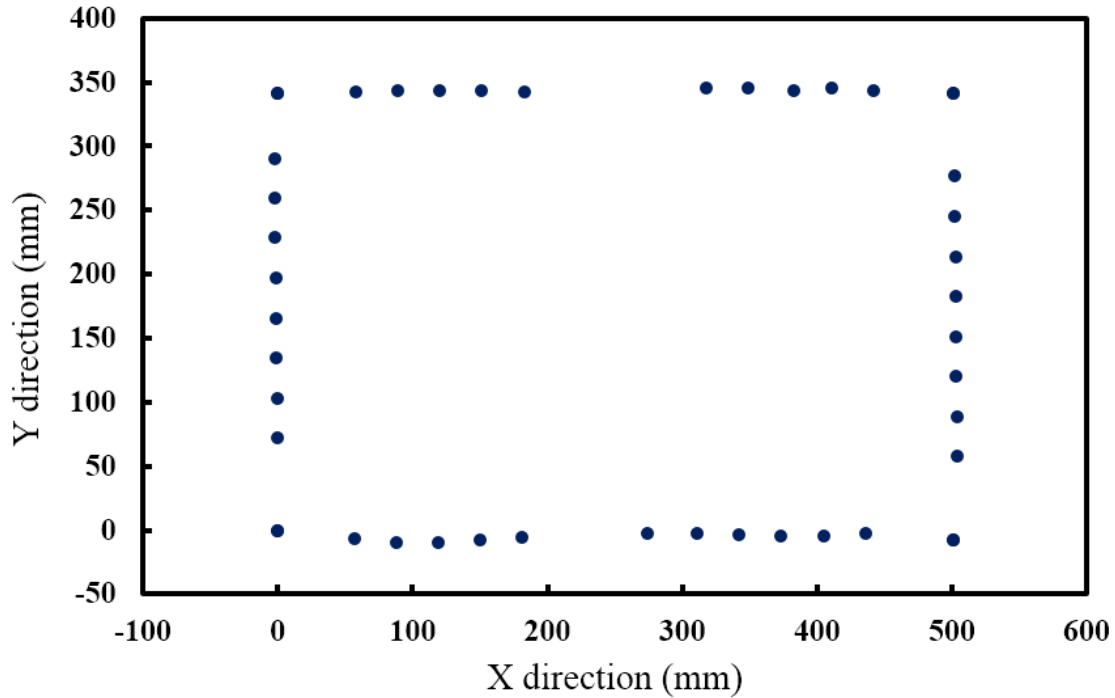
Fig 5.21. Deformed shape of SPSW-OP35% opening at the end of experiment

The shape of SPSW-OP50% opening before loading and at yielding are shown in Fig 5.22 and Fig 5.23 respectively. The deformed shape of SPSW-OP50% at 2% drift and at the end of the experiment are shown in Fig 5.24 and Fig 5.25 respectively. The maximum horizontal and vertical deflection at 2% drift were 3.2 mm and 3.3 mm respectively. Out-of-plane deformation at this drift was under 1 mm for all points. At the end of the experiment, the maximum horizontal deflection was 7.6 mm which was at the right side of the opening in the top half part. The maximum vertical deflection was 11.8 mm and it was observed at the right half of the top side of the opening. The out-of-plane deformation of only two points reached 1 mm and the rest were under 1 mm.
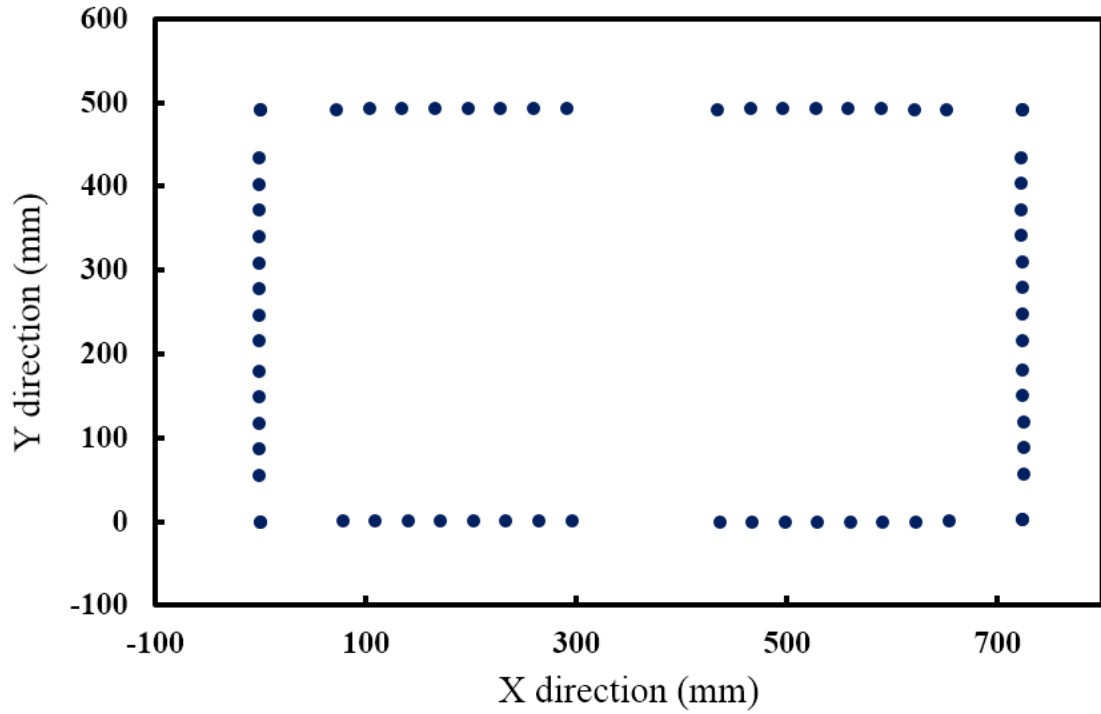
Fig 5.22. Shape of SPSW-OP50% opening before loading
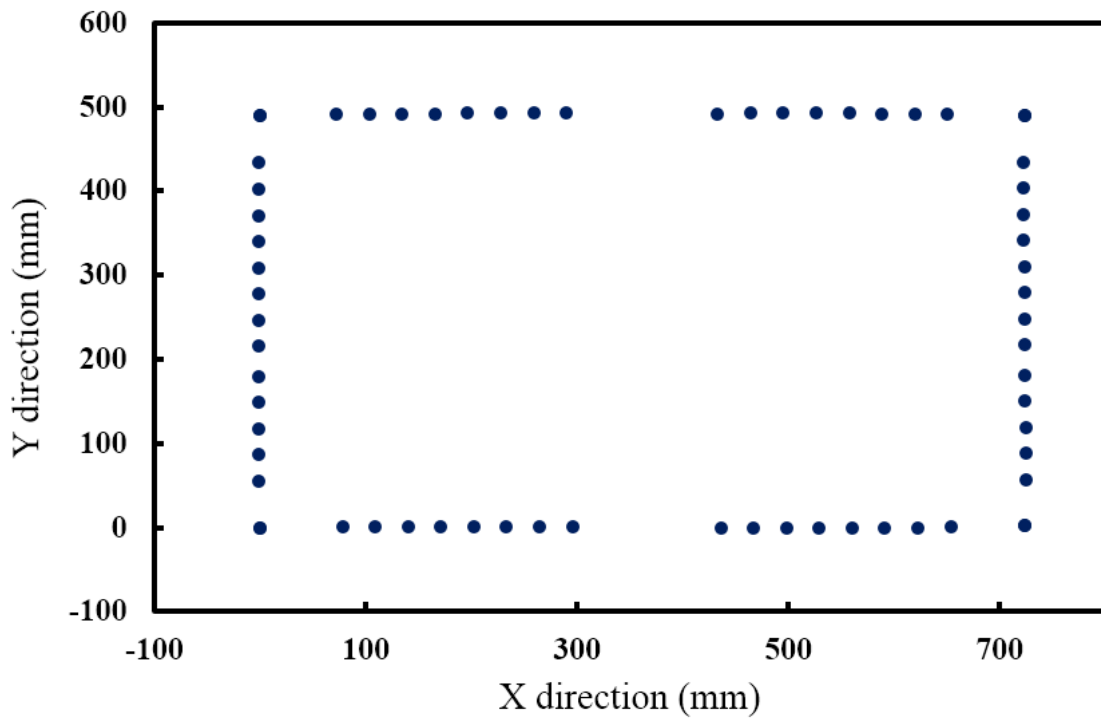
Fig 5.23. Deformed shape of SPSW-OP50% opening at yielding

112
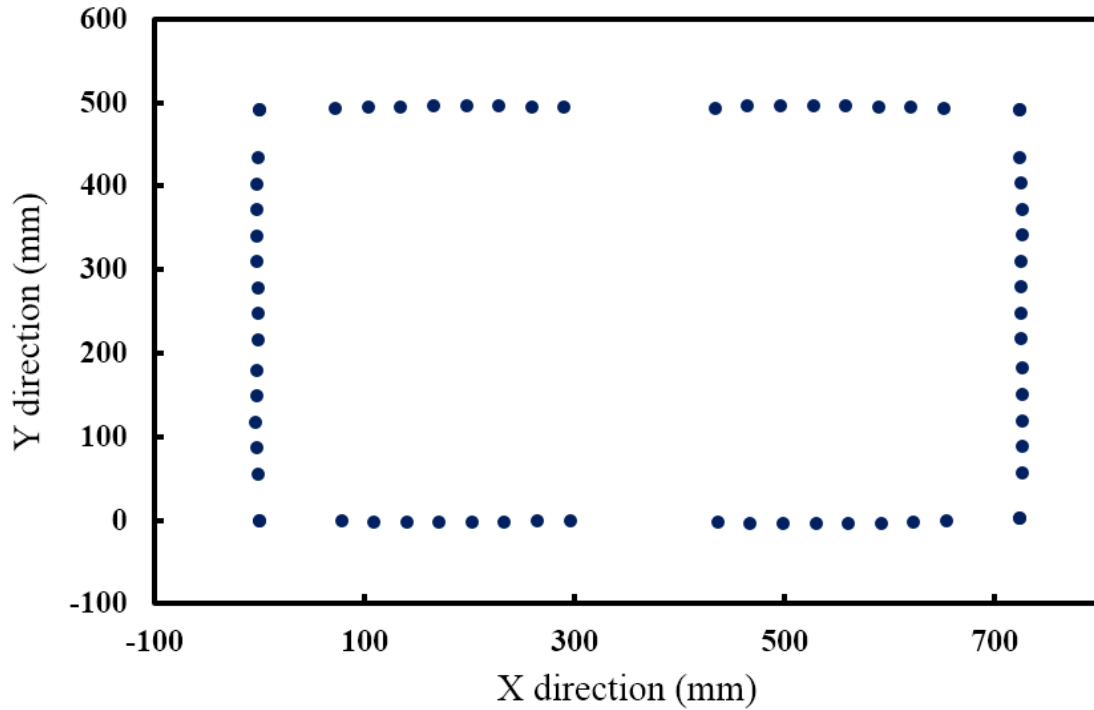
Fig 5.24. Deformed shape of SPSW-OP50% opening at 2% drift

The results of the experiments showed that the proposed stiffener layout studied in this research can be a very effective solution for limiting the deformation around the opening. Out-of-plane deformation for both models was successfully prevented until the end of the experiment. In-plane deformation was also limited for both models even at large drifts, at the end of the experiment. The two different approaches for welding stiffeners to the infill plates were proved effective, and no difference in the final results was observed. The stiffeners in both cases remained attached to the infill plate until the end of the experiment and only minor deformations happened around the openings.
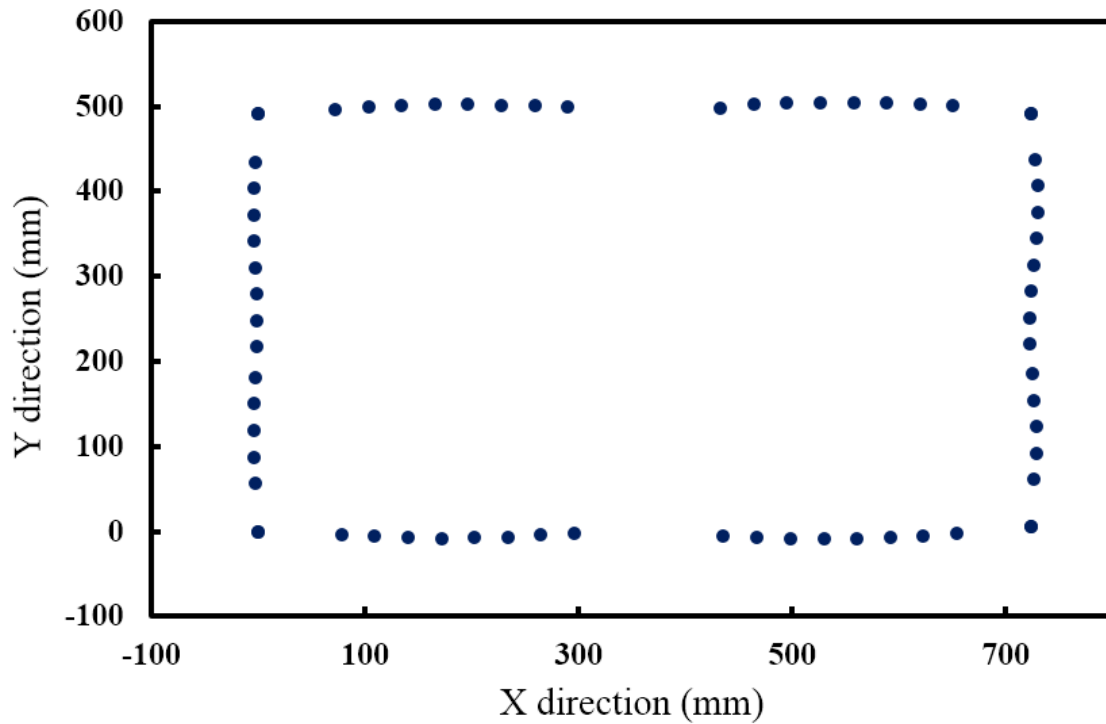
Fig 5.25. Deformed shape of SPSW-OP50% opening at the end of experiment

5.8. Finite element (FE) analysis of SPSWs with rectangular openings

As mentioned before, prior to the experiment finite element analysis was carried out to provide predictions for the specimens' behaviour. Nonlinear push over analysis was conducted to find out the buckling mode of the infill plate and also estimate the yield points of the specimens. The finite element analysis for this study was carried out by using ABAQUS software (ABAQUS 2014). All elements of the FE models such as boundary members, infill plate and stiffeners were modeled by using 4-node general-purpose shell (S4R) element. Details such as the top beam stiffeners and the fishplates were also modeled to characterize the test specimens more accurately. Similar to the test setup, the base of the model was fixed to the ground and the top beam out-of-plane movement was restrained. An initial imperfection was applied to the model to initiate the buckling of the infill plate. In order to incorporate initial imperfection, an eigenvalue buckling analysis was first carried out for the FE model. The initial imperfection shape was assumed as the first buckling mode, obtained from eigenvalue analysis, with a peak amplitude of 1 mm. For meshing the models, a

structured mesh control was assigned to the models. Fig 5.26 presents the deformed shapes of the two tested specimens obtained from FE analyses.

Previous research on SPSWs showed that large displacements and local buckling of infill plates could cause difficulties in the convergence of the FE model. This was overcome by using general-purpose shell elements (S4R element), which can accommodate large displacements. In this study, ABAQUS/Standard was adopted for all FE analyses. ABAQUS/Standard uses an implicit dynamic integration method and automatically adjusts the time increment to achieve convergence in analysis for highly nonlinear problems. In addition, convergence is more easily obtained in the dynamic (seismic) analysis as the inertia terms provide mathematical stability to the system, making the method more robust.

SPSW-OP35%   **SPSW-OP50%**
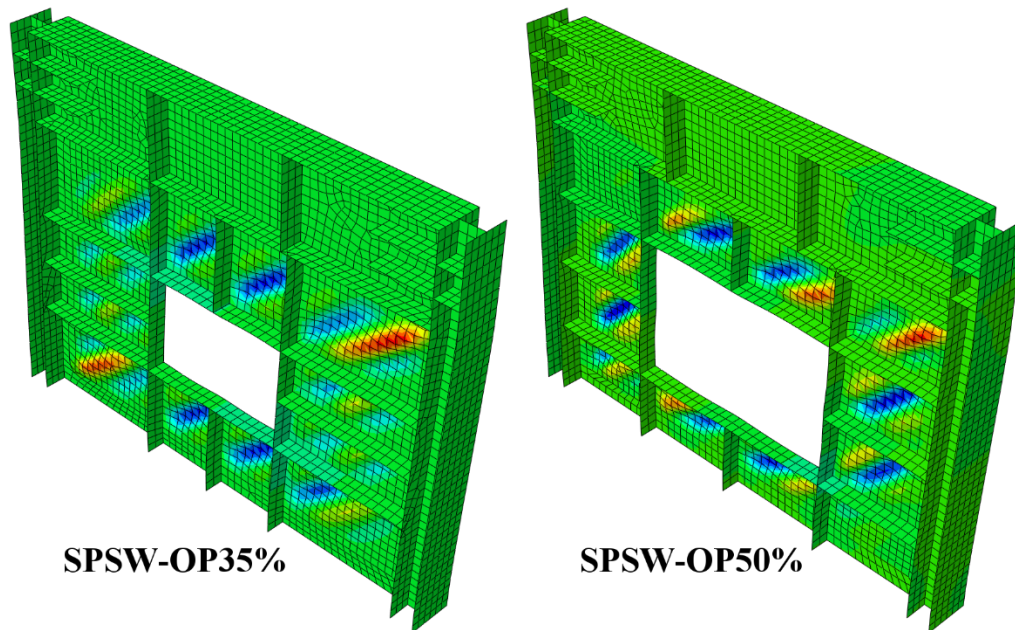
Fig 5.26. Deformed shapes of the two FE models after the analysis showing local buckling

Fig 5.27 and Fig 5.28 show the comparison between the backbone of the hysteresis curves and the results from the FE analysis. As observed, FE analysis results for SPSW-OP50% are very close to the experiment results. FEA results predicted both yield points and the ultimate strength of the specimen with good accuracy. For the SPSW-OP35% specimen, FE analysis shows a close agreement with the experiment result, especially for the elastic part, but it slightly overestimated

the ultimate strength of the specimen. For this model, the ultimate strength predicted by FE analysis was around 2.5% higher than the experiment.
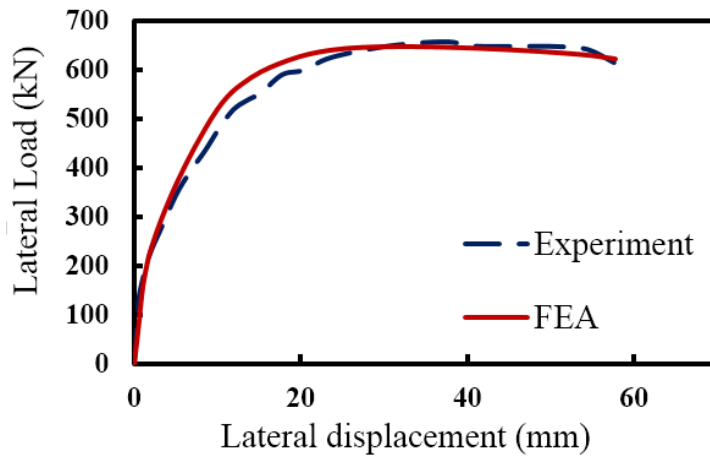
Fig 5.27. Experiment results compared to finite element analysis for SPSW-OP35%
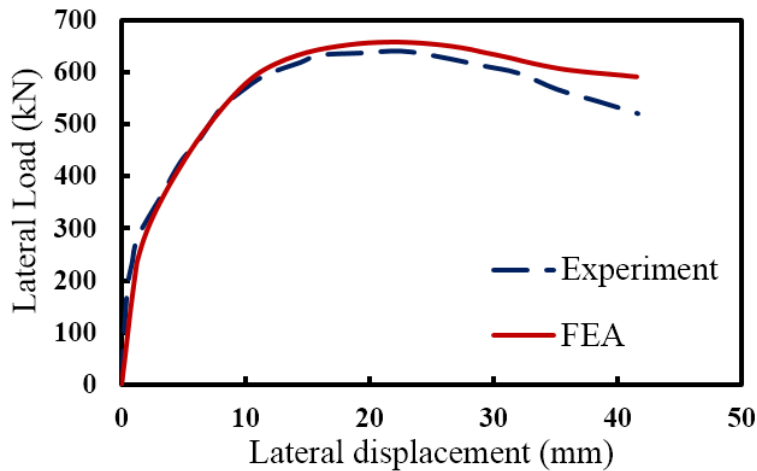
Fig 5.28. Experiment results compared to finite element analysis for SPSW-OP50%

5.9. Seismic analysis of SPSWs with rectangular openings

5.9.1. Selection of the steel plate shear walls

A hypothetical 4-storey office building located in Vancouver, Canada with SPSW system was designed for this part. A symmetrical plan with an equal bay width of 6 m was considered for the building and a storey height of 3.8 m was selected for all levels. The building was considered to

have two SPSWs in each direction to resist lateral loads. The building was assumed to contain a foundation built on soft rock or dense soil, corresponding to site class C in NBCC 2015. At the roof level, the dead load was considered 3 kPa, and the snow load was calculated as 1.64 kPa. The typical dead load and live load for the floors were considered as 4.1 kPa and 2.4 kPa respectively. To calculate the seismic forces, equivalent static force procedure was adopted according to NBCC 2015. For design of SPSWs, ductility-related force modification factor (Rd) and overstrength-related force modification factor (Ro) were assumed as 5.0 and 1.6, respectively.

A rectangular opening with the size of 50% was considered at the center of the SPSWs at all storeys. The infill plate thickness was selected as 3.0 mm for all floors. Wide flange sections were considered for the boundary beams and columns of the selected 4-storey SPSWs and they were designed for the resulting forces from the infill plate yielding. The selected beam and column sections for the SPSWs are presented in Table 5.2.

Table 5.2. Section properties for the 4-storey SPSW frames

Storey	Column Section	Beam Section
4	W360x262	W460x193
3	W360x262	W310x129
2	W360x287	W310x129
1	W360x287	W310x129

The FE model for seismic analysis includes one SPSW and a gravity dummy column. Truss elements were used to model the "dummy" columns and pin-ended rigid links were used at each level to connect to the main SPSW model. The vertical load for half of the building columns were supported by the "dummy" columns. In the FE analysis, the storey gravity loads were represented as lumped masses on the columns at every floor. Frequency analyses were conducted for both unstiffened and stiffened SPSW models to determine the periods for the first two modes of

vibrations. The results for frequency analyses are shown in Table 5.3. As observed, the stiffened SPSW model has slightly lower fundamental period, indicating higher stiffness for the system. The periods for the first two modes of vibration were used to select a 5% Rayleigh proportional damping ratio for seismic analyses.

Table 5.3. Periods for the first two modes of vibration of the structure

Mode	Stiffened SPSW	Unstiffened SPSW	NBCC 2015
First	0.769	0.869	0.384
Second	0.285	0.312	

5.9.2. Ground motion selection and scaling

According to NBCC 2015 guidelines, a set of at least eleven ground motion records are required for dynamic analysis. Although the guideline allows using synthetic time histories, records from historical earthquakes are preferred. To ensure variability in time history characteristics, it is also recommended to select no more than two records for the same earthquake. Thus, eleven historical earthquake time histories were selected from eleven different events. The selected records, their date, station name, magnitude and the value of maximum acceleration to maximum velocity for each record are presented in Table 5.4. The records were obtained from the Pacific Earthquake Engineering Research (PEER) Center NGA-West2 database (Ancheta et al. 2014). These records were also scaled to be compatible with Vancouver response spectrum. NBCC guidelines define an appropriate period range in which the mean response spectrum for the selected earthquakes should be equal or above the target spectrum (Vancouver spectrum in this case). The lower bond and upper bond of this period range are defined as:

$$T_{min} = min\ (0.2T_1\ , T_{90\%}) \tag{5.1}$$

$$T_{max} = max\ (2.0T_1\ , 1.5\ sec) \tag{5.2}$$

where, T_1 is the fundamental period of the building and $T_{90\%}$ is the period of the highest vibration mode for a minimum of 90% mass participation.

Using the guidelines, the mean response spectrum was scaled for the range between $0.2T_1$ and 1.5 sec. In order to maintain the records' frequency content, NBCC recommends using a linear scale factor for scaling the records, and spectral matching methods are not recommended. Although NBCC does not suggest a specific scaling method, methods such as equating the area under the ground motions' response spectrum to the area under the target's response spectrum over the appropriate range are accepted. A scale factor between 0.2 and 4.0 is considered acceptable. Thus, in this study, the area under the target's response spectrum over the appropriate range was first calculated. Then the scale factor for the records was calculated so that the area under the ground motions' response spectrum over the appropriate range remained equal to the calculated area in the first step. The unscaled and scaled mean response spectrums compared to Vancouver response spectrum for site class C are shown in Fig 5.30. Two examples of the unscaled and scaled earthquake records are also shown in Fig 5.29.

Table 5.4. Selected records names and specifications

Number	Event Name	Date	station Name	Mag	A/V
1	Imperial Valley	5/19/1940	El Centro	6.95	0.70
2	San Fernando	2/9/1971	LA - Hollywood Stor	6.61	0.86
3	Kern County	7/21/1952	Taft Lincoln School	7.36	0.97
4	Cape Mendocino	4/25/1992	Fortuna Fire Station	7.01	1.00
5	Northridge	1/17/1994	LA - Brentwood VA Hospital	6.69	0.78
6	Morgan Hill	4/24/1984	Halls Valley	6.19	1.25
7	Nahanni Canada	12/23/1985	Site 1	6.76	2.39

8	Borrego Mtn	4/9/1968	San Onofre - So Cal Edison	6.63	1.14
9	Parkfield	6/28/1966	Cholame - Shandon	6.19	1.58
10	San Simeon	12/22/2003	San Luis Obispo - Lopez Lake Grounds	6.52	0.92
11	Landers	6/28/1992	Morongo Valley Hall	7.28	1.13

Table 5.5. Periods for the first two modes of vibration of the structure

Mode	Stiffened SPSW	Unstiffened SPSW	NBCC 2015
First	0.769	0.869	0.384
Second	0.285	0.312	
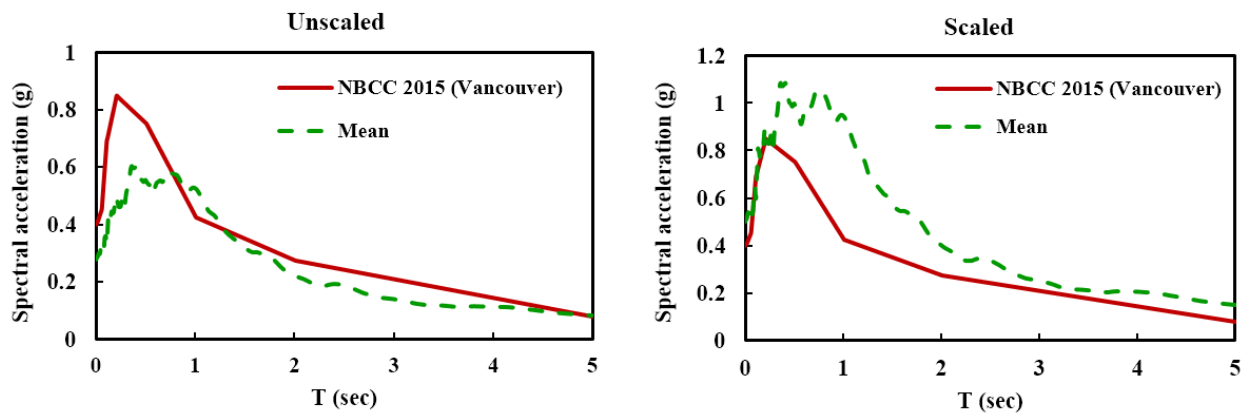
Fig 5.30. Design and mean spectrums for unscaled ground motions (left) and scaled ground motions (right)
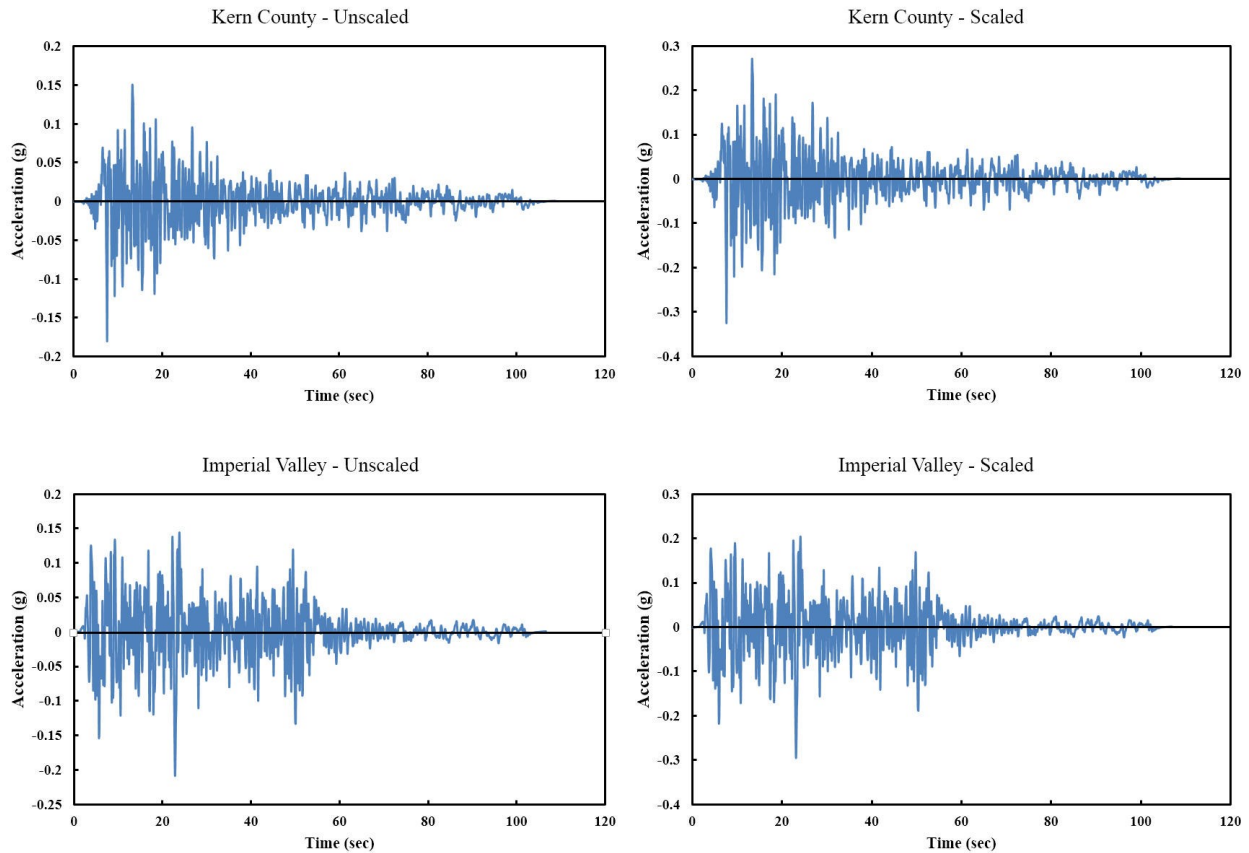
Fig 5.31. Unscaled (left) and scaled (right) records of Kern County and Imperial Valley earthquakes

5.9.3. Seismic analysis results

For all the scaled selected seismic records, nonlinear dynamic analysis was carried out for the selected 4-storey stiffened and unstiffened SPSWs. For all seismic records, Results showed large out-of-plane deformations around the openings in all stories of the unstiffened SPSW. The maximum out-of-plane deformation around the opening for each record is presented in Table 5.6. The minimum out-of-plane deformation is for the Borrego Mtn record and is 76.4 mm. For all other records, the out-of-plane deformation is more than 100 mm. The maximum out-of-plane deformation is 287 mm for the Cape Mendocino record. For the 4-storey SPSW stiffened with the proposed stiffener layout around the rectangular opening, the maximum out-of-plane deformation around the opening is 4.4 mm for the Cape Mendocino record. For all other records, the out-of-

plane deformation around the opening is equal to or less than 2 mm. The significant difference between the results of the stiffened SPSW and the unstiffened SPSW demonstrates the effectiveness of using the proposed stiffener layout in limiting the out-of-plane deformation around the rectangular opening. It was also observed that the in-plane deformations for all the records were very small for the 4-storey stiffened SPSW. The maximum in-plane deformation for the Cape Mendocino record was about 5 mm.

The deformed shapes of the 4-storey stiffened and unstiffened SPSWs for the Imperial Valley record are shown in Fig 5.32. In the stiffened model, local buckling was observed for all records. Local bulking is generally more visible in the first storey and the second storey. Similar to the experiment, deformations can be observed in the subpanels of the first two stories. Local deformations at the top storey are usually very small because of the lower drifts in this storey.

Table 5.6. Maximum values of out-of-plane deformations around the opening for each record

Event	Maximum deformation around the opening (mm)	
	Stiffened SPSW	Unstiffened SPSW
Imperial Valley	2.0	268.6
San Fernando	1.0	142.5
Kern County	1.1	137.7
Cape Mendocino	4.4	287.5
Northridge	1.9	245.0
Morgan Hill	0.8	102.5
Nahanni Canada	2.4	201.8
Borrego Mtn	0.9	76.4

Parkfield	0.9	158.4
San Simeon	1.9	160.1
Landers	1.1	150.2
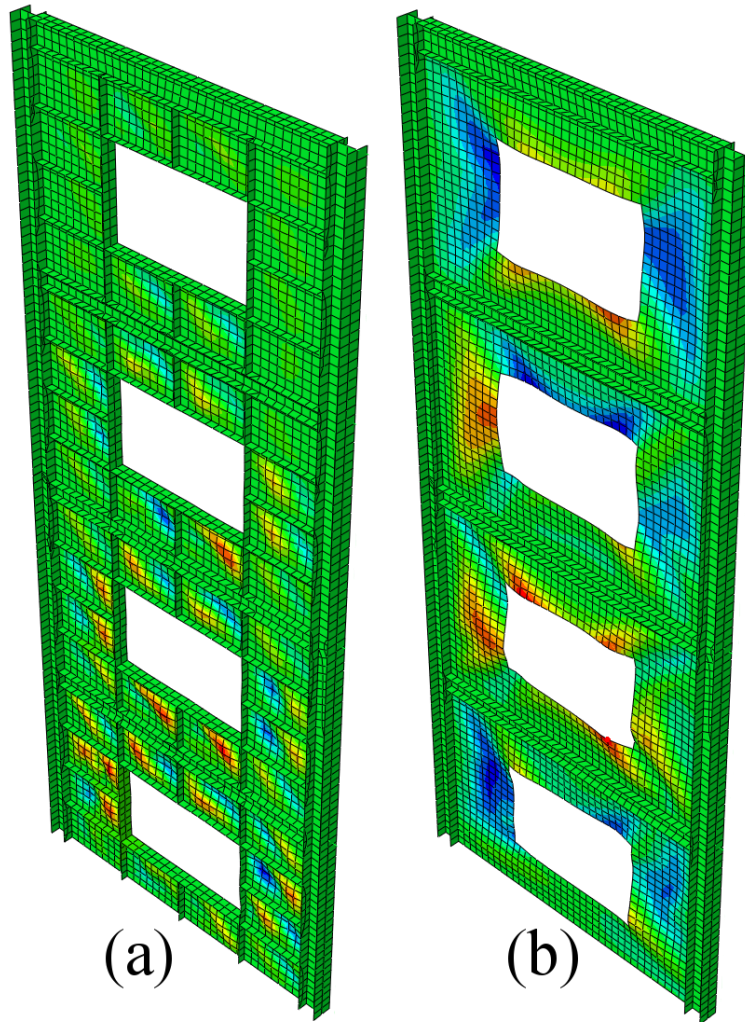
Fig 5.32. Deformed shapes of (a) stiffened and (b) unstiffened models for the Imperial Valley record

Seismic drift demands between 4-storey stiffened and unstiffened SPSWs for records number 1 to 6 are shown in Fig 5.33 and for records number 7 to 11 in Fig 5.34. Fig 5.34 also presents average drifts for all records. It also compares the drifts between stiffened SPSW and unstiffened SPSWs with rectangular openings for the Cape Mendocino record, and the Northridge record (the two records that caused the largest drifts). In the unstiffened 4-storey SPSW, the maximum interstorey drift demand is 2.4% for the Cape Mendocino record. The maximum interstorey drift demand for the 4-storey stiffened SPSW is 2.3% for the Northridge record. The results for the 4-storey stiffened model show an overall reduction in the interstorey drift demand in comparison to the unstiffened model. For the first storey, mean drift demand is reduced by 10% when the proposed stiffener layout is used around the rectangular opening. The reduction in the interstorey drift is 18% and 37% for the second and third stories, respectively. The maximum reduction in mean drift demand is for the top storey, which is about 57%. Thus, a reduction in the interstorey drift demand is another advantage of using the proposed stiffened SPSW system when a rectangular opening is present on the plate.

In the SPSW model stiffened with the proposed stiffener layout, it was observed that yielding occurred in most parts of the infill plates of the first three levels. Due to the lower drifts in the top storey, in most cases, only partial yielding was only observed in the infill plates at the top storey. In the unstiffened model, only partial yielding was observed in the infill plates at all levels. Complete yielding was not observed in any of the infill plates of the unstiffened SPSW model. Thus, the proposed stiffener layout helped achieve uniform yielding in the infill plates of the stiffened SPSW with a rectangular opening. In addition, in most cases, the frame members remained essentially elastic for both stiffened and unstiffened models. In some cases, where the models experienced larger drifts, yielding was observed at the end of the beams. This indicates that in both models, energy was dissipated mostly by the infill plate yielding.
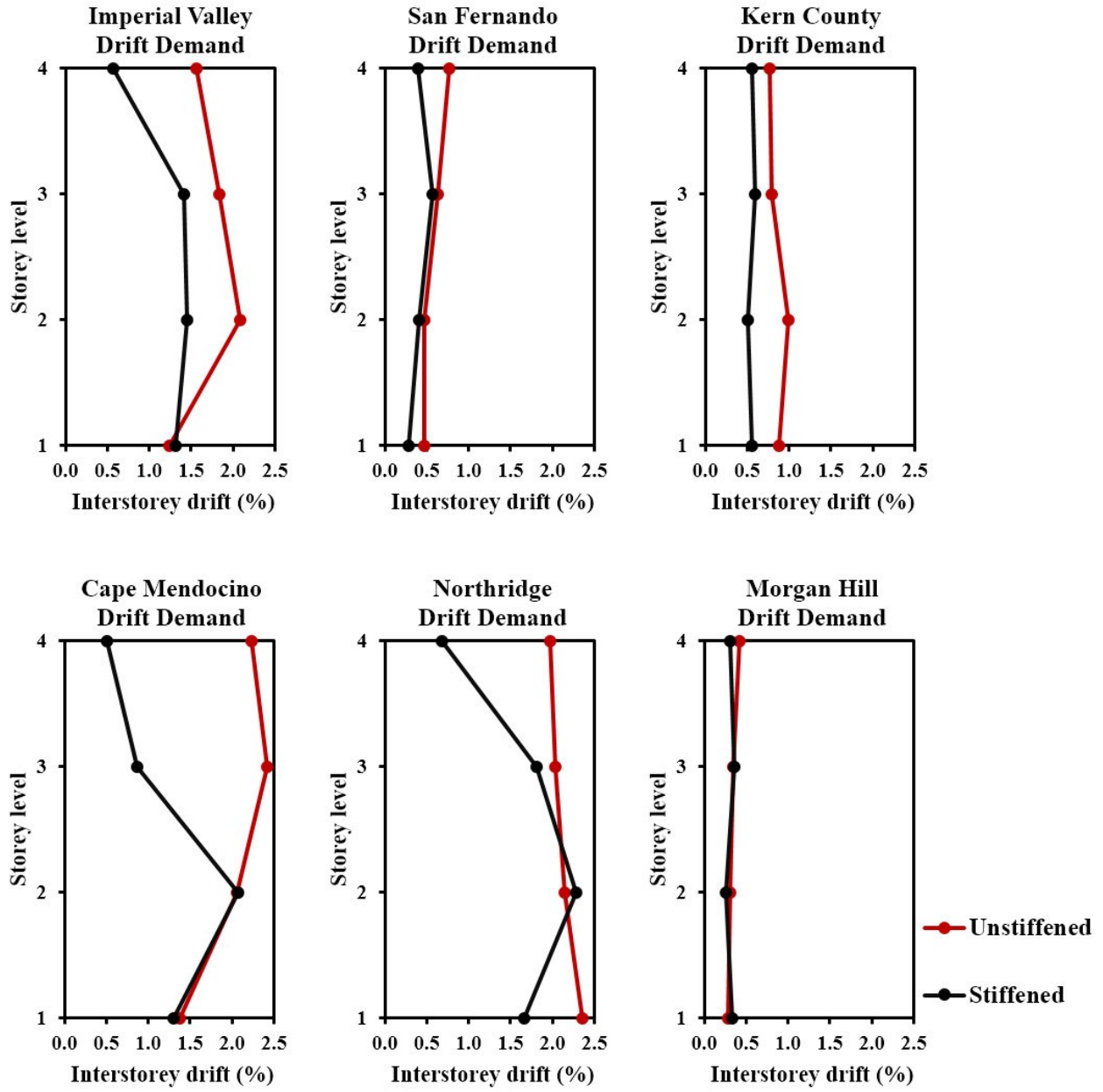
Fig 5.33. Drift demand of all storey levels for records number 1 to 6 for stiffened and unstiffened models
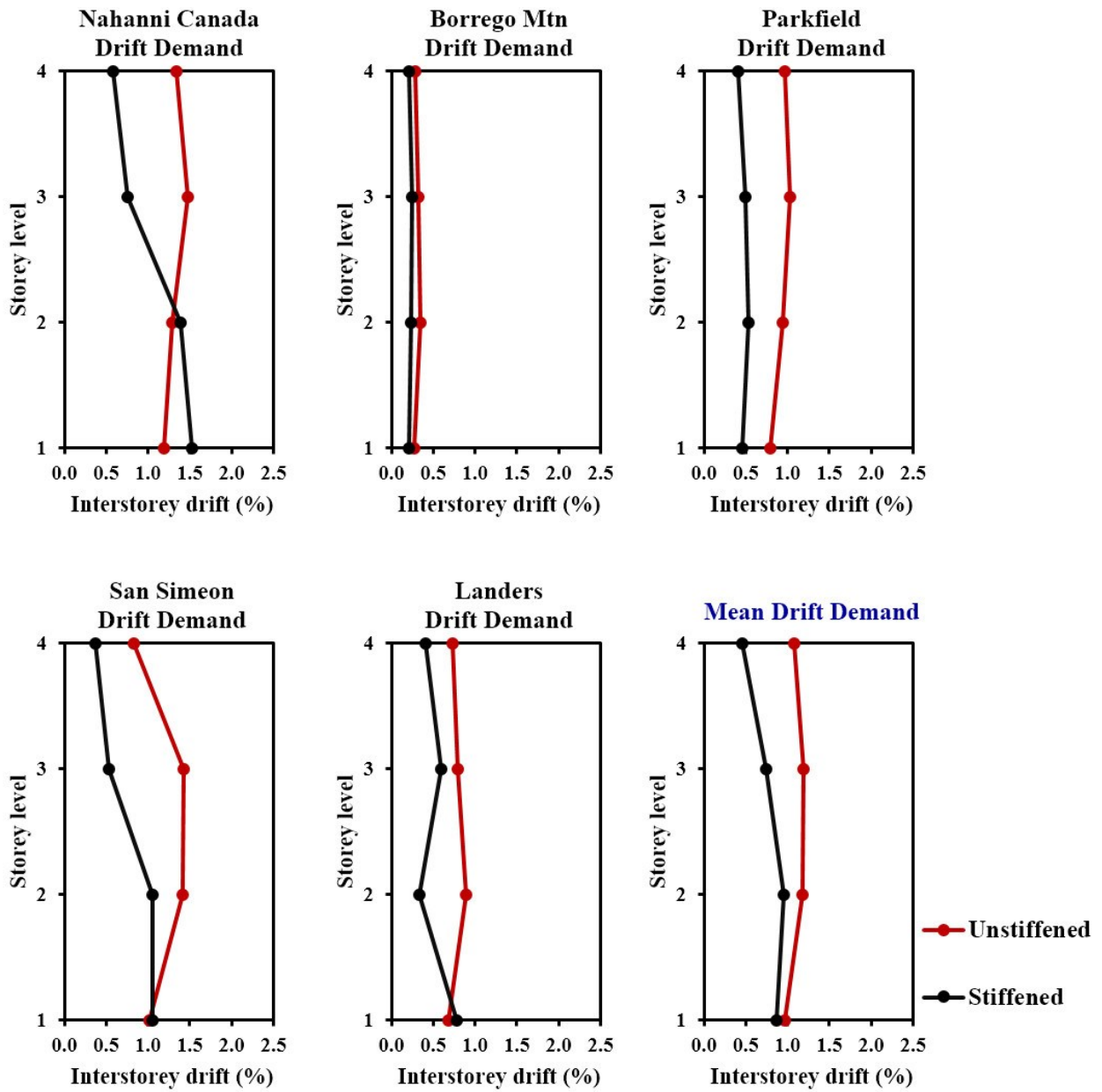
Fig 5.34. Drift demand of all storey levels for records number 7 to 11 and mean demand for stiffened and unstiffened models.

5.10. Summary and conclusions

Experimental and numerical studies were conducted on two single-storey SPSWs with a centrally placed rectangular openings. A recently proposed stiffener layout was used around the rectangular openings. The objective of using the proposed stiffener layout was to prevent the global buckling of the infill plate and consequently limit the deformations around the opening. The results of the tests showed that the proposed stiffener arrangement fully prevented the out-of-plane deformations around the openings. Local buckling was observed in the subpanels in both tests and the amount of out-of-plane displacements around the openings were negligible even at large drifts. In addition, the stiffeners were also successful in restricting the in-plane deformations around the rectangular openings. At 2% drift, maximum in-plane deformation for both specimens was under 4 mm, and at the end of the experiment maximum, in-plane deformations for SPSW-OP35% and SPSW-OP50% were 5.7 mm and 11.8 mm, respectively.

Stable hysteresis behaviour was also observed for both tested specimens. Use of the lower yield point steel for the infill plate caused the specimens to start absorbing energy in smaller drifts. The amount of energy dissipation capacity at similar displacements was close for the two specimens. The ultimate shear strength was also found to be close for both specimens but the initial shear stiffness for the model with the smaller rectangular opening was higher.

The developed finite element model provided very good predictions of behaviour of the SPSW specimens tested under quasi-static loading. Essential features of the test specimens such as initial stiffness and ultimate strength were reasonably predicted by nonlinear pushover analyses of the tested specimens.

Nonlinear seismic analyses using eleven historical records also showed significant reduction in the out-of-plane deformations around the rectangular openings when the proposed stiffener layout was used around the opening. For the 4-storey FE model, the maximum out-of-plane deformation around the opening was reduced from 287 mm to 4.4 mm. Reduction in interstorey drift demand was also observed from the seismic analyses. The mean interstorey drift demand was reduced in all storey levels when the proposed stiffener layout around the rectangular opening was used in SPSW.

CHAPTER 6

Summary, conclusions, and recommendations for future work

6.1. Summary

The main objective of this study was to propose a solution for preventing the deformation around rectangular openings in steel plate shear walls. To the best of the author's knowledge, the issue of deformation around rectangular openings has not been investigated before. Therefore, when rectangular openings are required in the design of the SPSW system, engineers usually use heavily reinforced plates. This study intended to propose a simple and efficient approach to improve the behaviour of SPSWs with rectangular openings. Thus, the research began with studying stiffened SPSWs and the effects of the number of stiffeners on the behaviour of the infill plate. Theoretical and numerical investigations were carried out on plates with different numbers of vertical and horizontal stiffeners. The numerical models were validated before the analysis against available experimental data. The results showed that there is no significant advantage in using only a few stiffeners on the plate, and at least four or five stiffeners are required to improve parameters such as shear strength or stiffness. However, it was also proved that it is inefficient to add more stiffeners on the plate after a certain number since it will not increase the benefits of using stiffeners.

After studying solid stiffened plates, unstiffened and stiffened SPSWs with rectangular openings were investigated. Numerical analysis of unstiffened plates with five different sizes of rectangular openings showed decreased shear strength, stiffness, and very large out-of-plane deformations around the opening. Thus, four various stiffener layouts were considered around the opening and their performance was evaluated. The results showed that all of the considered stiffener arrangements were successful in limiting the deformation around the opening. The stiffener layout providing the best results was selected as the solution for this research. It was also

shown that this stiffener layout would increase the shear strength and stiffness of SPSWs with rectangular openings.

In the last and most important part of the research, the performance of the solution proposed in the second part was studied experimentally. Two one-third-scale SPSW test specimens with a rectangular opening at the center of the plate were designed and constructed. Both specimens had identical infill plates and boundary frames, and the difference was the size of the opening on the plate. Stiffeners were attached to the plates using the layout proposed in the second part. Various instruments were employed to record data during the tests. Since the most important part of the study was to measure the deformations around the opening, photogrammetry was used at four different stages during the tests for this purpose. Quasi-static cyclic loading was applied at the top beam of the specimens by a hydraulic actuator following ATC-24 guidelines. The specimens experienced large drifts, and stable hysteresis curves were observed for both specimens. The results showed that the stiffeners successfully prevented out-of-plane deformations around the opening. The in-plane deformations were also observed to be minor. Thus, the effectiveness of the stiffener layout proposed in this research study was verified experimentally.

A hypothetical four-storey building with steel plate shear walls as the lateral load-resisting system was also designed. A large rectangular opening was considered in the infill plates at all storey levels. Finite element models of the four-storey SPSWs were developed with and without the proposed stiffener layout. Nonlinear seismic analyses using eleven historical records were carried out on the two models. The maximum amount of out-of-plane deformation was observed to be very large in the unstiffened model. However, this amount was minor in the stiffened model, indicating the success of the proposed stiffener layout. In the model with the proposed stiffener layout around the rectangular opening, the mean interstorey drift demand was also reduced at all storey levels.

6.2. Conclusions

The outcomes of this research contribute to a better understanding of stiffened steel plate shear walls and improve the performance of plates with rectangular openings. Designers can use the findings of Chapter 3 to determine the number of stiffeners on a stiffened plate depending on how

much increase is required in parameters such as shear strength and stiffness. These parameters can be calculated for a stiffened plate with good accuracy using the theoretical method discussed in Chapter 3.

The results of Chapter 4 and Chapter 5 provide a simple and efficient approach to improving the behaviour of SPSWs with rectangular openings. One of the main concerns related to plates with rectangular openings, the deformation of the opening, is addressed, and the issue is solved by the proposed solution in this study. Since the Canadian design standard does not provide any provisions for SPSWs with rectangular openings, the findings of this research can be a foundation for providing guidelines and provisions for this type of SPSW in the future. Engineers can use the findings of this research to reliably use SPSWs with rectangular openings as a lateral load-resisting system in buildings. The key findings of this research are categorized for chapters 3, 4, and 5 respectively as follow:

6.2.1. Obtained conclusions for Theoretical and numerical investigation on the design and behaviour of stiffened steel plate shear walls

- Theoretical study on solid stiffened plates showed that the shear strength of a plate can be increased up to 15% by attaching vertical and horizontal stiffeners on the plate. The yield displacement of the plate can be reduced as much as 25% and consequently the shear stiffness can be increased up to 53%.
- Finite element analysis showed the increase in shear strength was 10-14%. The decreases in yield displacement was between 20-26% and the increase in elastic stiffness was between 41 and 53%.
- Comparison between the PFI method and FE analysis showed that the PFI method is capable of reasonably predicting the shear strength, stiffness and yield displacement of stiffened plates. The accuracy of predictions is higher for plates with only a few stiffeners or fully stiffened plates.
- Both theoretical and numerical methods showed that the advantages of using stiffeners became noticeable when the slenderness ratio of the plate is about 20% to 16%. There are not any noticeable benefits when using only one or two stiffeners

in each for the SPSWs. It is also not beneficial to add more stiffeners after the critical buckling stress of the subpanels reached its upper limit.

- The currently used design criterion for stiffeners to force the plate into local buckling, is reliable when there are at least five stiffeners in each direction. Using the design criterion for plates with less number of stiffeners, may not be adequate to prevent the global buckling of the plate.

- A calibration factor, based on the numerical study is proposed to improve the currently used stiffness criterion. This calibration factor is a function of the number of horizontal and vertical stiffeners. Finite element results showed using proposed calibration factor is effective in ensuring local buckling of stiffened plates with any number of stiffeners.

6.2.2. Numerical analysis of steel plate shear walls with rectangular openings

- Numerical investigation on unstiffened SPSWs with a rectangular opening at the center showed a decrease in shear strength and stiffness. As the size of the opening increases, shear strength and stiffness decrease more significantly. In the model with the largest opening, decrease in shear strength was more than 50%.

- The results also showed large out-of-plane deformations around the opening due to early buckling of the plate. The maximum amount of out-of-plane deformation around the opening varied between 120-209 mm, depending on the size of the opening.

- Stiffeners were attached to the numerical models and four different stiffener layouts were investigated. It was observed that all of the selected stiffener layouts were successful in restraining the deformation around the opening. For all of the models the maximum amount of out-of-plane deformation was under 10 mm.

- The stiffener layout providing the best results was proposed as the solution to prevent the deformation around the opening. This layout has four full stiffeners and four short stiffeners around the opening.

131

- FE results showed that using the proposed stiffener layout can reduce the out-of-plane deformation around the opening to under 5 mm. The shear strength and stiffness of infill plates with rectangular openings using this stiffener configuration was increased significantly. It was also observed that changing the opening location had a negligible effect on these parameters.

- The shear strength of the models was observed to be depended only on the length of the opening and not the height of the opening.

- The linear reduction factor, currently used to predict the shear strength of perforated plates, was found to provide very conservative results. This reduction factor was modified for plates using the proposed stiffener layout. FE analysis results showed that using the revised reduction factor will lead to much more accurate results.

6.2.3. Experimental and numerical study of stiffened steel plate shear walls with rectangular openings

- Experimental tests on two SPSW specimens with rectangular openings confirmed that the proposed stiffener layout can successfully prevent deformations around the opening.

- For the specimen with the smaller opening size, the amount of deformation around the opening at yielding was negligible. At 2% drift, out-of-plane deformation around the opening was under 1 mm. The maximum in-plane deflection was 3.2 mm. At the end of the experiment, the maximum in-plane deflection was 5.7 mm. The out-of-plane deformation remained under 1 mm.

- The amount of deformation around the opening at yielding for the specimen with the larger opening size was also negligible. At 2% drift, out-of-plane deformation around the opening for this specimen was under 1 mm. The maximum in-plane deflection was 3.3 mm. At the end of the experiment, the maximum in-plane deflection was 11.8 mm. The maximum out-of-plane deformation was 1 mm.

- For both tested specimens, stable hysteresis behaviour was observed. Energy dissipation process began in smaller drifts due to use of the lower yield point steel

132

for the infill plate. At similar displacements, the amount of energy dissipation capacity was found to be close for the two specimens. The ultimate shear strength was also close for both specimens; however, the initial shear stiffness for the model with the smaller rectangular opening was higher.

- In both specimens, early tearing on the subpanels was found to have no noticeable effects on the shear strength or the hysteresis behaviour of the specimens.

- Two different approaches were used to install the stiffeners on the plate. For one specimen, continuous welding on one side of the stiffeners was used and for the other specimen, staggered intermittent welding was used. No difference was found between the performances of these two approaches. The stiffeners remained attached to the plate until the end of the experiment and no visible deflection was on observed them. The stiffeners of both specimens caused local buckling to take place on the plates as intended.

- The developed finite element model was found to provide very good predictions of behaviour of the tested SPSW specimens. Essential features of the test specimens such as initial stiffness and ultimate strength were reasonably predicted by nonlinear pushover analyses of the tested specimens.

- Nonlinear seismic analyses on a four-storey finite element model also showed the effectiveness of using the proposed stiffener layout. The model was analyzed using eleven historical records. The results showed when the four-storey model was unstiffened, the maximum amount deformation around the opening for the selected earthquake records was between 76 and 287 mm. This amount was less than 5 mm when the proposed stiffener layout was used on the models.

- The seismic analyses results also showed an overall reduction in interstorey drift demand when using stiffened plates. The maximum interstorey drift demand was found to be 2.4% for the unstiffened model and 2.3% for the stiffened model. The mean drift demand for the first, second, third, and fourth storey levels was found to be reduced by 10, 18, 37, and 57 percent respectively when the proposed stiffener layout is used around the rectangular opening.

6.3. Recommendations for future work

This research proposed an innovative stiffener layout for steel plate shear walls with rectangular openings. The effectiveness of using such a layout was proved by conducting numerical and experimental investigations. The findings of this research provide a foundation that can be built upon and improved in the future. Thus, the following list of points is recommended for future research.

- A single rectangular opening was considered for all the numerical and experimental models in this study. Investigating the behaviour of the suggested layout when there are multiple rectangular openings in the infill plate can be the next step for this research.

- The tested specimens in this research were one-storey. A multi-level finite element model was also analyzed. Conducting experimental tests on a multi-level specimen can also contribute to studying the behaviour of the stiffener layout proposed in this study. Furthermore, shake table testing for such a specimen can be used to evaluate the performance of such a system in an actual earthquake event.

- The stress distribution on the plate is much more complicated than on solid plates, and there is no analytical model available for perforated plates. Thus, a linear reduction factor is used to estimate the shear strength and stiffness of perforated plates. In this study, this reduction factor is modified for plates using the proposed stiffener layout. Finding an analytical model for perforated plates is an important issue that has not been solved yet. If an analytical model is proposed, the shear strength and stiffness of stiffened plates with rectangular openings can also be calculated more reliably and accurately.

- When using the stiffener layout proposed in this study, it is essential to ensure the stiffeners are strong enough to cause local buckling on the plate. The size of the stiffeners in this study was acquired using numerical methods. Proposing a simpler method to acquire the size of stiffeners can help simplify the design of this type of SPSW. This topic, again, requires a much deeper understanding of how perforated plates behave. If the global and local critical buckling stresses of perforated plates are calculated accurately, it will be possible to propose a method to reliably select the size of the stiffeners for plates with rectangular openings.

- It is acknowledged that the 5% Rayleigh proportional damping used for seismic analysis of the 4-storey stiffened and unstiffened steel plate shear walls is slightly on the higher side. While the objective of the seismic performance study, which was to investigate the effectiveness of the proposed stiffener layout when compared to unstiffened SPSW with a rectangular opening, was achieved, a smaller damping (2 to 3% Rayleigh proportional damping) can be used in future studies to estimate the seismic response parameters for both 4-storey stiffened and unstiffened SPSSWs with rectangular openings.

- In this study, an initial imperfection of 1 mm was applied to the plate corresponding to the first buckling mode of the steel infill plate. The objective for applying initial imperfection was to initiate buckling in the infill plate. A sensitivity study can be conducted in future to see the effect of the magnitude of initial imperfections on the behaviour and strength of the stiffened and unstiffened SPSW systems.

References

ABAQUS 6.14. Dassault Systemes Simulia.

Afshari, M. J., and Gholhaki, M. 2018. "Shear strength degradation of steel plate shear walls with optional located opening." *Archives of Civil and Mechanical Engineering* 18: 1547-1561.

Agisoft Metashape User Manual 1.7. Agisoft.

ANSI/AISC. 2016. Seismic Provision for Structural Steel Buildings, ANSI/AISC 341-16. American Institute of Steel Construction, Chicago, IL, USA.

Ancheta, T. D., Darragh, R., Stewart, J. P., Seyhan, E., Silva, W. J., Chiou, B., Wooddell, K. E., Graves, R. W., Kottke, A. R., and Boore, D. M.. 2014. "NGA-West2 database." *Earthquake Spectra* 30 (3): 989-1005.

Astaneh-Asl, A. 2001. "Seismic behavior and design of steel shear walls." SEOANC Seminar, San Francisco.

Astaneh-Asl, A., and Zhao, Q. 2002. "Cyclic behavior of steel shear wall systems." Annual Stability Conference.

ATC-24. 1992. *Guidelines for Cyclic Seismic Testing of Components of Steel Structures*. Redwood City, CA: Applied Technology Council.

Barua, K., and Bhowmick, A. K. 2019. "Nonlinear seismic performance of code designed perforated steel plate shear walls." *Steel and Composite Structures, An International Journal* 31 (1): 85-98.

Basler, Konrad. 1961. "Strength of plate girders under combined bending and shear." *Journal of the Structural Division* 87 (7): 181-198.

Berman, J. W., and Bruneau, M. 2003. "Plastic Analysis and Design of Steel Plate Shear Walls." *Journal of Structural Engineering* 129 (11): 1448-1456.

Berman, J. W., and Bruneau, M. 2005. "Experimental investigation of light-gauge steel plate shear walls." *Journal of Structural Engineering* 131 (2): 259-267.

Berman, J. W, and Bruneau, M. 2008. "Capacity design of vertical boundary elements in steel plate shear walls." Engineering Journal, American Institute of Steel Construction, 45: 57–71.

Bhowmick, A. K. 2009. "Seismic analysis and design of steel plate shear walls." Ph.D. dissertation. University of Alberta, Edmonton, AB, Canada.

Bhowmick, A. K. 2014. "Seismic behavior of steel plate shear walls with centrally placed circular perforations." *Thin-Walled Structures 75*: 30-42.

Bhowmick, A.K., Driver, R., and Grondin, G.. 2009. "Seismic analysis of steel plate shear walls considering strain rate and P-delta effects." *Journal of Constructional Steel Research* 65: 1149-1159.

Bhowmick, A.K, Driver R.G, Grondin G.Y. 2011. "Application of indirect capacity design principles for seismic design of steel-plate shear walls." *Journal of Structural Engineering* 137(4): 521–530.

Bhowmick, A.K, Grondin, G.Y., and Driver R.G. 2010. "Performance of Type D and Type LD steel plate walls." *Canadian Journal of Civil Engineering* 37(1): 88-98.

Bhowmick, A. K., Grondin G. Y., and Driver R. G. 2011. "Estimating fundamental periods of steel plate shear walls." *Engineering Structures* 33:1883–1893.

Bhowmick, A. K., Grondin, G., and Driver, R. 2014. "Nonlinear seismic analysis of perforated steel plate shear walls." *Journal of Constructional Steel Research* 94: 103-113.

Bruneau, M., and Sabelli, R. 2006. "AISC Design Guide No. 20." *Steel Plate Shear Walls*.

Caccese, V., Elgaaly, M., and Chen, R. 1993. "Experimental Study of Thin Steel-Plate Shear Walls under Cyclic Load." *Journal of Structural Engineering*: 573-587.

Chatterjee A.K., Bhowmick A., Bagchi A. 2015. "Development of a simplified equivalent braced frame model for steel plate shear wall systems." *Steel and composite structures* 18(3):711–737.

Choi, I. R., and Park, H. 2009. "Steel Plate Shear Walls with Various Infill Plate Designs." *Journal of Structural Engineering-asce* 135: 785-796.

CSA. 2009. *CAN/CSA-S16-09 Limit states design of steel structures*. Toronto, ON, Canada: Canadian Standards Association.

CSA. 2014. *CAN/CSA-S16-14 Limit states design of steel structures*. Mississauga, ON, Canada: Canadian Standards Association.

Dhar, M. M., and Bhowmick, A. K. 2016. "Seismic response estimation of steel plate shear walls using nonlinear static methods." *Steel and Composite Structures* 20: 777-799.

Driver, R., Kulak, G. L., Kennedy, D., and Elwi, A. L. 1998a. "Cyclic test of four-story steel plate shear wall." *Journal of Structural Engineering* 124 (2): 112-120.

Driver, R., Kulak, G. L., Kennedy, D., and Elwi, A. L. 1998b. "Cyclic Test of Four-Story Steel Plate Shear Wall." *Journal of Structural Engineering* 124 (2): 112-120.

Farahbakhshtooli, A., and Bhowmick, A. K. 2021. "Nonlinear seismic analysis of perforated steel plate shear walls using a macro-model." *Thin-Walled Structures* 166: 108022.

Farahbakhshtooli, A., and Bhowmick, A. K.. 2019. "Seismic collapse assessment of stiffened steel plate shear walls using FEMA P695 methodology." *Engineering Structures* 200: 109714.

Fujitani, H., Yamanouchi, H., Okawa, I., Sawai, N., Uchida, N., and Matsutani, T. 1996. "Damage and performance of tall buildings in the 1995 Hyogoken Nanbu earthquake." 67th Regional Conference (in conjunction with ASCE Structures Congress XIV).

Guo, H. C., Hao, J. P., and Liu, Y. H. 2015. "Behavior of stiffened and unstiffened steel plate shear walls considering joint properties." *Thin-Walled Structures* 97: 53-62.

Hosseinzadeh, S. A. A., and Tehranizadeh, M. 2012. "Introduction of stiffened large rectangular openings in steel plate shear walls." *Journal of Constructional Steel Research* 77: 180-192.

Ikarashi, K., Shimomura, H., Yasunaga, J., Ueki, T., Ono, J., and Ohyama, T. 2020. "Effect of surrounding frame members on the buckling behavior of steel shear walls restrained by stiffeners." *Japan Architectural Review* 3 (4): 481-495.

Kaveh, A., and Farhadmanesh, M. 2019. "Optimal seismic design of steel plate shear walls using metaheuristic algorithms." *Periodica Polytechnica Civil Engineering* 63 (1): 1-17.

Kulak, G. L. 1991. "Unstiffened steel plate shear walls." In *Structures subjected to repeated loading*, 247-286. CRC Press.

Lubell, A., Prion, H., Ventura, C., and Rezai, M. 2000. "Unstiffened Steel Plate Shear Wall Performance under Cyclic Loading." *Journal of Structural Engineering-asce* 126: 453-460.

Mamazizi, A., Shafi Khani, Gharehbaghi, V. R., and Noroozinejad Farsangi, E. 2022. "Modified plate frame interaction method for evaluation of steel plate shear walls with beam-connected web plates." *Journal of Building Engineering* 45: 103682.

NBCC. 2015. National building code of Canada 2015, Canadian commission on building and fire codes. National Research Council of Canada Ottawa.

Purba, R., and Bruneau, M. 2009. "Finite-element investigation and design recommendations for perforated steel plate shear walls." *Journal of structural engineering* 135 (11): 1367-1376.

Purba, R., and Bruneau, M. 2015. "Seismic performance of steel plate shear walls considering two different design philosophies of infill plates. II: Assessment of collapse potential." *Journal of Structural Engineering* 141 (6): 04014161.

Rezai, M. 1999. *Seismic behaviour of steel plate shear walls by shake table testing*. University of British Columbia Vancouver, Canada.

Rezai, M., Ventura, C., and Prion, H. 2004. "Simplified and detailed finite element models of steel plate shear walls." Proc. 13th world conference on earthquake engineering.

Roberts, T., and Sabouri-Ghomi, S. 1992. "Hysteretic characteristics of unstiffened perforated steel plate shear panels." *Thin-walled Structures* 14: 139-151.

Sabouri-Ghomi, M., Bhowmick, A. K., and Sabouri-Ghomi, S. 2022. "Behavior improvment of steel plate shear walls with rectangular openings." CSCE Annual Conference, Whistler, British Columbi.

Sabouri-Ghomi, S., Ahouri, E., Sajadi, R., Alavi, M., Roufegarinejad, A., and Bradford, M. 2012. "Stiffness and strength degradation of steel shear walls having an arbitrarily-located opening." *Journal of Constructional Steel Research* 79: 91-100.

Sabouri-Ghomi, S., and Mamazizi, S. 2015. "Experimental investigation on stiffened steel plate shear walls with two rectangular openings." *Thin-walled Structures* 86: 56-66.

Sabouri-Ghomi, S., and Roberts, T. M. 1991. "Nonlinear dynamic analysis of thin steel plate shear walls." *Computers & Structures* 39: 121-127.

Sabouri-Ghomi, S., and Sajjadi, R. 2012. "Experimental and theoretical studies of steel shear walls with and without stiffeners." *Journal of Constructional Steel Research* 75: 152-159.

Sabouri-Ghomi, S., Ventura, C., and Kharrazi, M. 2005. "Shear Analysis and Design of Ductile Steel Plate Walls." *Journal of Structural Engineering-asce* 131: 878-889.

Sabouri-Ghomi, S., Kharrazi, M,. Mam-Azizi, S., and Sajadi, R. 2008. "Buckling behavior improvement of steel plate shear wall systems." *The Structural Design of Tall and Special Buildings* 17 (4): 823-837.

Sayed-Ahmed, E. Y. 2001. "Behaviour of steel and (or) composite girders with corrugated steel webs." *Canadian Journal of Civil Engineering* 28 (4): 656-672.

Shishkin, J. J., Driver, R., and Grondin, G. 2009. "Analysis of steel plate shear walls using the modified strip model." *Journal of Structural Engineering* 135 (11): 1357-1366.

Takahashi, Yasuhiko, Takemoto, Takeda, and Takagi. 1973. "Experimental study on thin steel shear walls and particular bracings under alternative horizontal load." Preliminary Report, IABSE, Symp. On Resistance and Ultimate Deformability of Tsructures Acted on by Well-defined Repeated Loads, Lisbon, Portugal.

Thorburn, L. J., Kulak, G. L., and Montgomery, C. J. 1983. *Analysis and Design of Steel Shear Wall Systems.* Structural Engineering Report No. 107 (Department of Civil Engineering,).

Timler, and Kulak. 1983. *Experimental study of steel plate shear walls.* University of Alberta (Department of Civil Engineering,).

Timler, Ventura, Prion, and Anjam. 1998. "Experimental and analytical studies of steel plate shear walls as applied to the design of tall buildings." *Structural Design of Tall Buildings* 7: 233-249.

Timoshenko, S. P., and Gere, J. M. 1961. *Theory of Elastic Stability*. Dover Publications.

Timoshenko, S. P., and Goodier N. J. 1970. Theory of Elasticity 3rd ed., 567. McGraw-Hill, New York.

Troy, R. G. 1988. "Steel plate shear wall designs." *Stuctural Engineering Reviews* 1: 35-39.

Vian, D., Bruneau, M., and Purba, R. 2009. "Special perforated steel plate shear walls with reduced beam section anchor beams. II: Analysis and design recommendations." *Journal of Structural Engineering* 135 (3): 221-228.

Vian, D., Bruneau, M., Tsai, K. C., and Lin, Y. C. 2009. "Special perforated steel plate shear walls with reduced beam section anchor beams. I: Experimental investigation." *Journal of Structural Engineering* 135 (3): 211-220.

Vian, D., Lin, Y. C., Bruneau, M., and Tsai, K. H. 2003. "Cyclic performance of low yield strength steel panel shear walls."

Wagner, H. 1931. *Flat sheet metal girders with very thin metal web. Part I: general theories and assumptions.*

Zirakian, T., and Zhang, J. 2015. "Structural performance of unstiffened low yield point steel plate shear walls." *Journal of Constructional steel research* 112: 40-53.